

**Identification of novel sarcomeric modifiers of
hypertrophy in hypertrophic cardiomyopathy using
the yeast two-hybrid system**

C Todd

*Thesis presented in partial fulfilment of the requirements for the degree of
Master of Science in Medical Science (Human Genetics) in the Faculty
of Medicine and Health Sciences at Stellenbosch University*



Promoter: Dr CJ Kinnear

Co-promoter: Prof JC Moolman-Smook

March 2013

DECLARATION

By submitting this thesis electronically, I declare that the entirety of the work contained therein is my own, original work, that I am the sole author thereof (save to the extent explicitly otherwise stated), that reproduction and publication thereof by Stellenbosch University will not infringe any third party rights and that I have not previously in its entirety or in part submitted it for obtaining any qualification.

Date: March 2013

ABSTRACT

Left ventricular hypertrophy (LVH) occurs when the cardiomyocytes in the left ventricle become enlarged by increasing in mass in response to haemodynamic pressure overload. This can either be attributed to a normal physiological response to exercise or can be the result of a maladaptive process or disease state, such as chronic hypertension. Hypertrophic cardiomyopathy (HCM) is the most common form of Mendelian-inherited cardiac disease. A defining characteristic thereof is primary LVH that occurs when there are no other hypertrophy-predisposing conditions present. Therefore, HCM provides a unique opportunity to study the molecular determinants of LVH in the context of a Mendelian disorder, instead of in more complex disorders such as hypertension. Over 1000 HCM-causing mutations in 19 genes have been identified thus far, most of them encoding sarcomeric proteins residing in the sarcomeric C-zone. However, for many HCM patients no disease-causing genes have been identified. Moreover, studies have shown phenotypic variation in presentation of disease in, as well as between, families in which the same HCM-causing mutation segregates. This has led many investigators to conclude that genetic modifiers of hypertrophy exist.

The aim of the study was to identify novel plausible HCM-causing or modifier genes by searching for interactors of a known HCM-causing protein, namely titin. The hypothesis was that genes encoding proteins, which interact with proteins that are encoded by known HCM-causative genes, may also be considered HCM-causing or may modify the HCM phenotype. To this end, the aim was to identify novel interactors of the 11-domain super-repeat region of titin, which resides within the

sarcomeric C-zone, using yeast two-hybrid analysis. Five putative interactors of the 11-domain super-repeat region of titin were identified in this study. These interactions were subsequently verified by colocalisation in H9C2 rat cardiomyocytes, providing further evidence for possible interactions between titin and these proteins.

The putative interactor proteins of titin determined from the Y2H library screen were: filamin C (FLNC), phosphatidylethanolamine-binding protein 4 (PEBP4), heart-type fatty acid binding protein 3 (H-FABP3), myomesin 2 (MYOM2) and myomesin 1 (MYOM1).

The *FLNC* gene could be a candidate for cardiac diseases, especially cardiomyopathies that are associated with hypertrophy or developmental defects. The putative interaction of titin and PEBP4 is speculated to be indicative of the formation of the interstitial fibrosis and myocyte disarray seen in HCM. Heart-type fatty acid-binding protein 3 has prognostic value to predict recurrent cardiac events. Its suggested interaction with titin is speculated to play a role in inhibiting its functional abilities. Myomesin 2 is jointly responsible, with MYOM1, for the formation of a head structure on one end of the titin string that connects the Z and M bands of the sarcomere. This is speculated to be linked to a developmental error with the result being a defect in sarcomeric structure formation, which could result in pathologies such as HCM.

Therefore, these identified proteins could likely play a functional role in HCM due to their interactions with titin. This research could thus help with new insights into the further understanding of HCM patho-aetiology.

OPSOMMING

Linker ventrikulêre hipertrofie (LVH) ontstaan wanneer die kardiomyosiete in die linkerventrikel vergroot as gevolg van 'n verhoging in massa in reaksie op hemodinamiese drukoormoed. Dit kan toegeskryf word aan 'n normale fisiologiese respons op oefening of kan die gevolg wees van 'n wanaangepaste of siektetoestand, soos chroniese hipertensie. Hipertrofiese kardiomiopatie (HKM) is die mees algemene vorm van Mendeliese oorerflike hartsiekte. 'n Bepalende eienskap daarvan is primêre LVH, wat plaasvind wanneer daar geen ander hipertrofie-predisponerende voorwaardes teenwoordig is nie. Gevolglik bied HKM 'n unieke geleentheid om die molekulêre determinante van LVH te bestudeer, in die konteks van 'n Mendeliese oorerflike siekte, in plaas van om dit in die meer komplekse siektes soos hoë bloeddruk te bestudeer. Meer as 1000 HKM-veroorsakende mutasies is tot dusver in 19 gene geïdentifiseer. Die meeste van hulle kodeer vir sarkomeriese proteïene wat in die C-sone voorkom. Egter, vir baie HKM-pasiënte is geen siekte-veroorsakende gene al geïdentifiseer nie. Daarbenewens het studies getoon dat variasie in fenotipiese aanbieding van die siekte in, sowel as tussen, families voorkom wat dieselfde HKM-veroorsakende mutasie het. Dit het daartoe gelei dat baie navorsers tot die gevolgtrekking gekom het dat genetiese wysigers van hipertrofie wel bestaan.

Die doel van die studie was om nuwe moontlike HKM-veroorsakende of wysiger-gene te identifiseer deur te soek vir interaktors van 'n bekende HKM-veroorsakende proteïen, naamlik titin. Die hipotese was dat gene wat vir proteïene kodeer, wat in wisselwerking is met proteïene wat geïnkripteer word deur bekende HKM-veroorsakende gene, ook oorweeg kan word om HKM te veroorsaak.

Dit kan ook die HKM fenotipe verander. Dus was die doel om nuwe interaktors van die 11-domein super-herhaalstreek van titin, soos gevind binne die sarkomeriese C-sone, te identifiseer deur middel van gis-twee-hibried-analise. Vyf vermeende interaktors van die 11-domein super-herhaalstreek van titin is in hierdie studie geïdentifiseer. Hierdie interaksies is later geverifieer met behulp van ko-lokalisering in H9C2-rotkardiomyosiete, wat verdere bewyse vir moontlike interaksies tussen titin en hierdie proteïene verskaf.

Die vermeende interaktor-proteïene van titin wat bepaal is vanaf die gis-twee-hibried-biblioteeksifting was as volg: filamin C (FLNC), phosphatidylethanolamine-bindingsproteïen 4 (PEBP4), hart-tipe-vetsuur bindingsproteïen 3 (H-FABP3), myomesin 2 (MYOM2) en myomesin 1 (MYOM1).

Die *FLNC*-geen kan 'n kandidaat vir kardiaal siektes, veral kardiomiopatieë, wees wat geassosieer word met hipertrofie of ontwikkelingsafwykings. Die vermeende interaksie van titin en PEBP4 dui daarop om 'n aanduiding te wees vir die vorming van die interstisiële fibrose en miokardiale wanorde, soos gesien in HKM. Hart-tipe-vetsuur bindingsproteïen 3 het prognostiese waarde om herhalende kardiaal gebeure te voorspel. Verder dui sy voorgestelde interaksie met titin moontlik daarop dat dit 'n rol kan speel in die inhibering van sy funksionele vermoëns. Myomesin 2 tesame met MYOM1 is verantwoordelik vir die vorming van 'n kopstruktuur aan die een kant van die titinstring wat dan die Z- en M-bande van die sarkomeer verbind. Daar word vermoed dat dit gekoppel is aan 'n ontwikkelingsfout, met die gevolg dat daar 'n defek is in sarkomeriese struktuurvorming, wat weer kan lei tot patologieë soos HKM.

Gevolgtik kan hierdie geïdentifiseerde proteïene waarskynlik 'n funksionele rol in HKM speel, as gevolg van hul interaksies met titin. Hierdie navorsing kan dus help om met nuwe insigte vorendag te kom in die verdere begrip van HKM se pato-etologie.

INDEX

	PAGE
ACKNOWLEDGEMENTS	x
LIST OF ABBREVIATIONS	xi
LIST OF FIGURES	xviii
LIST OF TABLES	xx
1. INTRODUCTION	3
2. MATERIALS AND METHODS	54
3. RESULTS	91
4. DISCUSSION	112
APPENDIX I	139
APPENDIX II	148
APPENDIX III	150

APPENDIX IV **151**

REFERENCES **155**

ACKNOWLEDGEMENTS

I would like to express my sincere gratitude to the following people and institutions that assisted me in various ways during the course of this degree:

Dr Craig Kinnear and Prof Hanlie Moolman-Smook for their invaluable expertise, guidance, time and effort. I am grateful to have the opportunity to work with such role models.

Jomien Mouton for culturing the H9C2 cells used for the verification of this study.

Prof Dirk Lang and Susan Cooper, Department of Human Biology, University of Cape Town, for their extensive help and expertise with the confocal microscope used in the verification of this study.

Dr Ben Loos, Department of Physiology (University of Stellenbosch) for all the help and patience with the fluorescence microscope techniques.

Lizzie, Candice, Carmen, Martmari, Carin and William for technical support with the yeast two-hybrid system. The whole MAGIC lab team, especially Ilze, for emotional support and other assistance in times of need. I truly enjoyed my time with all of you!

A special thank you to the late Rowena Keyser for being a wonderful bench partner and for always being willing to answer questions that I probably should have known the answer to.

My family and friends: My mom and dad for their incredible, unwavering support and belief in me. My sister, Melvi, for understanding what nobody else could. Matthew, for putting up with my idiosyncrasies and mood swings, as well as being there for me almost every step of the way. Sunley, Lizette, Jane, Chandré, Elsje-Marie and Elize for always knowing what to say to cheer me up. A special thanks to An-Maree Nel!

Mrs Wendy Ackerman, Prof Paul van Helden, the University of Stellenbosch and the National Research Foundation (NRF) for their generous financial support and funding, enabling me to complete my studies.

The Lord, for giving me both the ability and the perseverance to conquer anything.

LIST OF ABBREVIATIONS

α	alpha
β	beta
γ	gamma
#	number
μg	micrograms
μm	micrometres
μM	micromolar
μL	microlitre
$^{\circ}\text{C}$	degrees Celsius
2D	two-dimensional
3D	three-dimensional
3'	three prime
3'-UTR	3 prime untranslated region
5'	five prime
5'-UTR	5 prime untranslated region
aa	amino acid
Ade	adenine
<i>ADE2</i>	Phosphoribosylaminoimidazole carboxylase gene
ABI	Applied Biosystems Incorporated
AD	activation domain
ADP	adenosine diphosphate
Amp	ampicillin
ATP	adenosine triphosphate
AV	atrioventricular

BD	binding domain
BLAST	Basic Local Alignment Search Tool
BLASTn	nucleotide Basic Local Alignment Search Tool
BLASTp	protein Basic Local Alignment Search Tool
bp	base pair
BP	blood pressure
BPB	bromophenol blue
C	cytosine
Ca ²⁺	calcium ²⁺
CaCl ₂	calcium chloride
CAF	Central Analytical Facility
cm	centimetre
cDNA	complementary DNA
cfu	colony forming units
cMyBPC	cardiac myosin binding protein C
CO ₂	carbon dioxide
co-IP	co-immunoprecipitation
DCM	dilated cardiomyopathy
ddH ₂ O	double distilled water
DIC	differential interference contrast
DMEM	Dulbecco's modified Eagle's medium
DMSO	dimethyl sulfoxide
DNA	deoxyribonucleic acid
dNTP	deoxy-nucleotide triphosphate
E	glutamate

ECG	Electrocardiography
<i>E.coli</i>	<i>Escherichia coli</i>
EDTA	ethylene-diamine-tetra-acetic acid
F actin	filamentous actin
FACS	fluorescence-activated cell sorting
FATZ	γ -filamin/ABP-L, α -actinin and telethonin binding protein of the Z-disk
FLNC	filamin C
Fn	fibronectin-like / fibronectin type
G	guanine
G actin	globular actin
H ⁺	hydrogen
H ₂ O	water
HCM	hypertrophic cardiomyopathy
HF	heart failure
H-FABP3	heart-type fatty acid binding protein 3
His	histidine
<i>HIS3</i>	Imidazoleglycerolphosphate dehydratase gene
HOPE	Heart Outcomes Prevention Evaluation
HR	heart rate
HRM	high resolution melt
Ig	immunoglobulin-like
IVS	interventricular septum
K	lysine
K ⁺	potassium

Kan	kanamycin
kb	Kilo bases
kDa	Kilo Dalton
KESTREL	kinase substrate tracking and elucidation
L	litre
LB	Luria-Bertani
LBB	left bundle branch
Leu	leucine
LiAc	lithium acetate
LIFE	Losartan Intervention for Endpoint reduction
LIM	lin-11, islet-1 and mec-3
LMM	light meromyosin
Ltd	limited
LV	left ventricular
LVH	left ventricular hypertrophy
LVM	left ventricular mass
M	Molar
MAPK	mitogen-activated protein kinase
MCS	multiple cloning site
MDa	Mega Dalton
<i>MEL1</i>	Alpha-galactosidase gene
mg	milligram
Mg ²⁺	magnesium ²⁺
min	minute
mL	millilitre

MLP	muscle-specific lin-11, islet-1 and mec-3 (LIM) protein
mm	millimetre
mM	millimolar
mRNA	messenger ribonucleic acid
MURF	muscle-specific ring finger
MyBPC	myosin binding protein C
myHCs	myosin heavy chains
MYOM1	myomesin 1
MYOM2	myomesin 2
Na ⁺	sodium
NaCl	sodium chloride
NCBI	National Centre for Biotechnology Information
NLO	two photon laser
ng	nanograms
nm	nanometre
OD	optical density
ORF	open reading frame
P	proline
PBS	phosphate buffered saline
PCI	phenol:chloroform:isoamyl alcohol
PCR	polymerase chain reaction
PDK1	3-phosphoinositide-dependent kinase 1
PEBP4	phosphatidylethanolamine-binding protein 4
PEG	polyethylene glycol
PEVK	proline (P), glutamate (E), valine (V) and lysine (K)

Pi	inorganic phosphate
PIPES	Piperazine-N,N'-bis(2-ethanesulfonic acid)
PKB	protein kinase B
PMTs	photomultiplier tubes
QDO	quadruple dropout
R	correlation coefficient
RAF1-MEK	proto-oncogeneserine/threonine-protein kinase1- mitogen-activated protein kinase/extracellular-signal- regulated kinase
RasGAP	RasGTPase-activating protein
RBB	right bundle branch
RNA	ribonucleic acid
rpm	revolutions per minute
RSA	Republic of South Africa
SA	sinoatrial
SB	sodium borate / di-sodium tetraborate-decahydrate
SCD	sudden cardiac death
<i>S.cerevisiae</i>	<i>Saccharomyces cerevisiae</i>
SD	synthetic dropout
SDS	sodium dodecyl-sulphate
sec	second
Ser	serine
SH3	Src homology 3
SNP	single nucleotide polymorphism
SR	sarcoplasmic reticulum

T	thymine
T _a	annealing temperature
T-cap	titin cap / telethonin
TDO	triple dropout
Thr	threonine
TK	titin kinase
T _m	melting temperature
Tm	tropomyosin
Tn	troponin
Trp	tryptophan
TTN	titin protein
<i>TTN</i>	titin gene
U	units
UCT	University of Cape Town
UK	United Kingdom
Ura	uracil
USA	United States of America
UV	ultra-violet
V	valine and Volts
W	Watts
w/v	weight per volume
www	World Wide Web
X- α -Gal	X-alpha-galactosidase
Y2H	yeast two-hybrid
YPDA	yeast peptone dextrose adenine

LIST OF FIGURES

FIGURE	PAGE
CHAPTER 1	
Figure 1.1. The cardiac conduction system.	4
Figure 1.2. Confocal microscopy of cardiac muscle cells.	6
Figure 1.3. Origins of the striations in muscle are from the arrangement of the myofilaments.	7
Figure 1.4. Electron micrograph of sections of three myofibrils in vertebrate striated muscle.	9
Figure 1.5. Schematic diagram of a sarcomere, summarizing the organization and locations of the main sarcomeric components.	11
Figure 1.6. The sliding-filament model of muscular contraction.	13
Figure 1.7. Schematic diagrams of the thin-filament structure.	16
Figure 1.8. Molecular structure of the titin filament as well as the location of alternative splicing sites that result in different titin isoforms.	22
Figure 1.9. Schematic representation of titin's arrangement within the sarcomere.	25
Figure 1.10. Models of titin's functioning.	29
Figure 1.11. Models of the Z-line's structure.	31
Figure 1.12. Schematic diagrams indicating the intermediate filaments.	33
Figure 1.13. Transverse section of muscle in the M-line region ($\times 125000$).	37
Figure 1.14. M-line models.	38

Figure 1.15. The pathology of hypertrophic cardiomyopathy.	46
---	----

CHAPTER 2

Figure 2.1. Normal transcription.	56
--	----

Figure 2.2. The principle of Y2H.	56
--	----

Figure 2.3. Outline of the methodology used to perform the present study.	57
--	----

CHAPTER 3

Figure 3.1. Linear growth curves of untransformed <i>S.cerevisiae</i> AH109 strain transformed with either non-recombinant pGBKT7 or pGBKT7- <i>TTN</i> bait constructs.	93
---	----

Figure 3.2. Confocal imaging of titin and FLNC.	102
--	-----

Figure 3.3. Confocal imaging of titin and PEBP4.	103
---	-----

Figure 3.4. Confocal imaging of titin and H-FABP3.	104
---	-----

Figure 3.5. Confocal imaging of titin and MYOM2.	105
---	-----

Figure 3.6. Confocal imaging of titin and MYOM1.	106
---	-----

LIST OF TABLES

TABLE	PAGE
CHAPTER 2	
Table 2.1. Primer sequences and annealing temperatures used in the construct design and amplification of the inserts from cloning vectors.	60
Table 2.2. Phenotypic assessment of the untransformed <i>S.cerevisiae</i> strains, grown on specific SD selection media.	72
Table 2.3. Test for autonomous reporter gene activation by the pGBKT7- <i>TTN</i> bait construct.	73
Table 2.4. Mating efficiency test of <i>S.cerevisiae</i> AH109 (pGBKT7- <i>TTN</i>).	75
Table 2.5. Antibody properties of the primary bait and prey antibodies used during the colocalisation analysis.	85
Table 2.6. Excitation and emission spectra of the secondary antibodies used during the colocalisation analysis.	86
CHAPTER 3	
Table 3.1. Mating efficiency of AH109 pGBKT7- <i>TTN</i> as determined by growth of colonies on selection media.	94
Table 3.2. Mating efficiency of library mating (pACT2 heart cDNA in Y187 x pGBKT7-bait construct in AH109).	97

Table 3.3. Activation of the <i>HIS3</i> & <i>ADE2</i> and <i>MEL1</i> reporter genes by prey- <i>TTN</i> interactions.	98
Table 3.4. Identification of plausible TTN interacting clones from the Y2H screen.	100
Table 3.5. Colocalisation of titin and FLNC.	107
Table 3.6. Colocalisation of titin and PEBP4.	107
Table 3.7. Colocalisation of titin and H-FABP3.	108
Table 3.8. Colocalisation of titin and MYOM2.	108
Table 3.9. Colocalisation of titin and MYOM1.	109

CHAPTER 1
INTRODUCTION

INDEX

	PAGE
1.1 PREFACE: THE HEART	3
1.1.1 Impulse propagation throughout the heart	3
1.1.2 The cardiac muscle cell (cardiomyocyte)	5
1.2 STRUCTURE AND FUNCTION OF MUSCLE FIBRES	6
1.3 THE CARDIAC SARCOMERE	10
1.3.1 Molecular composition and functions of sarcomeres	10
1.4 CONTRACTION OF MUSCLES	12
1.4.1 The cross-bridge cycle	14
1.5 THE THIN FILAMENT	15
1.5.1 The Z line	18
1.5.1.1 Composition of the Z line	18
1.5.2 Titin filaments	19
1.5.2.1 Molecular structure, interactions and organization of titin filaments	21
1.5.2.2 Function of titin in myofibrillogenesis	26

1.5.2.3 Mechanical function of titin	28
1.5.3 Model of the Z line	30
1.6 INTERMEDIATE FILAMENTS	32
1.7 THE THICK FILAMENT	35
1.7.1 The M line	35
1.7.1.1 Structure of the M line	35
1.7.1.2 Protein components and interactions of the M line	39
1.7.2 Model of the M line	41
1.7.3 Function of the M line	41
1.8 LEFT VENTRICULAR HYPERTROPHY	42
1.9 HYPERTROPHIC CARDIOMYOPATHY	44
1.10 IN THE PRESENT STUDY	48

CHAPTER 1: INTRODUCTION

1.1 PREFACE: THE HEART

The heart, once thought to contain the soul of mankind, is no longer seen as some mystical life-force not meant to be understood. In the past the heart was seen as the emotional, spiritual, moral and intellectual core of humanity; believed to accommodate the mind, it is often still used to represent love. The human heart is in fact essentially a giant pump, used to transfer both oxygenated blood coming from the lungs to the various parts of the body (organs, tissues and cells) as well as deoxygenated blood from the body back to the lungs. During normal functioning, the pump system operates in a basically uninterrupted cycle throughout a human's life. It is only when there is a disturbance in this cycle that the human body no longer functions as expected. This study aims to shed some light on some of the many molecular mechanisms involved in cardiac contractility.

1.1.1 Impulse propagation throughout the heart

The heart is the first organ that develops in a foetus (Woodcock and Matkovich, 2005). During normal contraction, action potentials (electrical impulses) are spread systematically throughout the heart (**Figure 1.1**). This electrical excitation spreads in a wave-like manner along the plasma membranes of each adjacent cardiomyocyte (heart muscle cell), triggering the release of calcium. The sarcoplasmic reticulum, an intracellular membrane-bound compartment, releases the calcium and this stimulates the contraction of the myofibrils (muscle fibres) (Gaussin, 2004).

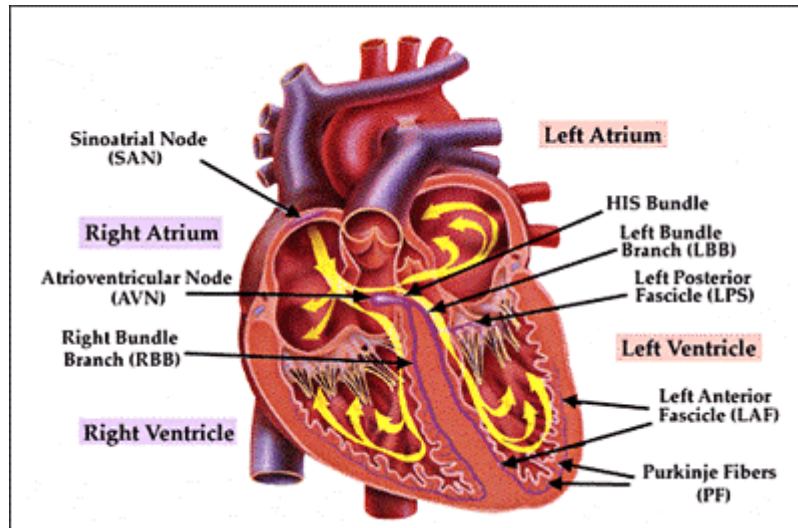


Figure 1.1. The cardiac conduction system. Yellow arrows indicate how an electrical impulse is conducted through the heart. [Adapted from www.pharmacology2000.com].

An electrical signal is initiated in the sinoatrial (SA) node (**Figure 1.1**) of the heart. The SA node is made up of fast autorhythmic (contractile) tissue and is found in the right atrium (Gaussin, 2004). An action potential is conducted through the atriums from right to left and superior to inferior, causing each contraction to be propagated downwards towards the ventricles. However, a thick non-conductive connective tissue septum prevents the electrical impulse from spreading directly to the ventricles. This causes a delay, as the impulse must pass through the atrioventricular (AV) node (**Figure 1.1**), found at the junction of the atria and ventricles. The electrical impulse is once again conducted rapidly along the AV bundle (bundle of His), separating into a left bundle branch (LBB) and right bundle branch (RBB) so as to excite the ventricles (**Figure 1.1**). The electrical signal is propagated by means of Purkinje fibres (**Figure 1.1**), to both left and right, throughout the cardiac muscles cells of the ventricles, ending at the apex (Gaussin, 2004). This results in a contractile wave

moving up through the ventricles and causing blood to be pumped into the pulmonary artery and the aorta. Electrocardiography (ECG) is a way to observe the conduction of an action potential through the heart, as well as to detect any disturbances thereof (Severs, 2000).

1.1.2 The cardiac muscle cell (cardiomyocyte)

The cardiac muscle is a unique muscle in composition as well as in function. It is capable of contracting on its own in the presence of an electrical impulse (Severs, 2000). The cardiac muscle cell or cardiomyocyte is elongated with the dimensions of 100 to 150 μm in length and 20 to 35 μm in width (Severs, 2000). The contractile myofilaments - including actin, myosin as well as associated proteins - form striated myofibrils that make up the cardiomyocytes (**Figure 1.2A**) (Severs, 2000). The myocytes are joined to each other at intercalated disks which form blunt ends (**Figure 1.2B**) (Severs, 2000).

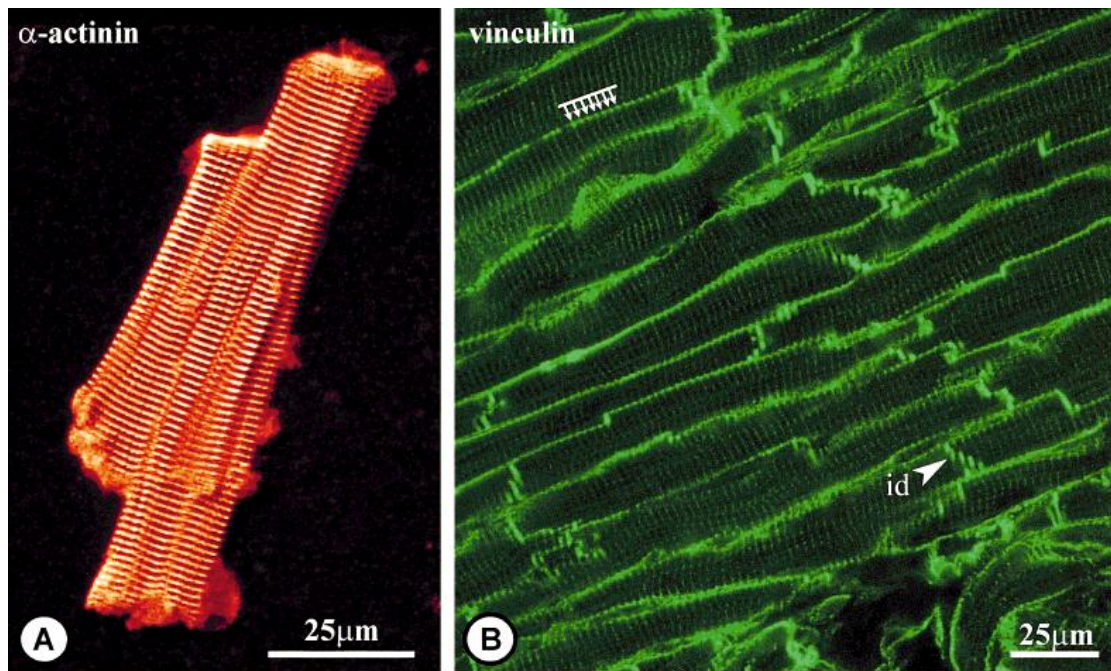


Figure 1.2. Confocal microscopy of cardiac muscle cells. (A) A single ventricular myocyte. The myofibrils are seen as striations. (B) A section of cardiac muscle. Numerous cells like that in panel (A) are joined together at intercalated disks (id). [Taken and adapted from Severs, 2000].

1.2 STRUCTURE AND FUNCTION OF MUSCLE FIBRES

Vertebrate striated muscle fibres are single, multinucleate, membrane-bound cells, about 10 to 100 μm in diameter and a number of centimetres long (Huxley, 1953a). When viewed under the light microscope, they show a pattern of transverse stripes which are indicative of the thick and thin filaments and how they are arranged in relation to one another (**Figure 1.3A**) (Huxley, 1953a). The fibres are filled with myofibrils (**Figure 1.3B**) of approximately one to three micrometres in diameter and enveloped by a sarcoplasmic reticulum (SR) membrane parallel to the fibre axis (Huxley, 1953a). The fibrils are striated which thus creates the striated appearance of the fibre as a whole (**Figure 1.3**) (Huxley, 1953a).

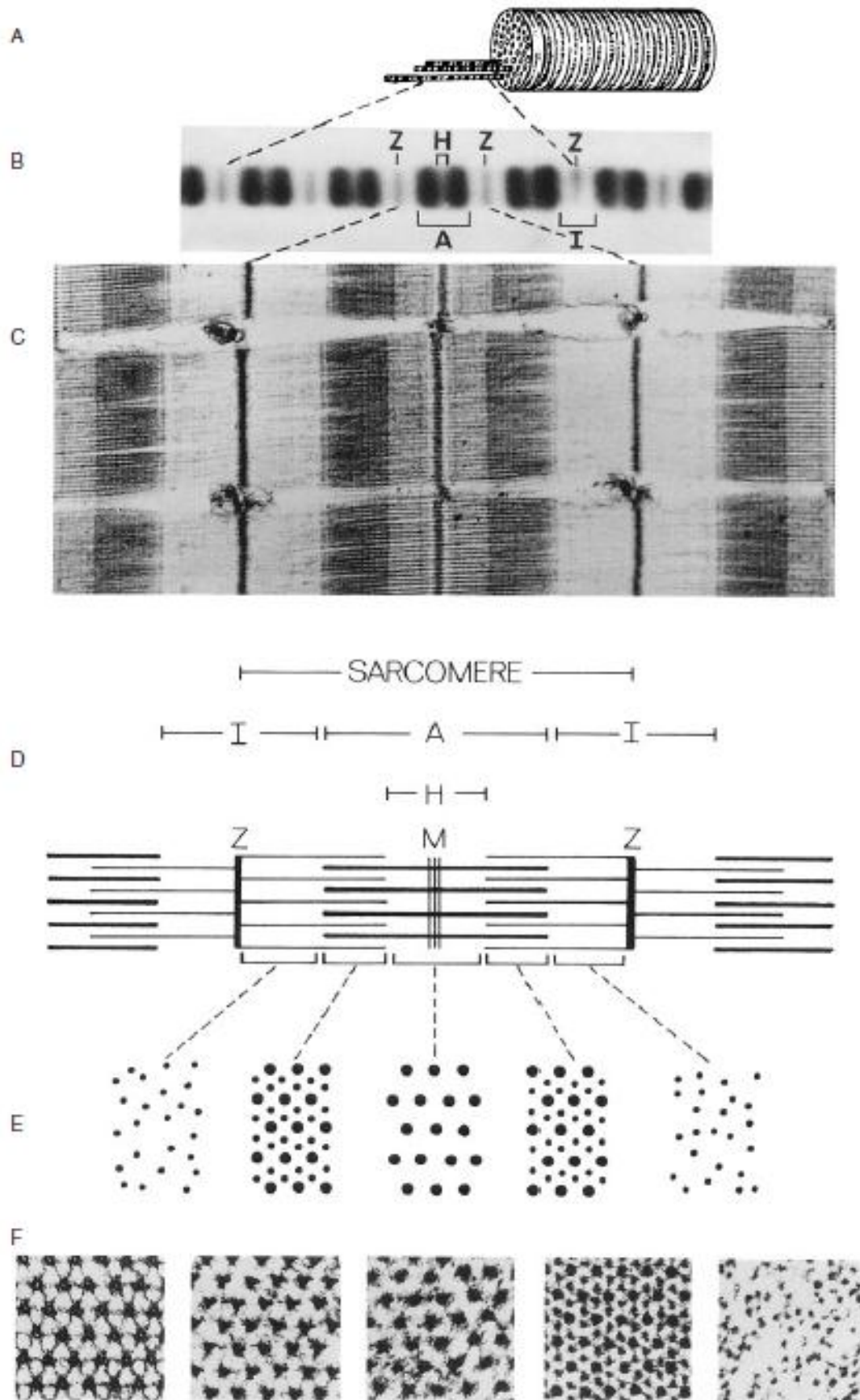


Figure 1.3. Origins of the striations in muscle are from the arrangement of the

myofilaments. (A) A single muscle fibre with three protruding myofibrils. (B) A phase-contrast light micrograph of a myofibril showing transverse striations ($\times 5400$). (C) An electron micrograph of three longitudinally sectioned myofibrils. Transverse stripes in the A band are due to myosin-binding proteins and in the I band due to troponin ($\times 23000$). (D) Interpretation of (B) and (C) in terms of thick (myosin-containing) and thin (actin-containing) filaments, arranged in register. (E) Cross-sectional appearance of sarcomere at different axial levels. (F) Electron micrographs of transverse sections at different points along the sarcomere. From left to right: the M line, the bare zone, the H zone, the zone of thick and thin filament overlap, the I band ($\times 120000$). [Taken and adapted from Craig and Padrón, 2004].

The pattern of striation on the myofibril repeats approximately every two to three micrometres (Huxley, 1953a). These repeating units are sarcomeres and they are known as the contractile units of striated muscle cells (Huxley, 1953a). The ends of sarcomeres have narrow (approximately $0.1\mu\text{m}$), dark lines known as Z lines (**Figure 1.3B-D**) (Huxley, 1953a). Each one of the Z lines intersects a lighter, approximately $1\mu\text{m}$ in length I band, shared by adjoining sarcomeres (Huxley, 1953a). A $1.6\mu\text{m}$ in length, dark A band is found in the middle of each sarcomere and is bisected by a less dense H zone (Huxley, 1953a). The centre of the H zone has an even lighter region, known as the pseudo-H zone (**Figure 1.3C**) (Huxley, 1953a). The pseudo-H zone contains a thin band (sometimes showing three or more fine stripes) of higher density known as the M line (**Figure 1.3C&D**) (Huxley, 1953a).

The pattern formed by the bands can be explained in terms of an accurately ordered arrangement of contractile filaments in each myofibril (**Figure 1.3**), which was first

obviously visible in ultrathin sections of muscle viewed with an electron microscope (**Figure 1.3** and **Figure 1.4**) (Huxley, 1953a; Huxley, 1957). The A band consists of a collection of thick (15nm in diameter) myofilaments that are 1.6 μ m long and lie parallel to the fibril axis (Huxley, 1953a). The half I bands consist of a group of thin (approximately 10nm in diameter) filaments, about 1 μ m in length that lie longitudinally (Huxley, 1953a). The thin filaments lie from their attachment at the Z line through the I band and into the A band, where they overlap partly with the thick filaments (Huxley, 1953a). The H zone is less dense than the remainder of the A band due to the lack of overlapping thin filaments (Huxley, 1953a).

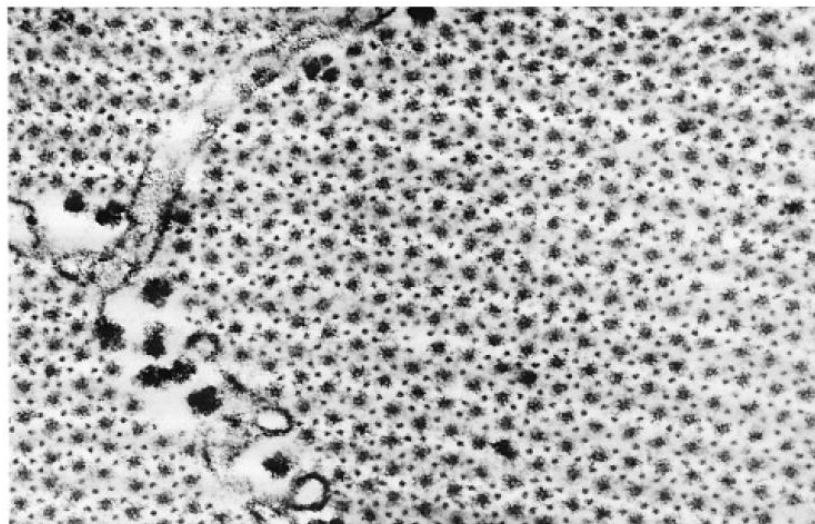


Figure 1.4. Electron micrograph of sections of three myofibrils in vertebrate striated muscle. As seen in transverse section within the overlap zone; illustrating the hexagonal arrangement of thick and thin filaments ($\times 130000$). [Taken from Craig and Padrón, 2004].

The filaments are arranged in a double hexagonal arrangement in the A band, as can be seen in a cross sectional view (**Figure 1.4**) (Huxley, 1953a); first suggested by x-ray diffraction studies of muscle (Huxley, 1953b). The H zone only contains thick

filaments, while in the overlap zone, thin filaments are equidistant from the nearest thick filaments (**Figure 1.3E&F** and **Figure 1.4**) (Huxley, 1953a). Only thin filaments can be found in the I band (Huxley, 1953a). The thin filaments are held together crossways in a square arrangement by the Z line and the thick filaments are interconnected by means of the M line (Huxley, 1953a).

1.3 THE CARDIAC SARCOMERE

1.3.1 Molecular composition and functions of sarcomeres

The sarcomere is the smallest contractile unit of the heart and its primary function is myocyte contractility (McElhinny *et al.*, 2005; King *et al.*, 2010; Nedrud *et al.*, 2011). The sarcomeres of vertebrate muscles are intricate and consist of a number of different proteins that have been identified thus far (**Figure 1.5**). Without actin and myosin the thin and thick filaments cannot exist, respectively (Hanson and Huxley, 1953). Actin accounts for 20 percent of myofibrillar protein, while myosin accounts for 54 percent (Huxley and Hanson, 1957; Hanson and Huxley, 1957).

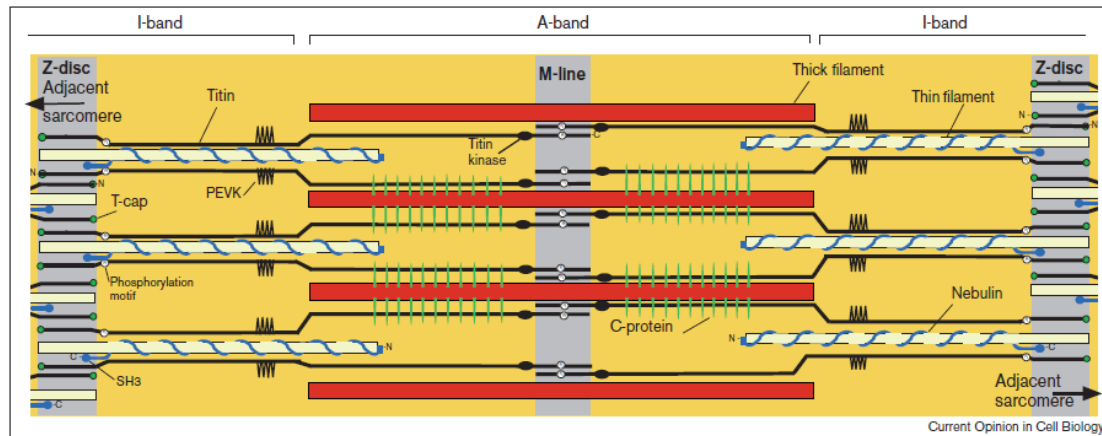


Figure 1.5. Schematic diagram of a sarcomere, summarizing the organization and locations of the main sarcomeric components. [Taken from Gregorio *et al.*, 1999].

The sarcomere has three important structure-function relations, namely the capacity to shorten rapidly and efficiently, being able to switch on and off in milliseconds as well as particular self-assembly and structural regularity (Craig and Padrón, 2004). The sarcomere is made up of different types of proteins, viz. contractile, regulatory and structural (Craig and Padrón, 2004). Actin and myosin are the contractile proteins known to assemble into thin and thick filaments, respectively, that interact with each other to generate both force and shortening in the sarcomere during muscle contraction (Craig and Padrón, 2004).

A number of structural proteins associated with actin and myosin filaments are responsible for the organisation of the sarcomere during development (Craig and Padrón, 2004). Together, the myosin-binding proteins are responsible for assisting in forming the structure of the myosin filament by contributing to the exact organization of its molecules during development as well as modulating contraction in cardiac muscles by means of calcium activated phosphorylation (McClellan *et al.*, 2001). Capping proteins, such as CapZ or β -actinin and tropomodulin, attached to the ends of

the thin filament, prevent either polymerization or depolymerisation of actin and therefore assist in the maintenance of the specific filament length needed for contraction (Xu *et al.*, 1999).

Cross-linking proteins found in the M and Z lines link the thick and thin filaments into well-organized, longitudinal, three-dimensional (3D) lattices (Craig and Padrón, 2004). Intermediate filaments attach to the M and Z lines, thereby reinforcing the structure of the sarcomeres and linking adjacent sarcomeres to each other longitudinally and diagonally (Craig and Padrón, 2004).

1.4 CONTRACTION OF MUSCLES

Muscle contraction is the product of filaments sliding past each other, thus creating a greater overlap of the filaments without a change in the lengths of the actual filaments (**Figure 1.6**) (Huxley and Hanson, 1954; Huxley and Niedergerke, 1954). The sliding-filament model of muscle contraction is generally accepted as the mechanism by which muscles contract and was based upon light microscope observations that the A band stayed constant in length during contraction, whilst the I band and H zone shortened (Huxley, 1957).

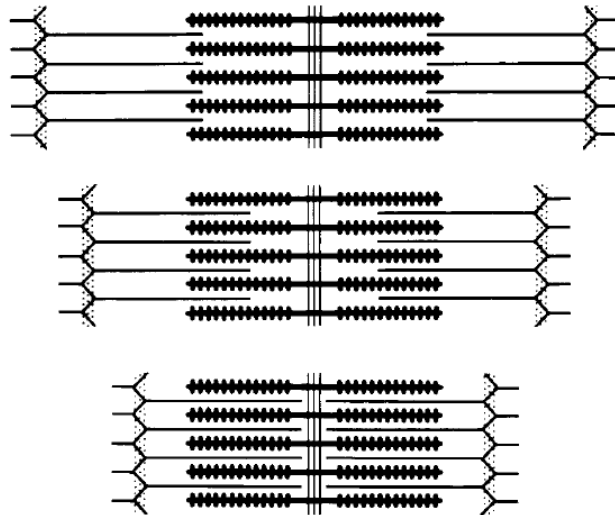


Figure 1.6. The sliding-filament model of muscular contraction. From top to bottom: the transition from the stretched to the contracted state. [Taken from Offer, 1974].

The sliding filament theory can explain how a muscle is able to contract and generate force without producing movement (Silverthorn, 2007). According to this sliding filament theory, tension created within a muscle fibre is directly proportional to the interaction between thick and thin filaments (Silverthorn, 2007).

Muscle fibre types fall into two main categories, namely, slow twitch (type I) and fast twitch (type II) muscle fibres (Lieber and Bodine-Fowler, 1993; Andersen *et al.*, 2000). Fast twitch muscle fibres can, however, be sub-categorized into type IIa and type IIb fibres (Lieber and Bodine-Fowler, 1993; Andersen *et al.*, 2000). Type I muscle fibres use oxygen more efficiently to create energy by generating adenosine triphosphate (ATP) and are thus able to contract continuously over a long period of time before fatigue would set in (Lieber and Bodine-Fowler, 1993; Andersen *et al.*, 2000). Type II muscle fibres make use of anaerobic metabolism to generate ATP and are thus fatigued faster (Lieber and Bodine-Fowler, 1993; Andersen *et al.*, 2000). Type IIa muscle fibres are known as intermediate fast twitch fibres and are able to

make use of both aerobic and anaerobic metabolism to generate ATP (Lieber and Bodine-Fowler, 1993; Andersen *et al.*, 2000). Type IIa is thus a combination of type I and type II fibres (Lieber and Bodine-Fowler, 1993; Andersen *et al.*, 2000). Type IIb muscle fibres only utilise anaerobic metabolism during energy production and have the fastest rate of contraction as well as fatigue (Lieber and Bodine-Fowler, 1993; Andersen *et al.*, 2000).

1.4.1 The cross-bridge cycle

The force that thrusts the actin filament along the sarcomere is the movement of myosin cross-bridges that connect actin to myosin (Huxley and Niedergerke, 1954; Silverthorn, 2007; Krans, 2010). Each myosin head has two binding sites: for an ATP molecule and for actin (Silverthorn, 2007). During the power stroke or cross-bridge cycle, movement of the myosin cross-bridges thrusts actin filaments towards the middle of the sarcomere (Huxley and Niedergerke, 1954; Silverthorn, 2007). When the cross-bridge cycle completes, each myosin head releases its bound actin, then swings backwards to bind a new actin molecule and is ready to start another cycle (Huxley and Niedergerke, 1954; Silverthorn, 2007). The cross-bridge cycle repeats many times as each muscle fibre contracts (Huxley and Niedergerke, 1954; Silverthorn, 2007; Krans, 2010). The myosin heads continually bind and release actin molecules as myosin thrusts the thin filaments closer to the middle of the sarcomere (Huxley and Niedergerke, 1954; Silverthorn, 2007). The movement of the myosin molecules is caused by energy from ATP hydrolysis, which causes the high-energy phosphate bond to break and release energy (Silverthorn, 2007; Krans, 2010). Myosin is therefore a motor protein with the capacity to produce movement by means of

converting the chemical bond energy of ATP into the mechanical energy of motion for contraction (Silverthorn, 2007). Each myosin molecule is able to bind to ATP and hydrolyse it to adenosine diphosphate (ADP) and inorganic phosphate (Pi), thus releasing energy (Silverthorn, 2007). This energy is then stored as potential energy in the angle between the myosin head and the long axis of the myosin filament, so as to fuel the power stroke that moves actin (Silverthorn, 2007).

1.5 THE THIN FILAMENT

Striated muscle thin filaments extend from the Z line to the edge of the H zone (**Figure 1.3C&D**) (Huxley, 1953a). Vertebrate thin filaments are approximately 1µm long and 10nm wide and are located in the filament lattice between the thick filaments (**Figure 1.3E&F** and **Figure 1.4**) (Huxley, 1953a; Huxley, 1957). Thin filaments are composed of mostly actin which is a major cytoskeletal protein, found in practically all eukaryotic cells (Pollard, 1990). Actin is a 42kDa globular protein, often referred to as G actin (G=globular), that is able to self-associate and create a helical polymer called F actin (F=filamentous), consisting of about 360 molecules (**Figure 1.7A**) (Offer, 1974). The F-actin backbone is attached at regular intervals to the proteins troponin and tropomyosin, that play a role in the regulation of contraction (Zot and Potter, 1987; Solaro and Rarick, 1998; Gordon *et al.*, 2000) (**Figure 1.7B&C**) and the giant protein nebulin, spanning the complete length of the filament while functioning to determine its length (Gregorio *et al.*, 1999; Horowitz *et al.*, 1996; Wang and Wright, 1988).

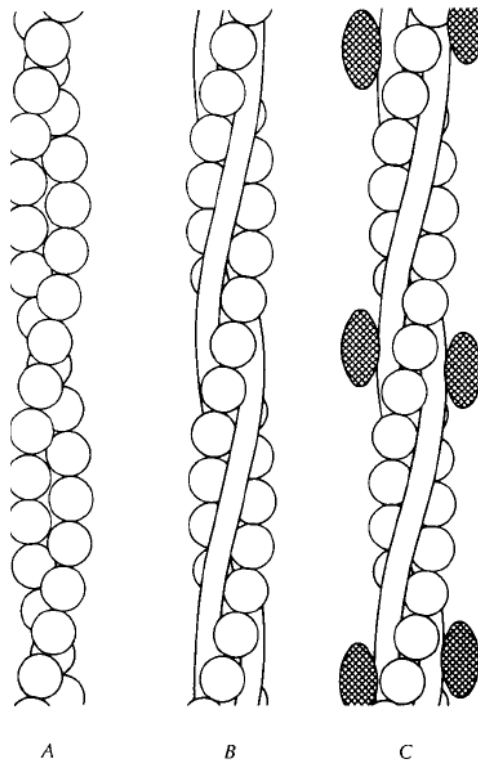


Figure 1.7. Schematic diagrams of the thin-filament structure. **(A)** F actin (actin subunits are drawn as spheres for simplicity). **(B)** F actin plus tropomyosin. **(C)** F actin-tropomyosin plus troponin. [Taken from Offer, 1974].

Troponin (Tn) and tropomyosin (Tm) are the most important thin filament components after actin and they are able to form a complex that is involved in the regulation of muscle contraction in response to calcium²⁺ (Ca²⁺) (Lehman *et al.*, 2009). Nebulin is found in the thin filaments and like titin, it is another giant myofibrillar protein which plays a role in sarcomeric length determination (Gregorio *et al.*, 1999; Horowitz *et al.*, 1996). The Z line contains, among other proteins, α -actinin which maintains the thin filaments in a systematic horizontal arrangement and connects sarcomeres into the linear grouping of the myofibril (Knöll *et al.*, 2002). Intermediate filaments and associated proteins function to attach the sarcomeres at the

M and Z lines and thus form crosswise links between the adjacent myofibrils, so as to maintain them in order with each other across the fibres (Craig and Padrón, 2004).

Troponin and tropomyosin are the main regulatory proteins in the sarcomere (Lehman *et al.*, 2009). These proteins both bind to actin and in so doing, regulate the actin and myosin interactions, thereby regulating sarcomeric contraction in response to changes in Ca^{2+} concentration (Lehman *et al.*, 2009).

The binding and dissociation of Ca^{2+} on troponin is coupled to the movement of tropomyosin on actin filaments (Solaro and Rarick, 1998), which regulates the contraction of muscles on a molecular level (Lehman *et al.*, 2009). Myosin cross-bridge dynamics and muscular contraction are therefore controlled by the fact that this process either blocks or exposes the myosin binding sites on actin (Lehman *et al.*, 2009).

According to Lehman *et al.*, 2009; troponin has two separate structural functions, namely: to function as an inhibitor in relaxed muscles when there is a low Ca^{2+} concentration and as a promoter to initiate contraction, in activated muscles when there is a high Ca^{2+} concentration (Lehman *et al.*, 2009). Changes in the sarcoplasmic free Ca^{2+} concentration and the subsequent binding or dissociation of Ca^{2+} from the troponin complex, switches contraction on or off in both cardiac and skeletal muscles (Lehman *et al.*, 2009).

Actin-myosin interaction is inhibited at low Ca^{2+} concentrations due to the myosin binding sites on actin being inaccessible (Lehman *et al.*, 2009). The myosin binding

is blocked because Ca^{2+} -free troponin has a bearing upon the elongated tropomyosin (Lehman *et al.*, 2009). Troponin's structural influence over tropomyosin at high Ca^{2+} concentrations is due to the Ca^{2+} -saturated troponin enabling the regulatory switching, by means of actively stimulating tropomyosin movement away from the blocking position (Lehman *et al.*, 2009).

1.5.1 The Z line

Interactions with a cytoskeletal lattice, the Z line; also referred to as the Z band/Z disk due to its predetermined thickness; are responsible for the noticeable uniformity of the thin filaments of sarcomeres (Knöll *et al.*, 2002). Z lines form the junction between one sarcomere and the next (**Figure 1.3B-D**) as they are found at the ends of the sarcomeres; this is also where the thin-filament polarity is reversed (Huxley, 1963). Z lines function as both connection points as well as mechanical links between thin filaments and between overlapping titin filaments from neighbouring sarcomeres (Knöll *et al.*, 2002). The transmission of force along the myofibril is therefore partially controlled by the Z lines (Vigoreaux, 1994). Attachment sites for intermediate filaments, forming lateral contacts with neighbouring myofibrils, are also found within the Z lines (Wang and Ramirez-Mitchell, 1983).

1.5.1.1 Composition of the Z line

The components of the Z line include: α -actinin, amorphin, FATZ (myozenin), Znin, Z protein, γ -filamin, ZASP, myotilin, myopodin and myopalladin; as well as sections of thin filaments overlaps: actin, CapZ and nebulin; the N-terminal ends of titin

filaments and telethonin (Vigoreaux, 1994; Stromer, 1995). The muscle-specific lin-11, islet-1 and mec-3 (LIM) protein (MLP) is also found in the Z line and MLP-deficient mice have been found to develop a severe form of dilated cardiomyopathy (DCM) (Knöll *et al.*, 2002). The muscle-specific ring finger (MURF) proteins are found at the Z line as well as the M line (Knöll *et al.*, 2002). MURF-3 deficient mice have been shown to possess a myopathic phenotype (Knöll *et al.*, 2002).

The main structural constituent of the Z line is α -actinin, which binds to several Z-line proteins and functions to cross-link anti-parallel actin filaments as well as anti-parallel titin filaments from neighbouring half sarcomeres (Knöll *et al.*, 2002). α -Actinin thus creates a ternary complex containing actin, titin and α -actinin (Young *et al.*, 1998).

In order to fully understand the structure and function of the Z-line, it is necessary to first discuss the protein titin.

1.5.2 Titin filaments

In addition to actin and myosin filaments, a third type of filaments is found in muscles (Trinick, 1991; Labeit and Kolmerer, 1995; Granzier and Labeit, 2007). This was discovered due to the integrity of sarcomeres being maintained when stretched beyond the actin-myosin overlap (Granzier and Labeit, 2007; Hudson *et al.*, 2011). The giant protein titin (also referred to as connectin) (Chung and Granzier, 2011; Nedrud *et al.*, 2011; Leinwand *et al.*, 2012), constitutes this set of filaments, separate from actin and myosin (Trinick, 1996; Gregorio *et al.*, 1999; Maruyama, 1999; Tskhovrebova and

Trinick, 2003; Lange *et al.*, 2005; Granzier and Labeit, 2007; Linke, 2008). Titin is the third most abundant protein found in muscles, after actin and myosin, making up approximately ten percent of myofibrillar mass (Gregorio *et al.*, 1999; Bang *et al.*, 2001b; Tskhovrebova and Trinick, 2003; Granzier and Labeit, 2007). Titin has been classified as a member of the intracellular immunoglobulin superfamily (Nave *et al.*, 1989; Labeit *et al.*, 1992; Soteriou *et al.*, 1993; Vinkemeier *et al.*, 1993; Labeit and Kolmerer, 1995; Tskhovrebova and Trinick, 2003; Linke, 2008).

Titin has two major functions in muscles; namely to supply a template for the exact organization of myofibrillar proteins during muscle development and to play a role as a molecular spring that is in charge of important aspects of mechanical stress sensing (Gautel, 2011) behaviour of muscles (Trinick and Tskhovrebova, 1999; Hudson *et al.*, 2011; Krüger and Linke, 2011; Stahl *et al.*, 2011 Anderson and Granzier, 2012; Leinwand *et al.*, 2012). Titin is thus often referred to as a protein ruler (Horowitz *et al.*, 1986; Trinick, 1994; Gautel and Goulding, 1996; Trinick and Tskhovrebova, 1999; Gautel, 2011; Leinwand *et al.*, 2012) and an entropic bi-directional spring (Cazorla *et al.*, 2000; Freiburg *et al.*, 2000; Linke, 2000; Chung and Granzier, 2011). Titin thus provides muscles with passive elastic properties (King *et al.*, 2010; Chung and Granzier, 2011; Nedrud *et al.*, 2011; Czajlik *et al.*, 2012), maintaining sarcomeric integrity and filament alignment in active and relaxed states (Granzier and Labeit, 2007; Leinwand *et al.*, 2012), so that they are not able to over-stretch, like the tension in a spring (Hudson *et al.*, 2011; Irving *et al.*, 2001 Anderson and Granzier, 2012).

1.5.2.1 Molecular structure, interactions and organization of titin filaments

Titin, the largest known polypeptide in humans, is a 3-4.2MDa (Granzier and Labeit, 2007; Czajlik *et al.*, 2012) single polypeptide chain consisting of about 38138 residues (Krüger and Linke, 2011; Leinwand *et al.*, 2012). Titin molecules are extremely long (approximately 1 μ m) (Nowak, 2012), thin (4nm in diameter) and are also very flexible (Means, 1998; Tskhovrebova and Trinick, 2003; Linke, 2008; Tskhovrebova and Trinick, 2010). Mammalian genomes have been shown to only contain a single titin gene (Mateja *et al.*, 2012) and in humans the titin gene has 363 exons (Granzier and Labeit, 2007; Krüger and Linke, 2011; Leinwand *et al.*, 2012; Nowak, 2012). Each titin molecule extends along the full length of a half-sarcomere, from the Z line (209kDa N-terminal region) all the way to the M line (250kDa globular C-terminal region) (**Figure 1.5**) (Fürst *et al.*, 1988; Fürst *et al.*, 1989; Nave *et al.*, 1989; Labeit *et al.*, 1992; Labeit and Kolmerer, 1995; Young *et al.*, 1998; Satoh *et al.*, 1999; Tskhovrebova and Trinick, 2003; Lange *et al.*, 2005; Granzier and Labeit, 2007; Linke, 2008; Tskhovrebova and Trinick, 2010; Chung and Granzier, 2011; Hudson *et al.*, 2011; Anderson and Granzier, 2012; Czajlik *et al.*, 2012; Leinwand *et al.*, 2012).

The N-terminal end of titin starts in the Z line (Granzier and Labeit, 2007; Tskhovrebova and Trinick, 2010) and was initially considered to be a separate protein, called zeugmatin (Turnacioglu *et al.*, 1997). Titin has been shown to interact in the Z line with a 19kDa protein called telethonin or titin cap (T-cap) (Gregorio *et al.*, 1998; Granzier and Labeit, 2007) which has been implicated in limb-girdle muscular dystrophy type 2G (Moreira *et al.*, 2000).

The middle section of titin is a 0.7 to 1.5MDa isoform dependent elastic region, with the shorter isoforms being less elastic (Mateja *et al.*, 2012), that passes through the I band parallel to the thin filaments (Gregorio *et al.*, 1998). The 2MDa C-terminal end of titin constitutes a part of the thick filament, binding to myosin and myosin binding protein C (MyBPC), concluding in the M line (Gregorio *et al.*, 1998; Stahl *et al.*, 2011). Each titin polypeptide overlaps with the titin polypeptides from the next half sarcomere at the Z and M lines, forming an uninterrupted arrangement of filaments right through the entire myofibril (Gregorio *et al.*, 1998). The binding of various myofibrillar proteins to specific titin domains implies that titin functions as a molecular outline during sarcomeric assembly due to specifying the particular arrangement of its ligands within each half sarcomere (**Figure 1.8**) (Fürst *et al.*, 1999).

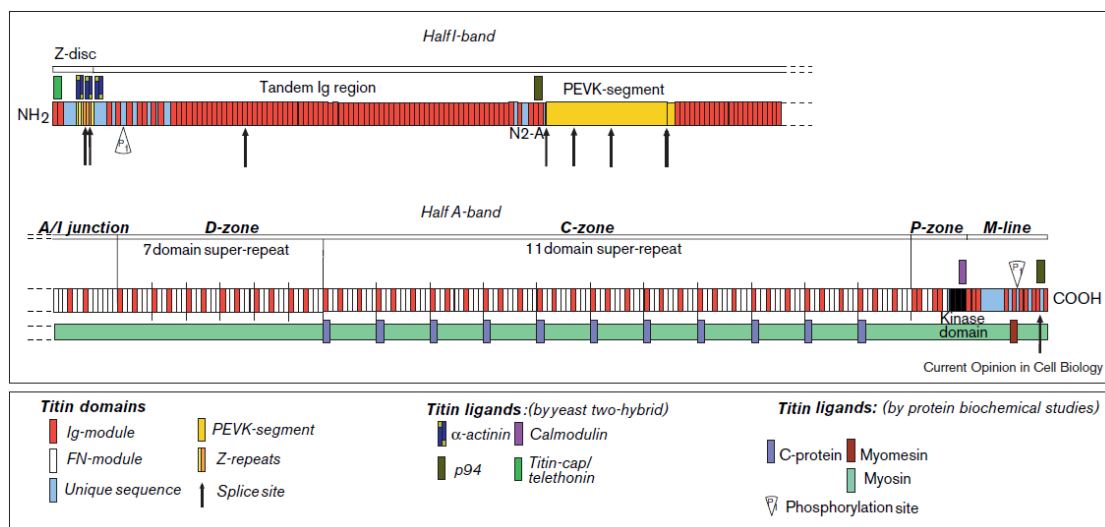


Figure 1.8. Molecular structure of the titin filament as well as the location of alternative splicing sites that result in different titin isoforms. Block above the corresponding titin domains indicate ligands that have been identified by yeast two-hybrid studies; while blocks below indicate putative titin ligands identified by *in vitro* studies using expressed domains. The modular structure of titin in relation to

the upper: Z line (Z repeats) and I band (tandem Ig repeats and PEVK segment); and the lower: myosin filament in the A band (Ig/Fn super-repeats – note the positions of non-myosin proteins on the myosin filament) and M line. [Taken and adapted from Gregorio *et al.*, 1999].

Titin is similar to other myosin-binding proteins because it has a modular structure comprising mostly (about 90 percent) of immunoglobulin-like (Ig) and fibronectin-like (Fn) domains (Tskhovrebova and Trinick, 2010; Czajlik *et al.*, 2012). Alternative splicing (Hudson *et al.*, 2011) of titin's mRNA as well as post-translational modifications causes these modules to be expressed in various arrangements in different muscle types; forming tissue-specific I-band titin isoforms (Leinwand *et al.*, 2012; Mateja *et al.*, 2012), with sizes from approximately 600kDa to 3.7MDa (Labeit *et al.*, 1997; Freiburg *et al.*, 2000; Bang *et al.*, 2001b; Tskhovrebova and Trinick, 2003; Tskhovrebova and Trinick, 2010; Hudson *et al.*, 2011; Anderson and Granzier, 2012).

However, titin also has a unique domain abundant in proline (P), glutamate (E), valine (V) and lysine (K) which is referred to as the PEVK domain (**Figure 1.8**) (Fürst and Gautel, 1995; Labeit and Kolmerer, 1995; Labeit *et al.*, 1997; Granzier and Labeit, 2007; LeWinter *et al.*, 2007; Anderson and Granzier, 2012; Mateja *et al.*, 2012). Cardiac PEVK titin has mechanical conformations of differing flexibility and functions as an entropic spring element (Linke *et al.*, 2002; Anderson and Granzier, 2012). This PEVK domain of titin has been shown by Linke *et al.*, 2002 to interact with actin filaments, therefore causing a slowing of sliding velocity of the actin filaments over myosin (Linke *et al.*, 2002). Titin's PEVK domain is dependent upon

Ca^{2+} concentration in cardiac muscles and contributes to the contractile properties as well as the extensibility of the sarcomeres (Linke *et al.*, 2002).

The tandem Ig domains as well as PEVK-rich sequences within the I-band region are responsible for the titin filaments' extensibility and elastic properties (Labeit *et al.*, 1997; Horowitz, 1999; Linke *et al.*, 1999; Hudson *et al.*, 2011). Muscle-specific alternative splicing also causes the length of PEVK titin to differ between 163 and 2200 residues (Kolmerer *et al.*, 1999) resulting in different mechanical properties for different striated muscle types (Labeit *et al.*, 1997).

The I-band region of titin (**Figure 1.8**) is responsible for the passive tension that is generated when a myofibril is stretched because it consists of spring-like (Ig) extensible elements that give rise to the variable degree of myofibril stiffness (LeWinter *et al.*, 2007; Anderson and Granzier, 2012). This passive tension plays a role in the diastolic filling of the heart and alterations in titin's extensibility have been shown to be associated with diastolic dysfunction as well as cardiac disease (Hudson *et al.*, 2011; Anderson and Granzier, 2012).

The Fn domains are only found within the A band and are arranged along with Ig domains into super-repeat patterns (**Figure 1.9**) (Gregorio *et al.*, 1999; Bennett *et al.*, 1999; Kolmerer *et al.*, 1999). Two separate blocks of Ig repeats are found in the I-band region, separated by the variable-length PEVK domain (Tskhovrebova and Trinick, 2010). The fact that this variation in titin isoforms is only found in the I-band region, results in titin molecules with varying elastic properties (Cazorla *et al.*, 2000; Freiburg *et al.*, 2000; Bang *et al.*, 2001b; Linke, 2008). This means that the titin

isoforms with additional Ig repeats are more elastic than those isoforms with fewer repeats.

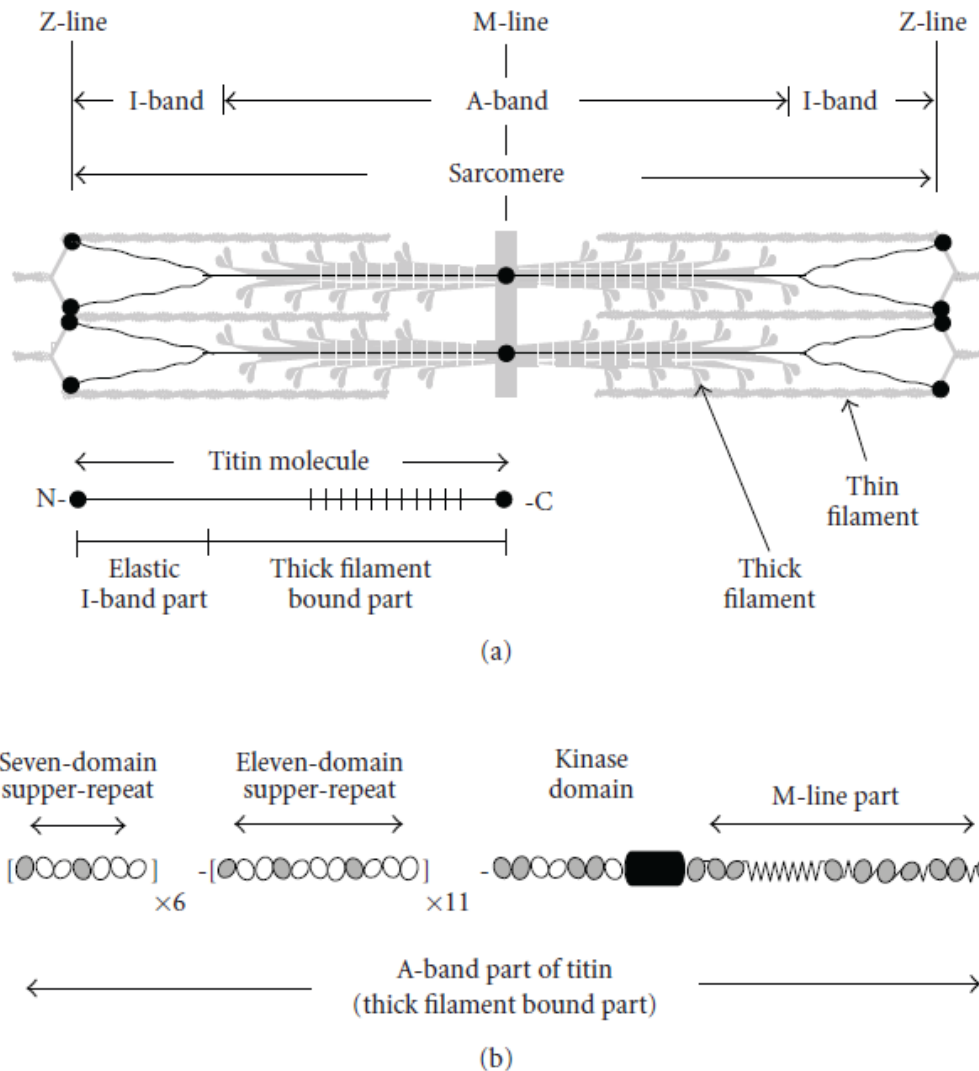


Figure 1.9. Schematic representation of titin's arrangement within the sarcomere. (a) Striated zones in the sarcomere and the titin molecule indicate the position of the large super-repeat. (b) The domain periodicity in the thick filament bound, A-band part of titin. [Taken and adapted from Tskhovrebova and Trinick, 2010].

Titin has two repeat regions (**Figure 1.9**) (Tskhovrebova and Trinick, 2010). Titin is attached to the thick filaments within the A-band, forming a large 11 super-repetitive

pattern in the domain structure (Czajlik *et al.*, 2012). This large super-repeat constitutes almost half of each titin molecule as it also occurs 11 times in the molecule (Czajlik *et al.*, 2012). The 11 repeat region (**Figure 1.9**) forms a pattern of Fn- and Ig-like domains: Ig, 2x Fn, Ig, 3x Fn, Ig, and 3x Fn that can be found in the MyBPC region of the A band (Gregorio *et al.*, 1999). The repeats are approximately 43nm long, with each domain having a length of 4 to 4.5nm (Gregorio *et al.*, 1999). Each one of the 11 repeats has multiple domains that are able to bind to the myosin tail as well as MyBPC (Gregorio *et al.*, 1999). The second repeat region is titin's seven repeat region (**Figure 1.9**), which comprises of five Fn3 and two Ig domains; where the myosin-binding proteins are missing towards the end of the A band (Tskhovrebova and Trinick, 2010). This seven repeat region is, in turn, repeated six times (Krüger and Linke, 2011).

1.5.2.2 Function of titin in myofibrillogenesis

Titin is one of the initial myofibrillar proteins to that assembles in the embryonic myofibril and it extends along the full length of the half sarcomere where it is able to interact with an assortment of sarcomeric proteins at precise locations; as well as anti-parallel connections with bordering titin molecules in the M and Z lines (Gautel *et al.*, 1999).

Correct sarcomere formation in both cardiac and skeletal muscles is dependent upon the interaction of a number of proteins, including titin, at the right time and place (Wang *et al.*, 1998). If any of these interactions are disturbed, then there could be interference in sarcomerogenesis because titin's assembly into the sarcomere would

thus be disrupted (Wang *et al.*, 1998). Turnacioglu *et al.* demonstrated in 1997 that the overexpression of N-terminal titin in cultured chicken cardiomyocytes and myotubes caused the disassembly of the myofibrils by means of interfering with titin's interaction with α -actinin (Turnacioglu *et al.*, 1997).

The section of titin found within the M-line (**Figure 1.14D-F**) consists of the C-terminal region which is the site of the catalytically active kinase domain; speculated to play a role in sarcomerogenesis and mechanotransduction (Labeit and Kolmerer, 1995; Leinwand *et al.*, 2012). M-line titin's main functions are to take part in thick filament assembly, M-band formation as well as maturation of other sections of the sarcomere within cardiac cells (Musa *et al.*, 2006). Titin's role in thick filament assembly is further supported by the fact that myosin interacts with its large super-repeats (Czajlik *et al.*, 2012; Kaiser *et al.*, 2012). The kinase domain also involves titin in protein turnover and signalling pathways (Granzier and Labeit, 2004).

The A-band region of titin (**Figure 1.8**) is approximately 2MDa in size and is suggested to play a role as a template for specific assembly and precise length of thick filaments (Lange *et al.*, 2006). The quick and efficient contraction and relaxation of striated muscles is due to the specific organization of the sarcomere, orchestrated by titin (Wang *et al.*, 1998).

Regulatory kinases phosphorylate titin domains within the Z line and T-cap/telethonin in the Z line can be phosphorylated by a serine/threonine kinase domain in the M-line area (Mayans *et al.*, 1998; Krüger and Linke, 2011). Therefore, during myofibril

assembly, developmental regulatory signals could potentially be relayed between the M and Z ends of titin (Gregorio *et al.*, 1999; Labeit *et al.*, 1997; Gautel *et al.*, 1999).

1.5.2.3 Mechanical function of titin

The different titin isoforms are responsible for passive tension and slack length of muscles at rest; fibres containing larger titin isoforms are able to develop passive tension at longer sarcomeric lengths, whilst smaller titin isoforms like those found in cardiac muscles, have an increased resting tension (Horowitz, 1999). In the event of skeletal muscle being stretched beyond its slack length, the Ig domain is initially straightened without much coupled force and with no unfolding of the individual Ig units (**Figure 1.10A**) (Horowitz, 1999). Any additional stretching then causes the PEVK domain to unravel, which demands a substantial force and creates considerable levels of passive tension (Horowitz, 1999). Unfolding of individual Ig domains is possible in exceedingly stretched sarcomeres, but it is unlikely to take place at physiological lengths (Linke *et al.*, 1999; Horowitz, 1999). The elevated levels of passive tension created at elongated muscle lengths may help to prevent damage that could occur during excessive muscle stretching (Horowitz, 1999).

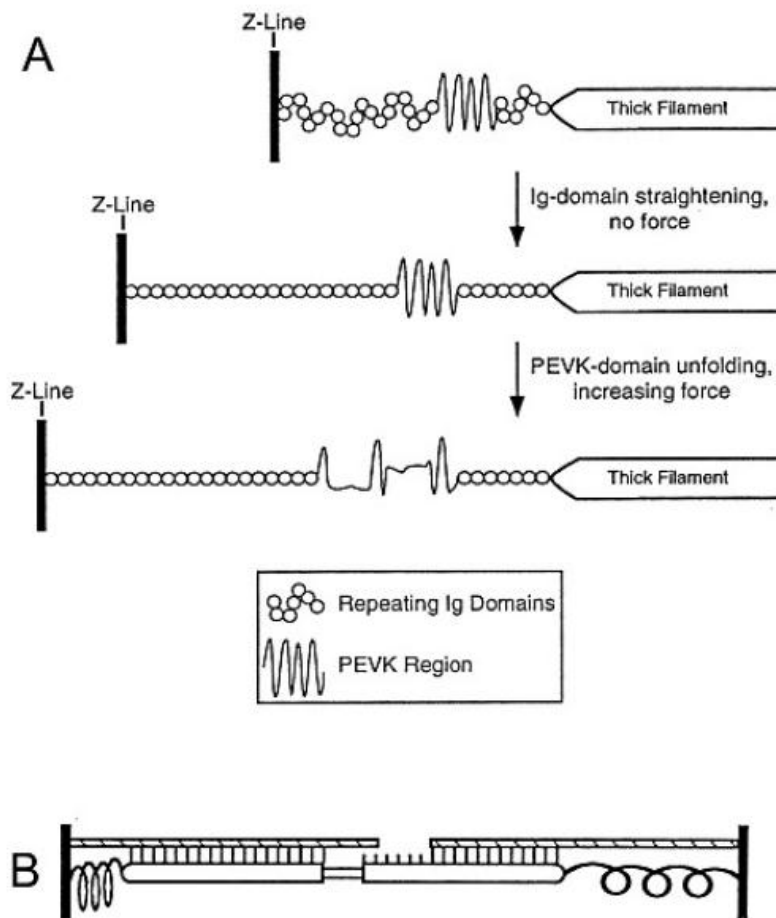


Figure 1.10. Models of titin's functioning. (A) When a slack sarcomere is stretched, domains containing tandem Ig modules are straightened first, with a minimal increase in tension. Further extension leads to unfolding of the PEVK domain, with tension increasing exponentially. (B) A model indicating how the stretch of titin (stretched spring on right) in an unequally contracted sarcomere, will tend to re-centre the thick filaments. [Taken from Horowitz, 1999].

Titin maintains the axial ordering of the filaments within the sarcomere which is vital for the fast and proficient generation of active tension during contraction (Horowitz, 1999). If the thick filaments were to become uncentred at some stage during prolonged contraction, a drop in tension would occur; thus titin functions to prevent

this (**Figure 1.10B**) (Horowitz, 1999). The most important organizational role of titin *in vivo* is therefore to keep the thick filaments centred during passive stretch and to avoid sarcomere asymmetry from accumulating over a period of several contractions, by recentring the thick filaments during muscle relaxation (Horowitz, 1999; Leinwand *et al.*, 2012).

1.5.3 Model of the Z line

Studies of the sequences, interactions and antibody labelling patterns of Z-line components have helped to elucidate the Z-line structure (**Figure 1.11B**) (Gautel *et al.*, 1996; Gautel *et al.*, 1999; Gregorio *et al.*, 1998; Gregorio *et al.*, 1999; Young *et al.*, 1998). The 30kDa N-terminals of titin molecules overlap at the edges of the Z lines in the neighbouring sarcomeres - where the first two titin Ig repeats (Z1 and Z2) bind to telethonin (titin was discussed in detail in **Section 1.5.2**) (Mayans *et al.*, 1998; Krüger and Linke, 2011). The next 60kDa of titin spans the Z line and contains up to seven copies of a 45-residue “Z repeat” which is able to bind to the carboxy terminus of α -actinin (Luther and Squire, 2002). α -Actinin could therefore play a role in cross-linking both actin filaments as well as anti-parallel titin filaments in the Z line (Wang *et al.*, 1998). Alternative splicing of the 45-residue Z repeats takes place in the central Z-line region of titin (Krüger and Linke, 2011). Varying lengths of titin’s N-terminal overlap and the number of α -actinin binding sites that cross-link the titin molecules to thin filaments could function to determine the Z-line’s width and internal arrangement (Craig and Padrón, 2004; Voelkel and Linke, 2011). Titin’s N-terminal region could be implicated in controlling fibril assembly due to the fact that sections

of Z-line titin and telethonin are phosphorylated by regulatory kinases (Craig and Padrón, 2004; Voelkel and Linke, 2011).

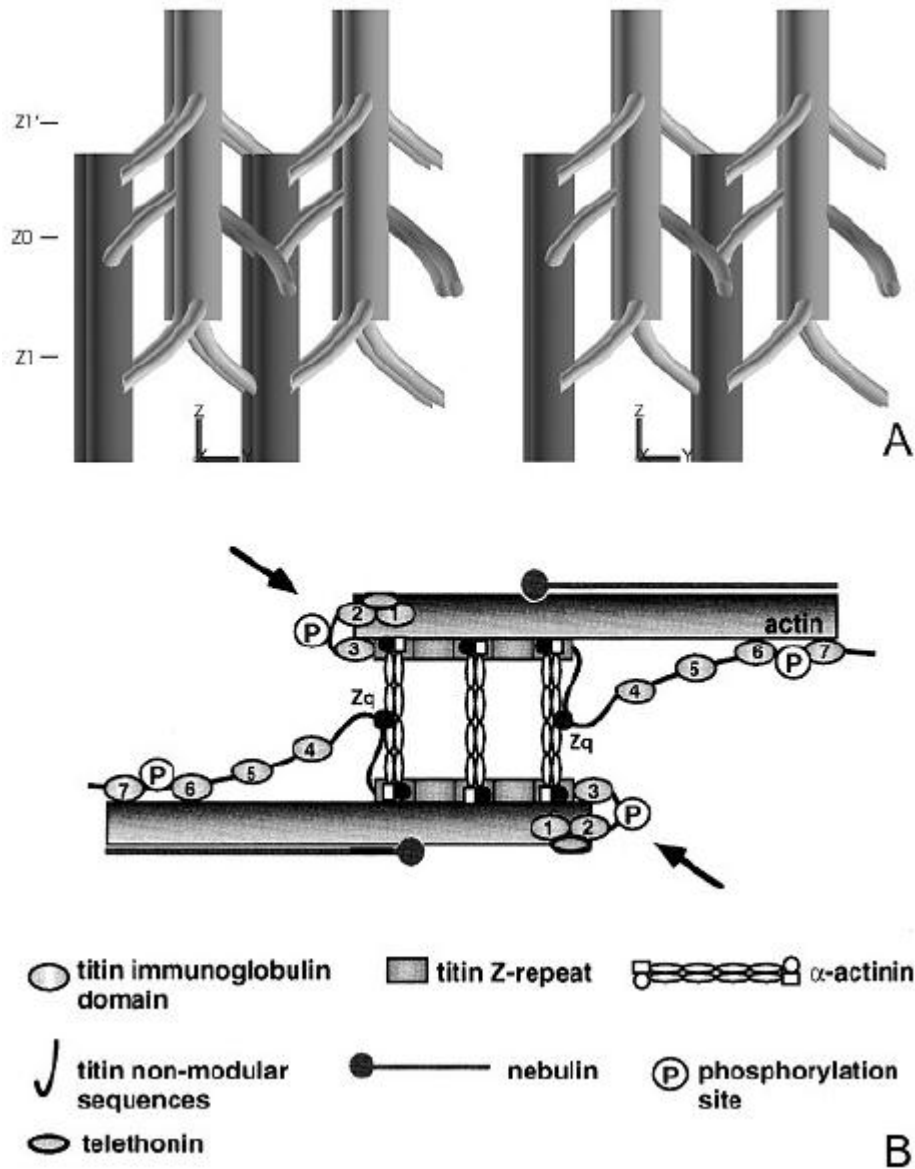


Figure 1.11. Models of the Z-line's structure. (A) Stereo view based on 3D reconstruction from tilted sections of intermediate-width Z lines. Actin filaments organized vertically overlap in the Z line and are connected there by obliquely oriented filaments; most likely mainly α -actinin. [Taken from Luther, 2000]. (B) Schematic diagram of proposed actin, α -actinin, titin, nebulin and telethonin

organization; established from sequence and immunoelectron microscopic data. [Taken from Gautel *et al.*, 1999].

The C-terminal, SH3-containing domain of nebulin allows it to insert into the periphery of the Z line (Millevoi *et al.*, 1998), which binds to α -actinin by way of myopalladin (Bang *et al.*, 2001a). Nebulin terminating at the boundary of the Z line determines where tropomyosin's actin binding ends and therefore where the binding of α -actinin, which competes with tropomyosin, is enabled (Craig and Padrón, 2004).

Nebulin is a large filamentous protein that extends the full length of the thin filament (Witt *et al.*, 2006). It is responsible for the regulation of the assembly and lengths of the thin filaments (McElhinny *et al.*, 2005). The contractility of the thin filaments as well as the Z disk structure is also regulated by nebulin (Witt *et al.*, 2006). Myopalladin functions in the assembly of the Z disk and I band proteins (Bang *et al.*, 2001a). It is responsible for linking nebulin and nebulin to α -actinin within the Z lines (Bang *et al.*, 2001a).

1.6 INTERMEDIATE FILAMENTS

A lattice of intermediate filaments 10nm in width attaches to the outside edge of the sarcomere and serves to arrange the structure of the muscle cell at a level beyond each individual sarcomere (**Figure 1.12**) (Wang and Ramirez-Mitchell, 1983). The intermediate filaments function to strengthen and hold the structure of each muscle cell together by means of the formation of crosswise connections between neighbouring myofibrils; which is due to their attachment to the SR or T-tubule

membranes, thus maintaining the membranes in order with each other across the muscle fibre and linking myofibrils to the sarcolemma and nucleus (Carlsson and Thornell, 2001; Nunzi and Franzini-Armstrong, 1981; Stromer, 1990; Stromer, 1995; Wang and Ramirez-Mitchell, 1983).

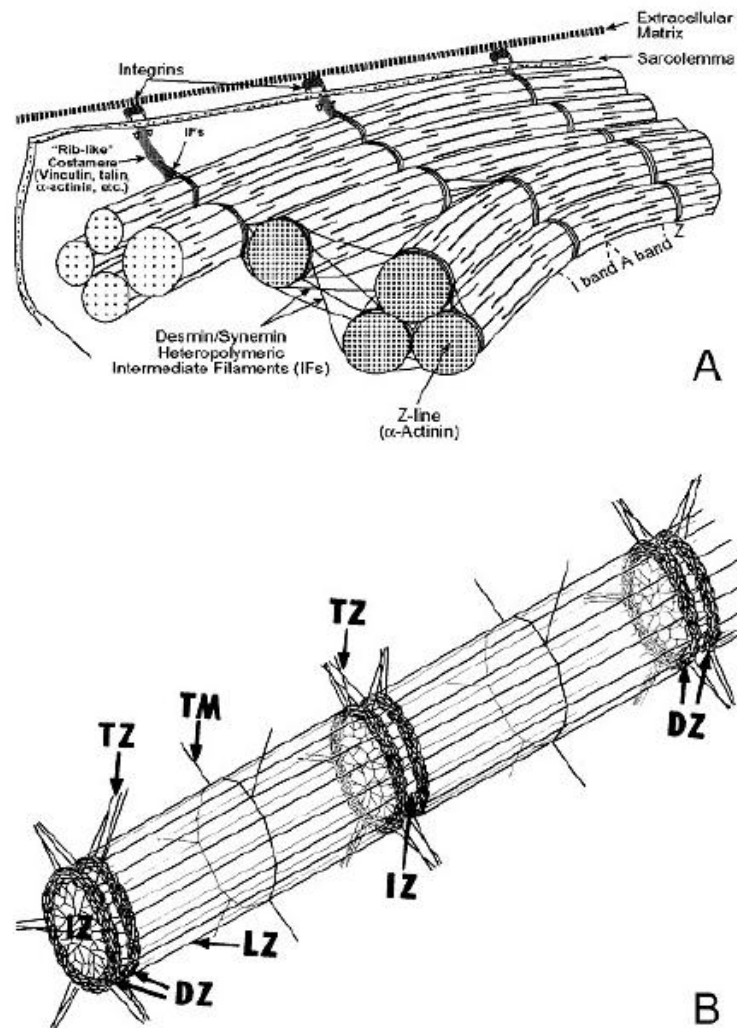


Figure 1.12. Schematic diagrams indicating the intermediate filaments. (A) Intermediate filaments encircling sarcomeres at the Z line and connecting to other sarcomeres as well as to the cell membrane. [Taken from Bellin *et al.*, 2001] (B) Intermediate filaments encircling and extending from the Z line (TZ) and M line (TM) as well as extending longitudinally from Z line to Z line (LZ). [Taken from Wang and Ramirez-Mitchell, 1983].

Desmin is the muscle-specific member of the intermediate filament family and constitutes the main component in mature muscles (Parry, 1999; Herrmann and Aebi, 2000). During development, vimentin is expressed and it coexists with desmin within the same filaments, however, it is not present in mature muscles (Parry, 1999; Herrmann and Aebi, 2000). Synemin, paranemin and nestin also associate with desmin filaments, but in lesser amounts; while plectin, an intermediate-filament-associated protein, is able to create contacts between the intermediate filaments and other cellular structures (Herrmann and Aebi, 2000).

Syncoilin is an extremely soluble 64kDa intermediate filament protein located within the neuromuscular junction, the sarcolemma and the Z line; it is able to bind to desmin as well as to the dystrophin protein complex, but does not form filaments (Poon *et al.*, 2002).

Skelemin is an approximately 200kDa protein and is encoded by the same gene as myomesin - it is considered a splice variant and contains two motifs that are intermediate-filament-like (**Section 1.7**) (Price and Gomer, 1993; Steiner *et al.*, 1999). Skelemin is able to form rings around the outside edge of the M line and connects these rings in neighbouring myofibrils (Price and Gomer, 1993). Myosin filaments, at the border of the sarcomere, could thus be connected to the intermediate filament cytoskeleton by means of skelemin's myosin-binding ability and its putative intermediate filament core-like motifs (Price and Gomer, 1993). Peripheral myofibrils could also be linked to the cell membrane at the M line because skelemin interacts with the cytoplasmic domain of sarcolemmal integrin molecules (Reddy *et al.*, 1998).

1.7 THE THICK FILAMENT

The thick filaments of muscle fibres are bipolar, spindle-shaped structures, 1.6 μ m long and approximately 15nm wide (Huxley, 1963). The cross-bridges cause thick filaments to have a rough appearance along most of their length due to them protruding, except for a central bare zone (**Figure 1.3C**) (Huxley, 1963).

The thick filaments also consist of non-myosin proteins: myosin-binding proteins C, H, and X (found in the middle third of each half of the thick filaments) (Craig and Padrón, 2004); myomesin, M protein and creatine kinase (found within the M line) (Wang *et al.*, 1998). Titin is also found to be associated along the length of the thick filaments, but it continues past the thick filaments through the I band to the Z line (Craig and Padrón, 2004). Titin is a giant elastic protein that maintains the A band in a centred position and makes sure that identical forces develop in the two halves of the A band (**Section 1.5.2**) (Craig and Padrón, 2004). During muscle development, titin appears to act as a molecular template to define the exact length and organization of myosin filaments (**Section 1.5.2**) (Craig and Padrón, 2004).

1.7.1 The M line

1.7.1.1 Structure of the M line

The sarcomeric filaments display a noticeable uniformity due to interactions with a cytoskeletal lattice, which is responsible for holding them in order (Fürst *et al.*, 1999). The M line forms this lattice structure in the thick filaments (**Figure 1.3**) (Huxley,

1953a). It is an approximately 80nm crosswise band found at the centre of the A band and consists of protein bridges that link the thick filaments to each of their six neighbours (**Figure 1.13**) (Luther and Squire, 1978). Intermediate filaments also connect at the M line and run diagonally; thus connecting adjacent myofibrils to each other (Craig and Padrón, 2004). In longitudinal sections of muscle, the M line is seen as an electron-dense band with other fine structures of three to five thin, densely stained lines approximately 20nm apart (**Figure 1.3C**) (Huxley, 1953a). The central line is termed M1, the strong lines 22nm on each side of M1 are known as M4 and M4' (**Figure 1.14C**) and the extra lines found in some M lines a further 22nm out are called the M6 and M6' lines (Sjoström and Squire, 1977).

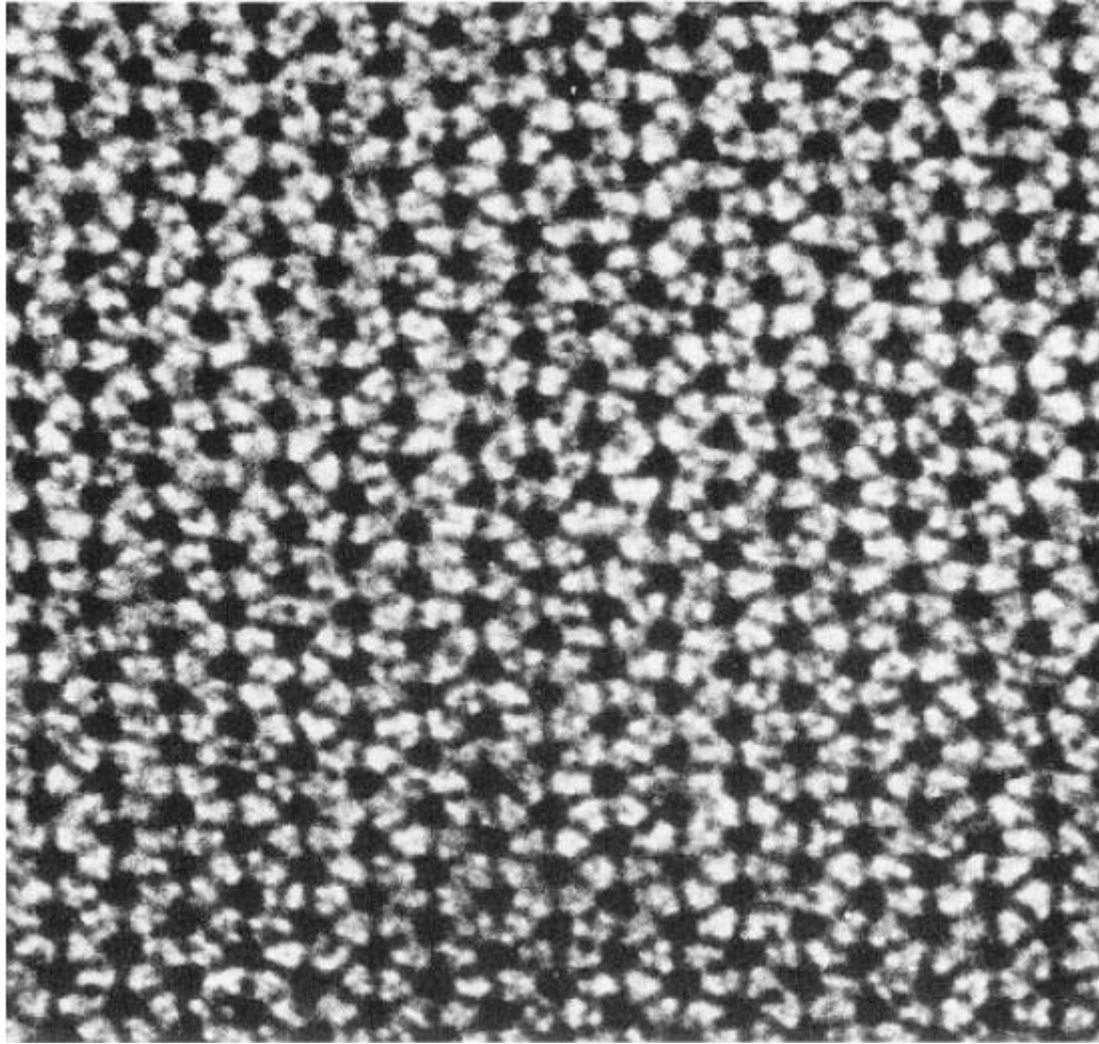


Figure 1.13. Transverse section of muscle in the M-line region ($\times 125000$). The big dark circles indicate the thick filaments and the dark lines indicate protein bridges that link the thick filaments to each of their six neighbours. [Taken from Luther and Squire, 1978].

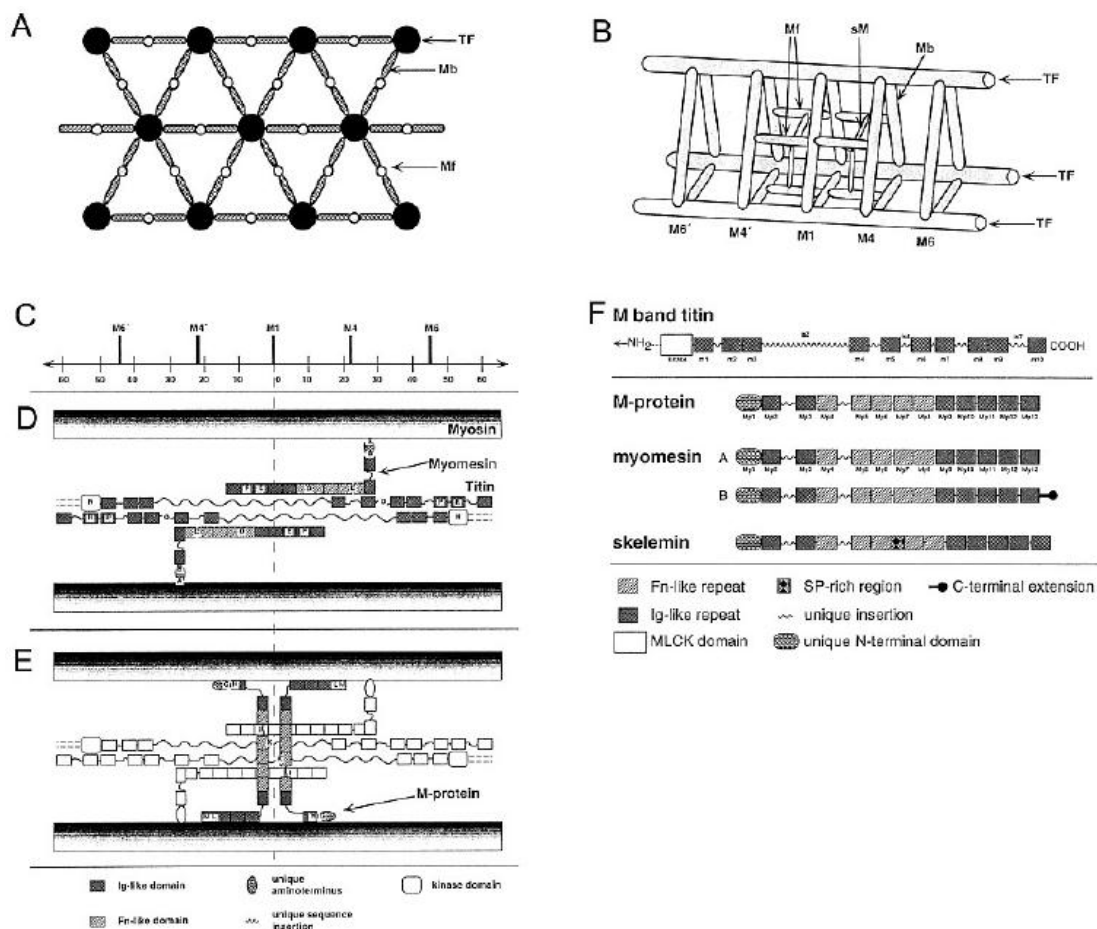


Figure 1.14. M-line models. **(A)** Transverse view at the M4 level indicating thick filaments (TF), M bridges (Mb) and M filaments (Mf). **(B)** Proposed 3D model based on electron microscopy; sM = secondary M bridges. **(C)** M-line nomenclature and scale in nanometres. **(D&E)** Suggested arrangement of titin, myomesin and M protein based on immune-electron microscopic observations. **(F)** The domain structures of M-line titin, M protein, myomesin and skelemin. [Taken from Fürst *et al.*, 1999].

The structure of the M line differs between fibre types, with fast (type II) fibres having three lines (M1, M4 and M4') and slow (type I) fibres showing four definite lines (M4, M4', M6 and M6'; with M1 being missing), whilst intermediate-speed fibres have all five lines present (Fürst *et al.*, 1999). The fact that M4 and M4' are

constantly present in all muscles, indicates that bridges in these locations are important in maintaining the integrity of the A band (Pask *et al.*, 1994).

1.7.1.2 Protein components and interactions of the M line

According to Fürst *et al.*, 1999, the M line consists of three main M line specific proteins; namely creatine kinase, M protein and myomesin; as well as overlapping sections of myosin tails, the C terminal end of titin and skelemin, which is a peripheral component that could play a role in linking M lines to the intermediate filaments (Fürst *et al.*, 1999).

Creatine kinase is a dimeric globular protein comprising two 43kDa subunits (Fürst *et al.*, 1999). Its function is to buffer cellular ATP and ADP concentrations by means of catalysing the reversible exchange of high-energy phosphate bonds between phosphocreatine and ADP, thus regenerating ATP from ADP that was formed during muscular contraction (Kushmerick, 1998).

M protein and myomesin are modular proteins containing mainly immunoglobulin-like (Ig) and fibronectin type (Fn) domains, similar to those found in MyBPC and titin (**Figure 1.14F**) (Fürst *et al.*, 1999). M protein and myomesin consist of the same core domain organizations and have more than 50 percent of the same residues; with only their C- and N-terminal regions differing (Fürst *et al.*, 1999). M protein is only found in cardiac and fast skeletal fibres (Eppenberger *et al.*, 1981) and is a flexible approximately 165kDa monomer that is 36nm long and 4nm wide (Masaki and Takaiti, 1974; Trinick and Lowey, 1977). Myomesin is found in both

fast and slow fibres and it is a flexible, segmented rod of 185kDa that is 50nm long and 4nm wide (Grove *et al.*, 1984). The N-terminal region of myomesin binds to light meromyosin (LMM), while its central section interacts with the C-terminus of titin (Obermann *et al.*, 1996). Both M protein and myomesin function to maintain the three-dimensional structure of neighbouring myosin filaments within the A band by binding to myosin and titin, thus providing the insertion sites for titin filaments (Wang *et al.*, 1998) They therefore link titin molecules to the thick filaments (Wang *et al.*, 1998). Wang and co-workers showed in 1998 that if M protein or myomesin are not expressed, then the assembly of titin into the sarcomere is disrupted (Wang *et al.*, 1998). Wang *et al.*, 1998 further stated that since titin is inserted into both the M line as well as the Z line, a disruption within the M line would cause titin disorganisation throughout the sarcomere (Wang *et al.*, 1998).

Skelemin consists of Fn and Ig domains in the same order as in M protein and myomesin and is a splice variant encoded by the same gene as myomesin (Fürst *et al.*, 1999; Steiner *et al.*, 1999). However, skelemin also has two different motifs that differentiate it from M protein and myomesin (Price and Gomer, 1993).

Obscurin is an 800kDa sarcomeric protein that resembles titin and has a modular design comprising of Ig- and Fn-like domains (Young *et al.*, 2001). It has a section similar to the elastic region of titin and its C-terminal end has sequences that could indicate a function in signal transduction; whilst some of its domains interact with the N-terminus Z line section of titin (Granzier and Labeit, 2007).

1.7.2 Model of the M line

Creatine kinase has been shown to play a role in the M4 bridges; while titin molecules cross the middle of the A band at the M line (bare zone region) and go a further 60nm into the adjacent half sarcomere, therefore forming an anti-parallel overlap region of 120nm (about the length of the bare zone) where they interact with each other (Fürst *et al.*, 1999). Myomesin molecules from the two halves of the M line are found parallel to the thick filament and titin and bind to titin in this area, while also forming an overlap region with myomesin molecules of differing polarity from the other half of the sarcomere (**Figure 1.14B,D&E**) (Fürst *et al.*, 1999). Myomesin has a perpendicular bend near its N-terminal end and extends in the direction of the bordering thick-filament, where it then binds to myosin (**Figure 1.14D**) (Fürst *et al.*, 1999). The C- and N-terminal ends of M protein are able to bind to the surfaces of adjoining myosin filaments while the middle section is perpendicular to the thick filaments, thus creating M1 bridges and reinforcing the links between thick filaments (**Figure 1.14E**) (Fürst *et al.*, 1999).

1.7.3 Function of the M line

The M line stabilizes the crosswise and longitudinal structure of the thick filament lattice by connecting adjoining filaments to each other, which is important for the fast and efficient contraction of the sarcomeres (**Figure 1.3C**) (Huxley, 1953a). During muscle shortening, the inter-filament distance can increase by up to 7nm (Elliott *et al.*, 1963) when a change in the conformation of an actin-myosin head complex (cross-bridge) takes place (Takezawa *et al.*, 1998).

The M line plays both a structural and enzymatic role (Fürst *et al.*, 1999). The M line is involved in sarcomeric assembly and turnover and the phosphorylation of a particular serine residue (Ser-482) found on M protein and myomesin causes the inhibition of their binding to myosin and titin, respectively (Fürst *et al.*, 1999; Kontrogianni-Konstantopoulos *et al.*, 2004).

Mutations found in titin have been shown to cause hypertrophic cardiomyopathy (HCM) which is a disease in which one of the primary features is left ventricular hypertrophy (Frey *et al.*, 2012).

1.8 LEFT VENTRICULAR HYPERTROPHY

Left ventricular hypertrophy (LVH) occurs when the cardiomyocytes in the left ventricle face a haemodynamic pressure overload, need to compensate and thus become enlarged by increasing in mass (Lorell and Carabello, 2000; Hudson *et al.*, 2011). This can either be attributed to a normal physiological response to exercise (Colan *et al.*, 1985; Hart, 2003; Rawlins *et al.*, 2009) or can be the result of a maladaptive process or disease state, such as chronic hypertension (elevated blood pressure) (Frey and Olson, 2003; Taylor *et al.*, 2011).

The enlargement occurs as a result of the hypertrophy (increase in size) of the existing myocytes, as opposed to hyperplasia (increase in number), due to the fact that myocytes are terminally differentiated shortly after birth (Lorell and Carabello, 2000). The hypertrophy only becomes pathological when it fails to regress, as is seen in the disease hypertrophic cardiomyopathy (HCM). Left ventricular hypertrophy is

recognised as a major risk factor for cardiovascular morbidity and mortality (Lorell and Carabello, 2000). Studies have shown that LVH is a strong predictor of sudden cardiac death (SCD) (Haider *et al.*, 1998; Lorell and Carabello, 2000), coronary heart disease (Devereux and Roman, 1993), congestive heart failure (HF), cardiac arrhythmias and stroke (Verdecchia *et al.*, 2001).

A better clinical prognosis (Verdecchia *et al.*, 1998) and higher life expectancy (Sharp and Mayet, 2002) is associated with a regression of LVH. This can also be inferred from the Losartan Intervention for Endpoint reduction (LIFE) and Heart Outcomes Prevention Evaluation (HOPE) studies (Stöllberger *et al.*, 2003). From the LIFE study, the risk for myocardial infarction, stroke and SCD were significantly reduced by a reduction in left ventricular mass (LVM). Left ventricular mass is an indicator of LVH that is independent of systolic blood pressure (BP) and treatment administered (Devereux *et al.*, 2004).

Left ventricular hypertrophy is the most common cardiac complication caused by hypertension (Levy *et al.*, 1990). Interestingly, morbidity and mortality from cardiovascular disease associated with LVH has not been reduced by antihypertensive treatment, even though there was a reduction in BP (Koren *et al.*, 1991). Left ventricular hypertrophy has been observed in normotensive patients as well (Levy *et al.*, 1990; Schunkert *et al.*, 1999), indicating that LVH is not only due to a pressure overload, but can also be attributable to non-haemodynamic factors such as gender and age (Lijnen and Petrov, 1999).

More effective therapeutic intervention for patients suffering from hypertension can therefore only be achieved by means of a better understanding of the underlying causes of LVH. Identification of novel sarcomeric modifiers associated with the development of LVH would thus enable an improved risk profiling for susceptible patients. Hypertrophic cardiomyopathy is an inherited cardiac disease which is characterised by LVH – seen in hypertensive patients - and is therefore used as a model disease to study the molecular mechanisms involved in the development of cardiac hypertrophy (Watkins *et al.*, 1995).

1.9 HYPERTROPHIC CARDIOMYOPATHY

Hypertrophic cardiomyopathy (HCM) is the most common form of Mendelian-inherited cardiac disease that has effects at molecular, cellular and systemic (whole body) levels (Frey *et al.*, 2012). It was first described by two French pathologists in 1869 (Roberts and Marian, 2003). A defining characteristic thereof is primary LVH that occurs when there are no other hypertrophy-predisposing conditions present (Keren *et al.*, 2008; Revera *et al.*, 2008); such as increased external loading conditions (Marian, 2002; Roberts and Marian, 2003), myocyte loss or gross cardiac dysfunction (Roberts and Marian, 2003). Other clinical characteristics of HCM include: diastolic dysfunction, arrhythmias and sudden cardiac death (SCD) (Lim *et al.*, 2001; García-Castro *et al.*, 2003; Kaufman *et al.*, 2007; Revera *et al.*, 2007; Frey *et al.*, 2012). Sudden cardiac death in people younger than 35 years of age, especially athletes, is most often due to HCM (McLeod *et al.*, 2009).

Population-based clinical studies have indicated the prevalence of HCM to be one in 500 to one in 1000 people; mostly young adults (Maron *et al.*, 1995; García-Castro *et al.*, 2003; Keren *et al.*, 2008; Frey *et al.*, 2012). Due to HCM penetrance being age dependent, a much higher prevalence can be predicted in older patients (Niimura *et al.*, 2002). It has been shown that there is a gender element involved in HCM as the prevalence is higher in males than in females, regardless of age (Andersen *et al.*, 2008; Keren *et al.*, 2008).

Hypertrophic cardiomyopathy is a genetic disorder resulting in the thickening of the muscle of the ventricular wall of the heart (Maron *et al.*, 2000; Patel *et al.*, 2001; Revera *et al.*, 2007; Revera *et al.*, 2008; Van der Merwe *et al.*, 2008), which leads to decreased cardiac output, due to reduced ventricular volume (**Figure 1.15**). Cardiac mass is increased in HCM due to left ventricular wall thickening that is often asymmetric and frequently involves a thickening of the interventricular septum (Seidman and Seidman, 2001). The degree and site of the muscle thickening in HCM is extremely variable and inconsistent, which could be due to the locus as well as allelic heterogeneity of the disease-causing genes (Wigle *et al.*, 1995; Van der Merwe *et al.*, 2008). The most commonly observed type of asymmetrical hypertrophy is ventricular septal hypertrophy; whilst midventricular, apical, right ventricular and concentric hypertrophy are less frequent (Wigle *et al.*, 1995).

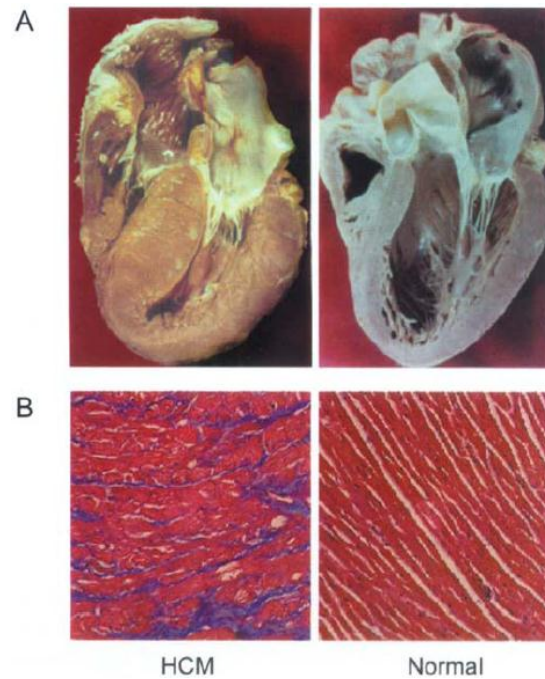


Figure 1.15. The pathology of hypertrophic cardiomyopathy. (A) Post-mortem examination of the heart of a patient with hypertrophic cardiomyopathy mutations showing vast asymmetrical hypertrophy of the left ventricle, along with related decrease in cavity size of the left ventricle, in comparison to a normal heart. (B) Histopathology of heart sections, stained with Masson's trichrome, indicating the difference between a normal heart and the extensive myofibrillar disarray and interstitial fibrosis present in hypertrophic cardiomyopathy. [Taken from Chung *et al.*, 2003].

Hypertrophic cardiomyopathy histopathology clearly shows abnormal hypertrophic growth of individual myocytes. Myocyte or myofibrillar disarray (Lim *et al.*, 2001; Arad *et al.*, 2002; Blair *et al.*, 2002) and interstitial fibrosis are important diagnostic criteria that can also be seen via histological examination (**Figure 1.15**) (Chung *et al.*, 2003; McLeod *et al.*, 2009).

Imaging of hypertrophied, nondilated left ventricular (LV) heart chamber by means of two-dimensional (2D) echocardiography is the simplest way to make a clinical diagnosis of HCM (Maron and McKenna *et al.*, 2003).

The clinical presentation of HCM can vary extensively, with symptoms manifesting from extreme hypertrophy with serious complications such as cardiac arrhythmias (a disturbance in or loss of regular rhythm) (Dorland's Illustrated Medical Dictionary, 2007) and HF (Blair *et al.*, 2002), along with sudden cardiac death (Tsoutsman *et al.*, 2006). However, HCM can also present with a form where carriers of a mutation have minimal to no symptoms and have a very benign or asymptomatic course, which is the reason for many cases of HCM remaining undiagnosed (García-Castro *et al.*, 2003). Familial segregation cannot always be determined because the disease tends to be intermittent in approximately 50% of known cases (García-Castro *et al.*, 2003; Frey *et al.*, 2012). This could also lead to an underestimation of the percentage of familial cases of hypertrophic cardiomyopathy, as there is incomplete penetrance of the hypertrophy phenotype in some mutation carriers (García-Castro *et al.*, 2003).

Left ventricular hypertrophy can develop at any age as well as increase or decrease dynamically throughout a patient's life (Maron, 2002). The HCM phenotype is thus not stagnant, as seen in a small subset of HCM subjects who progress to a burned-out phase; including features of HF, systolic dysfunction, left ventricular (LV) wall thinning and cavity enlargement (Maron *et al.*, 1987; Spirito *et al.*, 1997). Progressive cardiac remodelling can also be observed by some HCM subjects experiencing a slight regression in LV wall thickness when aging (Spirito and Maron, 1989).

The location of the causal mutations and the influences they have over sarcomeric proteins as well as myocytes do not specify the presence or severity of the HCM phenotype alone, because modifier genes and non-genetic environmental factors also play a role (Marian, 2000). Elucidation of the molecular pathogenesis of HCM is therefore necessary (Roberts and Marian, 2003) to better understand the effects of possible modifier proteins.

There is motivation to study the susceptibility to HCM in the South African population because this population is host to the largest number of founder mutations in the world (Moolman-Smook *et al.*, 2000; Van der Merwe *et al.*, 2008). It would thus serve as the ideal sample group to further investigate HCM as a model for cardiac hypertrophy.

1.10 IN THE PRESENT STUDY

The present study is based upon the findings of earlier Y2H studies, which identified C-zone titin as an interactor of cardiac myosin binding protein C (cMyBPC), known to be HCM causing (De Lange, 2004). Titin was therefore identified as being an HCM modifier protein, with the ability to contribute in a cumulative fashion to the HCM phenotype. The literature shows that mutations within the *TTN* gene are, however, also independently able to cause HCM (Taylor *et al.*, 2011; Frey *et al.*, 2012; Herman *et al.*, 2012).

Titin is able to sense mechanical stimuli and subsequently change them to biochemical signals, like the ones responsible for triggering hypertrophy, due to its

location within the sarcomere (Voelkel and Linke, 2011). Previous research regarding the role that titin plays in disease was complicated by the size of titin's coding region (Leinwand *et al.*, 2012) as well as its complex splicing pattern (Short, 2011). The *TTN* gene has thus been incompletely studied due to technical challenges involved with this approximately 100kb coding sequence (Herman *et al.*, 2012; Nowak, 2012).

Further research into the proteins that interact with titin was conducted in the present study, in order to elucidate more possible HCM modifier proteins. However, the focus was on the C-zone of the sarcomere, as previous studies on cMyBPC implicated titin in interactions within the C-zone, that were likely to play a role in modulating HCM (De Lange, 2004). The study also had to be limited to the C-zone due to titin's enormous size, as this has posed a problem with studying the properties of isolated titin in the past (Herman *et al.*, 2012). Thus, titin interactor proteins are likely to function in hypertrophy modulation in HCM as well.

The aim of the study was to identify novel interactors of the 11-domain super-repeat region of titin as candidate modifiers (or possible disease causing mutations) of hypertrophy in HCM in order to better understand the mechanisms leading to hypertrophy in complex disorders. This aim was achieved by the identification of a number of interactors of titin, by means of the yeast two-hybrid system, which were then subjected to further verification by colocalisation.

CHAPTER 2
MATERIALS AND METHODS

INDEX

	PAGE
2.1 THE PRINCIPLE OF THE YEAST TWO-HYBRID METHOD	54
2.2 POLYMERASE CHAIN REACTION (PCR) AMPLIFICATION	58
2.2.1 Oligonucleotide primer design and synthesis	58
2.2.1.1 Primers for the generation of a C-terminal <i>TTN</i> bait insert for Y2H analysis	58
2.2.1.2 Design of vector specific primers for insert screening	59
2.2.2 Bacterial colony PCR amplification	59
2.3 GEL ELECTROPHORESIS	60
2.3.1 Agarose gel electrophoresis for the visualisation of PCR-amplified products	61
2.3.1.1 Agarose gel electrophoresis for the purification of PCR products or plasmids purified from <i>E.coli</i>	61
2.4 AUTOMATED DNA SEQUENCING	62
2.5 ANALYSIS OF DNA SEQUENCES	62

2.6	BACTERIAL STRAIN, YEAST STRAINS AND CELL LINE	63
2.6.1	Bacterial strain	63
2.6.2	<i>S.cerevisiae</i> yeast strains	64
2.6.3	Cell line	64
2.7	PREPARATION OF <i>E.coli</i> DH5α COMPETENT CELLS FOR BACTERIAL TRANSFORMATIONS	64
2.8	CULTURING OF H9C2 CELL LINE	65
2.8.1	Culture of H9C2 cells from frozen stocks	65
2.8.1.1	Thawing the H9C2 cells	65
2.8.1.2	Removing dimethyl sulfoxide (DMSO) from stocks and culturing H9C2 cells	66
2.8.1.3	Sub-culturing of H9C2 cells	66
2.9	TRANSFORMATION OF PLASMIDS INTO <i>E.coli</i> AND <i>S.cerevisiae</i> CELLS	67
2.9.1	Bacterial plasmid transformation	67
2.9.2	<i>S.cerevisiae</i> plasmid transformations	68
2.10	DNA EXTRACTION	69
2.10.1	Bacterial plasmid purification using TOpure™ Plasmid Miniprep Purification Kit	69
2.10.2	Purification of DNA by means of Wizard® SV Gel and PCR Clean-up system	70

2.10.3	<i>S.cerevisiae</i> plasmid purification	70
2.11	VERIFICATION OF THE INTEGRITY OF THE Y2H CONSTRUCT	71
2.11.1	Phenotypic assessment of the <i>S.cerevisiae</i> strains	71
2.11.2	Test for autonomous reporter gene activation	72
2.11.3	Test for toxicity of the bait protein for the transformed <i>S.cerevisiae</i>	73
2.11.4	Testing of mating efficiency	74
2.12	YEAST TWO-HYBRID ANALYSIS	76
2.12.1	Adult human cardiac cDNA library	76
2.12.2	Establishment of the bait culture	76
2.12.3	The library mating	77
2.12.4	Establishment of a library titre	78
2.12.5	Control mating	79
2.12.6	Detection of the activation of nutritional reporter genes	79
2.12.6.1	Selection of transformed <i>S.cerevisiae</i> colonies	79
2.12.6.2	Selection of diploid <i>S.cerevisiae</i> colonies containing putative interactor peptides	80
2.12.7	Detection of the activation of colourimetric reporter genes by means of X-α-Galactosidase assay	81
2.12.8	Rescuing of prey plasmids from diploid colonies	81
2.12.9	Interaction specificity testing - exclusion of non-specific bait and prey interactions	82

2.13	COLOCALISATION	83
2.13.1	Immunostaining procedure	83

CHAPTER 2: MATERIALS AND METHODS

2.1 THE PRINCIPLE OF THE YEAST TWO-HYBRID METHOD

Yeast two-hybrid (Y2H) is a method to identify protein-protein interactions by means of manipulating the GAL4 transcription activator complex. The GAL4 gene encodes the yeast transcription activator protein Gal4. During normal transcription the GAL4-activation domain (AD), which binds to ribonucleic acid (RNA) polymerase and the GAL4 deoxyribonucleic acid (DNA) binding domain (BD), forms a transcription activator complex (**Figure 2.1**). In the Y2H system, the AD and BD are separated and fused to proteins that will potentially interact (i.e. a bait-BD fusion protein or prey-AD fusion protein) (**Figure 2.2**). If a fusion protein cannot activate transcription alone, it is able to become a target or “bait” protein, used to screen a complementary DNA (cDNA) library of clones by means of identifying other interactors or “prey” proteins. Therefore, transcription of downstream reporter genes will only occur if the bait-AD and prey-AD fusion proteins interact with each other, thus bringing the AD and BD into close enough proximity to initiate transcription. In the BD Matchmaker™ GAL4-based two-hybrid system (BD Biosciences, Clontech, Paulo Alto, CA, USA), the protein of interest is fused to the GAL4-BD and the potential interacting proteins are each separately fused to the GAL4-AD.

In the present study, interactions between the potential scaffold region of titin (TTN), known to be located within the C-zone of the sarcomere and proteins found in the human heart were investigated using the Y2H methodology (**Figure 2.3**). The region comprising of the 11-domain super-repeat region of TTN (**Figure 1.9**) was fused to

the GAL4 DNA-BD and transformed into the *S.cerevisiae* strain AH109 yeast. It was subsequently used as “bait” in a Y2H screen of a commercially available Y187 pre-transformed adult heart cDNA library (pACT2) to identify interacting proteins. The Y2H screen enabled the identification of interactions between TTN and putative ligands encoded by prey clones contained within the cDNA library. The mating culture (pACT2 heart cDNA in Y187 x pGBKT7-bait construct in AH109) was plated onto primary selection agar plates, known as triple dropout (TDO) plates, which selected for diploid histidine positive (His⁺) colonies (**Section 2.12.6.2**). Thereafter, the colonies that grew successfully were subjected to more stringent selection media, selecting for diploid adenine positive (Ade⁺) and His⁺ colonies (**Section 2.12.6.2**). Finally, the colonies were tested for the expression of the alpha-galactosidase (*MEL1*) reporter gene, by means of an X-alpha-galactosidase (X- α -Gal) assay. Colonies found to be positive for the activation of all three reporter genes showed strong bait-prey interactions. The prey plasmids were then rescued from the diploid colonies by means of yeast plasmid purifications and transformed into the yeast strain Y187 (**Section 2.12.8**). Each prey plasmid’s specificity of interactions was further tested by means of an interaction specificity test (**Section 2.12.9**). Prey colonies that passed all three of the reporter activation tests as well as the interaction specificity test were sequenced. The sequences were subsequently aligned against the Genbank DNA database (<http://www.ncbi.nlm.nih.gov/Entrez>) to identify the putative interacting prey proteins. Translated sequences were also aligned to Genbank protein sequences. In order to verify and further validate the Y2H results, colocalisation experiments (**Section 2.13**) were performed in cultured cardiomyocytes.

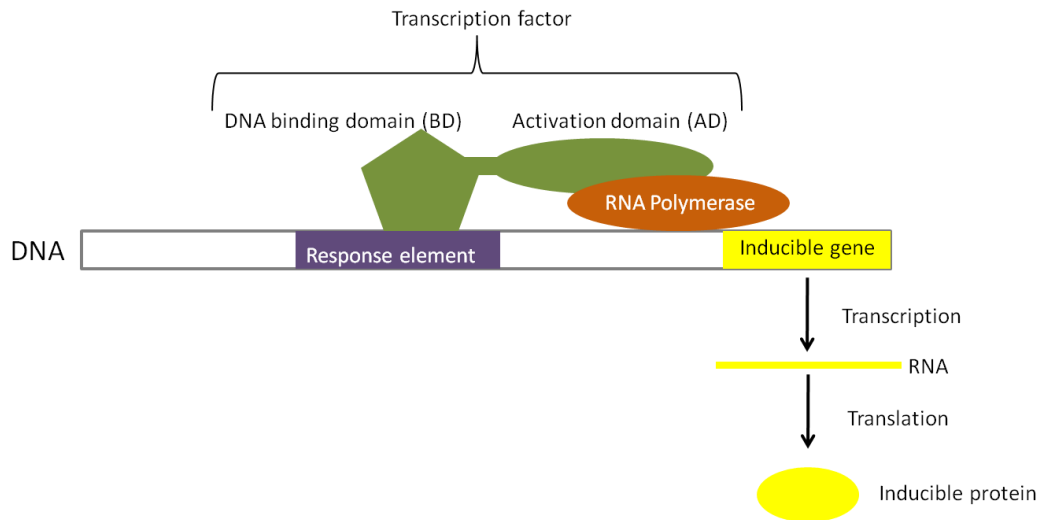


Figure 2.1. Normal transcription. Transcription factors bind to response elements in the DNA and activate transcription via RNA polymerase. Abbreviations: AD, activation domain; BD, DNA binding domain; cDNA, complementary DNA; DNA, deoxyribonucleic acid; RNA, ribonucleic acid.

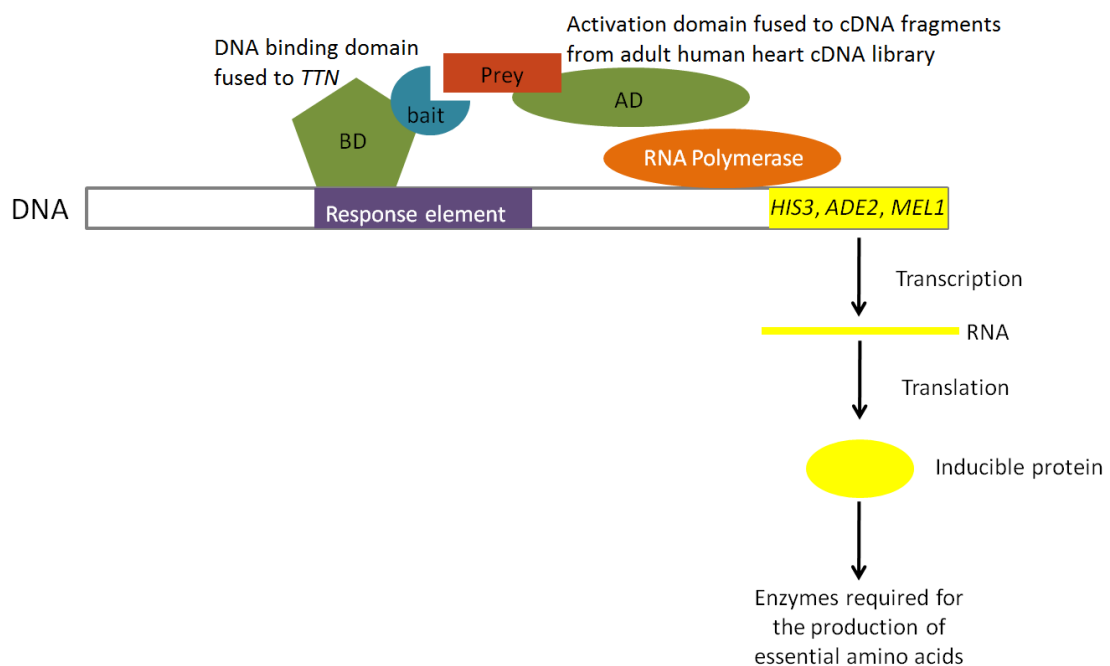


Figure 2.2. The principle of Y2H. The DNA binding domain (BD) is fused to the protein of interest (bait) and the activation domain (AD) is fused to the cDNA of an adult human heart cDNA library (prey). In diploid yeast cells containing bait and a

prey plasmid, fusion proteins are expressed and when interaction of the bait and prey proteins takes place, the AD and BD come into close enough proximity so as to activate the transcription of various reporter genes. The reporter genes encode enzymes required for the production of essential amino acids. Abbreviations: AD, activation domain; BD, DNA binding domain; cDNA, complementary DNA; DNA, deoxyribonucleic acid; RNA, ribonucleic acid.

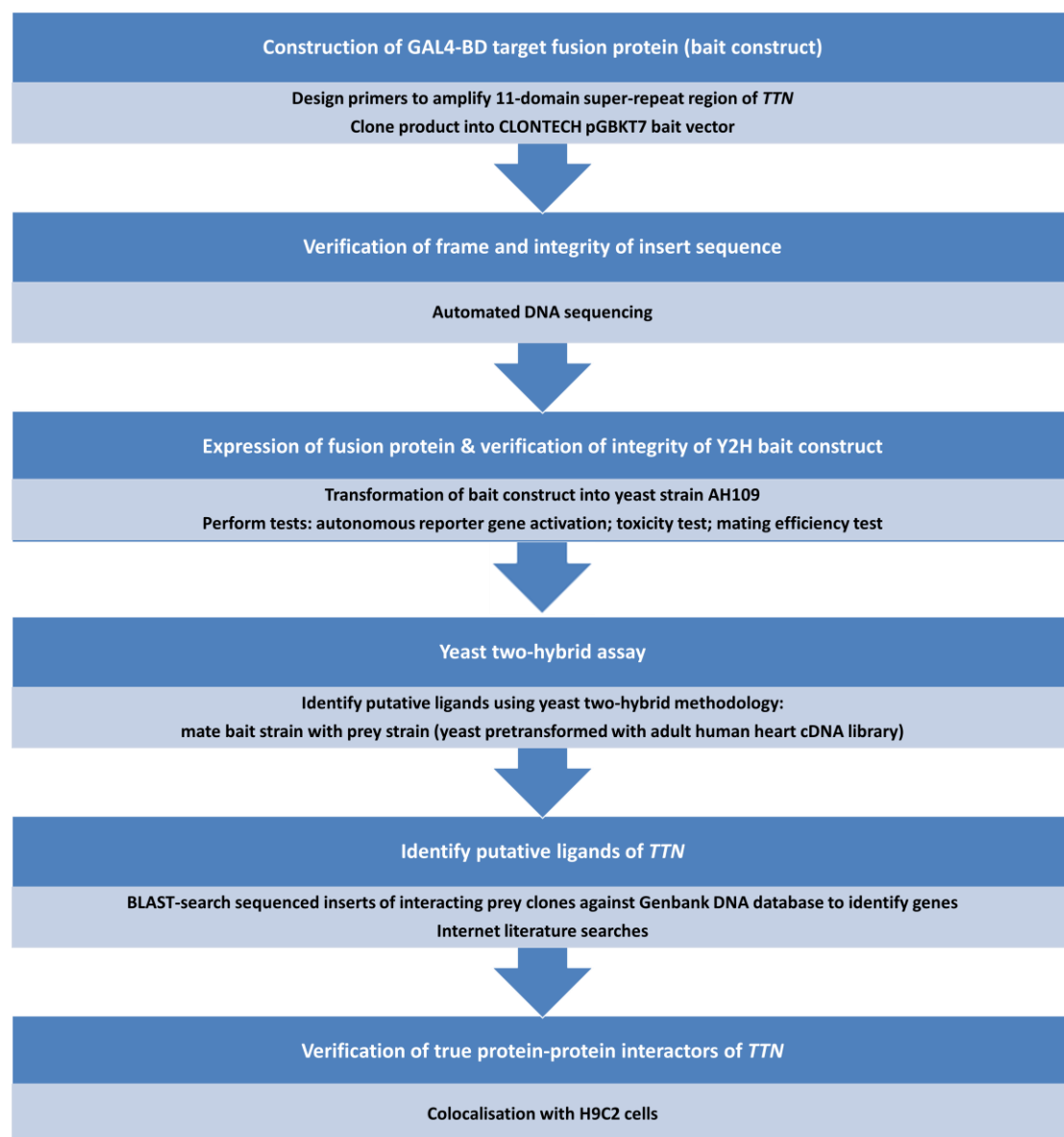


Figure 2.3. Outline of the methodology used to perform the present study.

2.2 POLYMERASE CHAIN REACTION (PCR) AMPLIFICATION

2.2.1 Oligonucleotide primer design and synthesis

Oligonucleotide primers were designed using sequence data available from the Genbank DNA database (<http://www.ncbi.nlm.nih.gov/Entrez>). The primers were designed using DNAMAN™ version 4 software (Lynnion Biosoft Corp©) and analysed for primer-primer complementarity and self-complementarity as well as compatibility of melting temperatures before synthesis, using IDT Scitools software (<http://eu.idtdna.com/Scitools/Scitools.aspx>). The oligonucleotide primers were synthesised according to standard phosphoramidite methodology at the Department of Molecular and Cell Biology, University of Cape Town (UCT), South Africa.

2.2.1.1 Primers for the generation of a C-terminal *TTN* bait insert for Y2H analysis

Human cardiac expressed TTN is approximately 34350 amino acids long (*ExpASy Proteomics Server* Swiss Institute of Bioinformatics, 2011). The DNA sequence of *TTN* was obtained from the Genbank DNA database (accession number CAD12456.1) (<http://www.ncbi.nlm.nih.gov/Entrez>). Domains A109 to A119 (residues 33791 to 34350) of *TTN* were amplified from a *TTN* open reading frame (ORF) clone (ImaGenes GmbH, Berlin, Germany). The primers were designed to incorporate restriction enzyme sequences on the forward (*NdeI*) and reverse (*EcoR1*) primers to enable the insertion of the amplified product into the pGBKT7 shuttle vector. The

reverse primer also possessed a stop codon. The primer sequences used for the amplification are provided in **Table 2.1**.

2.2.1.2 Design of vector specific primers for insert screening

Primers were designed that flanked the multiple cloning site (MCS) to amplify inserted DNA or putative prey DNA from either the pGBKT7 or pACT2 vectors (**Appendix IV**). The primer sequences were obtained from the individual vector datasheets at www.clontech.com and are summarized in **Table 2.1**. Vector-specific primers were designed to amplify and sequence the pGBKT7-*TTN* bait construct as well. The primers were designed and sent to ImaGenes for cloning.

2.2.2 Bacterial colony PCR amplification

Bacterial colony PCR is used to identify bacterial colonies that contain the chosen recombinant plasmid. A single bacterial colony was picked from an agar plate containing the appropriate antibiotic and was used as a template in a PCR reaction. Vector-specific primers (Table 2.1) were used to amplify the insert, nested within the vector. The PCR reaction mixture was made up as follows: 0.4 μ M reverse primer, 0.4 μ M forward primer, 12.5 μ L of 2x ReadyMix (1.25U of KapaTaq DNA Polymerase, a reaction buffer containing 1.5mM Mg²⁺ and 0.4mM of each dNTP) (Kapa Biosystems, Massachusetts, USA), the single of the bacterial colony and sterile double distilled water (ddH₂O). PCR amplification was performed in a GeneAmp® PCR system 9700 thermal cycler (Perkin-Elmer, Applied Biosystem Inc., Foster City CA, U.S.A.). The cycling parameters were set up as follows: a denaturing step of

94°C for five minutes, followed by 30 cycles of amplification consisting of 94°C for 30s each, appropriate annealing temperature for 30s (see Table 2.1) and an elongation step for one minute at 72°C. The amplification products were visualised by agarose gel electrophoresis (**Section 2.3.1**), including negative controls and co-electrophoresed with a 100bp DNA ladder (Promega Corporation, Madison, Wisconsin, USA) or with Hyperladder™ I (Bioline UK Ltd, UK).

Table 2.1. Primer sequences and annealing temperatures used in the construct design and amplification of the inserts from cloning vectors.

Name	Sequence	T _a (°C)
Construct primers for the generation of the Y2H bait insert		
BKA109F	5'-GCCATGGAGCATATGATAGAACTCGATGCTGATCTC-3'	64
BKA119R	5'-ACTCGAGAATTCCTAACTGGGGTCACTAGCACCAAC-3'	70
Vector specific primers – amplification and sequencing of inserts from cloning vectors		
pGBKT7-F	5'-TCATCGGAAGAGAGTAG-3'	50
pGBKT7-R	5'-TCACTTTAAAATTTGTATACA-3'	51
pACT2-F	5'- GATGATGAAGATACCCAC -3'	65
pACT2-R	5'- CAGTTGAAGTGAAGTGC -3'	65

Blue: universal enzyme seat; Red: enzyme restriction site; Green: stop codon; Black: gene specific sequences. Abbreviations: T_a, annealing temperature; °C, degrees Celsius.

2.3 GEL ELECTROPHORESIS

Agarose gel electrophoresis was used to visualize PCR-amplified fragments, to verify plasmid preparations and for excision of DNA fragments for purification.

2.3.1 Agarose gel electrophoresis for the visualisation of PCR-amplified products

Verification that PCR amplifications or plasmid preparations were successful was performed by agarose gel electrophoresis as follows: 10 μ L of the PCR product was mixed with 3 μ L bromophenol blue (BPB) loading dye. The prepared sample was loaded into wells of either one or two percent (dependant on the size of the amplified fragment) horizontal agarose gel, containing 1 μ g/mL ethidium bromide (**Appendix I**) and 1x sodium borate (SB) buffer (**Appendix I**). All the PCR products were co-electrophoresed with a 100bp molecular weight marker (Promega Corporation, Madison Wisconsin, USA) or with Hyperladder™ I (Bioline UK Ltd, UK). Electrophoresis was done at 10V/cm for 20 minutes in 1x SB running buffer (**Appendix I**). The DNA fragments were visualized with an ultra-violet (UV) transilluminator 20x20 using the G-BOX gel documentation system (Synoptics Ltd, Syngene, Cambridge, UK).

2.3.1.1 Agarose gel electrophoresis for the purification of PCR products or plasmids purified from *E.coli*

The PCR amplified product representing the correct base pair (bp) size was electrophoresed and then excised from the agarose gel to sequence the *TTN* bait-insert. For the excision of PCR-amplified products 30 μ L of the PCR amplified fragments were loaded onto a 2% agarose gel, as described in **Section 2.3.1.1**. The DNA fragments were visualized by means of a 3UV transilluminator (UVP Inc., Upland, CA, USA). The correct sized band was excised from the gel, using a sterile

scalpel blade. The gel band was subsequently purified using the Wizard® SV Gel and PCR Clean-up System (Promega Corporation, Madison Wisconsin, USA) (**Section 2.10.2**).

2.4 AUTOMATED DNA SEQUENCING

Bidirectional, automated DNA sequencing of PCR-amplified products and cloned inserts was done at the Central Analytical Facility (CAF) (University of Stellenbosch) on the ABI Prism™ 377 or ABI Prism™ 3100 automated sequencer (P.E. Applied Biosystems, Forster City, CA, USA). Sequencing was used as verification of the correct bait construct as well as to determine the nucleotide sequence of the prey proteins that interacted with the bait construct. Primer sequences used in the sequencing reactions are shown in Table 2.1. The sequencing of PCR-amplified products' primers was the same as for the original PCR reaction; whilst the vector-specific primers were used for the sequencing of the constructs (Table 2.1).

2.5 ANALYSIS OF DNA SEQUENCES

Bioedit (Ibis Bioscience, Carlsbad, CA, USA) and DNAMAN™ (Lynnon Biosoft, St. Louis, Pointe-Claire, Quebec, Canada) software were used to perform sequence analysis. Sequence analysis permitted the verification of the sequence integrity (reading frame and cloning sites) of the *TTN* bait-insert that was cloned into the pGBKT7 vector (**Section 2.4**) as well as the identification of putative interactor prey clones that were identified during the Y2H library screen (**Section 2.4**).

The nucleotide sequence of the *TTN* bait-insert, determined by automated sequencing (**Section 2.4**), was compared to cDNA and messenger RNA (mRNA) sequences found on the Genbank database (www.ncbi.nlm.nih.gov/Entrez). A nucleotide Basic Local Alignment Search Tool (BLASTn) analysis search of the Genbank database was performed with the prey-insert sequences obtained from the Y2H library screen. The insert sequences of the prey clones were translated in the frame determined by the previous GAL4AD reading frame (reading frame 1). The protein sequence was subsequently compared to proteins found in public protein databases by means of protein BLASTp analysis.

2.6 BACTERIAL STRAIN, YEAST STRAINS AND CELL LINE

2.6.1 Bacterial strain

The *E.coli* DH5 α strain (**Appendix III**) was routinely used to facilitate the selection, amplification and purification of constructs. Transformed bacterial colonies were selected based on their ability to grow on selection plates containing different antibiotics. The shuttle vector, pGBKT7 contains a kanamycin resistant gene and can therefore grow on Luria-Bertani (LB) plates containing kanamycin. pACT2 contains an ampicillin resistance gene and bacteria transformed with this vector are therefore able to grow on ampicillin containing media. Recombinant plasmids were previously identified by means of bacterial colony PCR, using suitable primers.

2.6.2 *S.cerevisiae* yeast strains

The pGBKT7-*TTN* bait construct was transformed into the *S.cerevisiae* strain AH109 (**Section 2.9.2**). The clones in the pre-transformed Clontech adult human heart cDNA library were transformed into the *S.cerevisiae* strain Y187 by the manufacturer (BD Biosciences, Clontech, Paulo Alto, CA, USA) (**Appendix III**).

2.6.3 Cell line

The H9C2 cardiac cell line (American Type Culture Collection, Manassas, VA, USA) was used for the colocalisation (**Section 2.13**) verification experiments. The H9C2 cells were a subclone of the original clonal line, derived from embryonic BD1X *Rattus norvegicus* deposited as *Rattus* sp. heart myocardium tissue (ATCC, Manassas, VA, USA).

2.7 PREPARATION OF *E.coli* DH5 α COMPETENT CELLS FOR BACTERIAL TRANSFORMATIONS

Stock of *E.coli* DH5 α competent cells are kept frozen in 50% glycerol at -80°C. To generate competent *E.coli* DH5 α cells, 200ul of the above mentioned stock was inoculated in 10mL LB media (**Appendix I**) and incubated overnight at 37°C in a YIH DER model LM-530 shaking incubator (SCILAB Instrument Co. Ltd, Taipei, Taiwan) at 200 revolutions per minute (rpm). After incubation, 300 μ L of the overnight starter culture was inoculated into a sterile 2L Erlenmeyer flask containing 200mL LB media. The culture was incubated at room temperature for 16 hours whilst

shaking at 100 rpm. The following morning the optical density (OD) was measured at 600nm (OD₆₀₀). Once the OD₆₀₀ reached 0.6 (indicating that the cells were in mid log phase), the culture was transferred to four separate 50mL polypropylene centrifuge tubes and centrifuged in a Beckman model TJ-6 centrifuge (Beckman Coulter, Scotland, UK) for 10 minutes at 3000 rpm. The supernatant was discarded and 8mL of ice-cold CAP buffer (**Appendix I**) was added to each tube to resuspend the pellets. The cells were re-pelleted by centrifugation at 3000 rpm for 10 minutes. The supernatant was again discarded and 4mL of ice-cold CAP buffer was added to resuspend each pellet. Two hundred microliters aliquots of the suspended cell mixtures were then pipetted into 2mL reaction tubes. The aliquots were stored overnight at 4°C in an ice box. The next morning the competent cells were stored at -80°C until required for further experiments.

2.8 CULTURING OF H9C2 CELL LINE

2.8.1 Culture of H9C2 cells from frozen stocks

2.8.1.1 Thawing the H9C2 cells

Frozen stocks of H9C2 cells were thawed by rapidly immersing the vials into a 37°C water bath (Mettmert®, Scwabach, Germany) for 10 minutes. Once thawed, the outside of the vials were sterilised with 70 % ethanol.

2.8.1.2 Removing dimethyl sulfoxide (DMSO) from stocks and culturing H9C2 cells

It is essential to remove the DMSO from the frozen cell stocks to ensure maximum viability of the cells upon plating. DMSO was removed as follows: 1mL of complete growth media (**Appendix I**), pre-heated to 37°C, was added to the thawed cell stocks and mixed by gentle pipetting. This mixture was transferred to a 12mL Greiner tube (Greiner Bio-one, Frickenhausen, Germany) and an additional 5mL of growth media was then added. The cells were pelleted by centrifugation at 1000 rpm for three minutes using a Sorval® GLC-4 General Laboratory centrifuge (Separations Scientific, Johannesburg, RSA) and the supernatant was removed thereafter. The pellet was resuspended in 5mL growth media and centrifuged at 1000 rpm for one minute. The pellet was finally resuspended in 10mL growth media and transferred into a T25 culture flask. The H9C2 cells were then spread evenly over the growth surface of the culture flask and subsequently incubated in a Farma-thermosteri-cycle 5% carbon dioxide humidified incubator (Farma International, Miami, Florida, USA).

2.8.1.3 Sub-culturing of H9C2 cells

The H9C2 cells were split every two to four days, until a confluency of approximately 70-80% was achieved. The cells were split into multiple flasks as follows: the growth media from the flask was removed, the adherent cells were washed with sterile phosphate buffered saline (PBS), containing no Ca^{2+} or magnesium²⁺ (Mg^{2+}) (Cambrex, Walkerville, MD, USA). In order to detach the cells from the surface of the flask, 2mL of trypsin (Highveld Biological, Lyndhurst, RSA) was added to the

flask. The cells were left to incubate at room temperature for five minutes with the trypsin. Thereafter, 5mL of growth media was added and the detached cells were gently resuspended in this volume. The cells were subsequently transferred to a 12mL Greiner tube and pelleted by centrifugation at 1000 rpm for three minutes in a Sorval® GLC-4 General Laboratory centrifuge. After the centrifugation, the cells were resuspended in 10mL complete growth media (**Appendix I**) and transferred to four other flasks, each containing 10mL growth media.

2.9 TRANSFORMATION OF PLASMIDS INTO *E.coli* AND *S.cerevisiae* CELLS

2.9.1 Bacterial plasmid transformation

Competent *E.coli* DH5 α cells were removed from the -80°C freezer and allowed to thaw on ice for approximately 20 minutes. One tube, containing 200 μ L of competent cells (**Section 2.7**), was used per bacterial transformation. When the cells were completely thawed, 1 μ L of plasmid preparation (**Section 2.10.1**), was added to the competent cells and gently mixed. The mixture was incubated on ice for 25 minutes, followed by incubation in a Memmert water bath (Memmert 854, Schwabach, Germany) at 42°C for precisely 45 seconds. The sample was removed from the water bath and kept at room temperature for two minutes. Subsequently, 1mL of LB media (**Appendix I**) was added to the mixture and it was incubated in a YIH DER model LM-530 shaking incubator (SCILAB instrument CO. Ltd, Taipei, Taiwan) at 37°C for one hour at 200 rpm. Two hundred microliters of the incubated mixture was subsequently plated onto LB agar plates, containing the appropriate selection

antibiotics. The plates were inverted and incubated overnight in an un-I-trol CO₂ incubator, model 329 (Forma Scientific, Ohio, USA).

2.9.2 *S.cerevisiae* plasmid transformations

The yeast strain to be transformed (either AH109 or Y187) was streaked onto yeast peptone dextrose adenine (YPDA) agar plates and incubated (Sanyo, Electronic Company Ltd, Ora-Gun, Japan) at 30°C for three to four days. A volume representing 20-50uL of yeast cells was picked and resuspended by vortexing in 1mL sterile ddH₂O. The cells were pelleted for 30 seconds at 15000 rpm (Hermle Labortechnik, Wehingen, Germany). The H₂O was removed and the pellet resuspended in 1mL 100mM lithium acetate (LiAc) (**Appendix I**) then incubated at 30°C for five minutes in a 311 DS incubator (Labnet International Inc., Edison, NJ, USA). The 1mL suspension was split into three 2mL reaction tubes. The yeast cells were then pelleted by centrifuging for 30 seconds at 15000 rpm. The LiAc was removed from each pellet with a pipette. The following was then sequentially added, as quickly as possible, to the pellet: 240uL 50% polyethylene glycol (PEG) (**Appendix I**), 36uL 1M LiAc (**Appendix I**), 25uL of 2mg/mL snap-cooled sonicated herring sperm DNA (Promega, Madison WI, USA), 10-20 uL of the plasmid and 29-39uL of sterile ddH₂O (depending on how much plasmid was added, so that plasmid + H₂O = 50µL), so as to bring the mixture to a final volume of 350uL. The transformation mixture was thoroughly vortexed for at least one minute then incubated in a Lasec 102 circulating water-bath (Lasec Laboratory and Scientific Company Pty Ltd, Cape Town, R.S.A) at 42°C for 25 minutes. After the incubation, the samples were pelleted for 30 seconds at 15000 rpm and the supernatant was removed. The pellet was then resuspended in

250uL sterile Millipore water. 150uL of this mixture was then plated onto appropriate selection agar plates (SD^{-Trp} for bait plasmid/pGBKT7; SD^{-Leu} for library/prey plasmids) (**Appendix IV**). Following plating, the plates were inverted and incubated at 30°C for two to five days in a Sanyo MIR262 stationary gravity ventilated incubator (Sanyo, Electronic Company Ltd, Ora-Gun, Japan).

2.10 DNA EXTRACTION

2.10.1 Bacterial plasmid purification using TOpure™ Plasmid Miniprep Purification Kit

A single *E.coli* colony, harbouring the plasmid of interest, was picked from an appropriate selection plate. The colony was then inoculated into 10mL of LB media, which was supplemented with appropriate antibiotic (**Appendix I**) in a 50mL polypropylene centrifuge tube. The culture was incubated at 37°C (shaking at 250rpm) overnight in a YIH DER model LM-530 shaking incubator (SCILAB instrument CO. Ltd, Taipei, Taiwan).

The following morning, the culture was centrifuged for ten minutes at 3000 rpm in a Beckman model TJ-6 centrifuge (Beckman Coulter, Scotland, UK). Four hundred microlitres of the supernatant was used to resuspend the *E.coli* pellet. The plasmid DNA was extracted using the TOpure™ Plasmid Miniprep Purification Kit (Gene Tech, Hong Kong), by following the manufacturer's instructions. The plasmid DNA was eluted in 30-50uL of the DNA elution buffer, dependent upon the required concentration. The concentration of each plasmid was then determined using the

Nanodrop model 1000 (Thermo Fisher Scientific, Waltham, MA, USA) and the plasmids stored at -20°C until needed for further experiments.

2.10.2 Purification of DNA by means of Wizard® SV Gel and PCR Clean-up system

PCR-amplified DNA products were purified to obtain DNA products of suitable quality for sequencing. The previously PCR-amplified products were gel-purified as follows: the applicable PCR-amplified DNA product was electrophoresed in a 1% agarose gel and viewed under UV light. The appropriate fragments were excised from the gel using a sterile blade. The excised fragments were then melted at 65°C in a waterbath, in membrane binding solution (10µL of membrane binding solution per 10mg of agarose gel slice). The DNA was then extracted from the solution using the Wizard® SV Gel and PCR Clean-up System, following the manufacturer's instructions (Wizard® SV Gel and PCR Clean-up System, Promega Corporation, Madison Wisconsin, USA). The process was similar for PCR reaction fragments besides that the PCR reaction was directly mixed with membrane binding solution in a 1:1 ratio.

2.10.3 *S.cerevisiae* plasmid purification

Yeast cells containing the plasmid of interest were inoculated into 1mL synthetic dropout (SD) media, containing the appropriate dropout supplement (BD bioscience, Clontech, Paulo Alto, CA, USA). The culture was then incubated overnight at 30°C and 150 rpm in a Labnet shaking incubator model 331DS (Labnet international, New

Jersey, U.S.A). Four millilitres of YPDA media was added early the following morning and the culture was incubated for a further four hours at 30°C. The cultures were then centrifuged in a Beckman model TJ-6 centrifuge (Beckman Coulter, Scotland, UK) for ten minutes at 3000 rpm. The supernatant was discarded and the culture resuspended in the residual liquid volume.

The following was subsequently added to a 2mL reaction tube: 200uL of yeast lysis buffer (**Appendix I**), 200uL of phenol:chloroform:isoamyl alcohol 25:24:1 (PCI) (Sigma-Aldrich, St. Louis Missouri, USA), 0.3g glass beads of diameter 450-600 µm as well as the above mentioned concentrated culture. The yeast cells were ground-up by vortexing the mixture for two and a half minutes and then centrifuging them at 15000rpm for five minutes in a Hermle model Z233M-2 centrifuge (Hermle Labortechnik, Wehingen, Germany) to separate the plasmid from the cell debris. The top aqueous layer was subsequently transferred to a new 1.5mL reaction tube and purified using the Wizard® SV Gel and PCR Clean-up System (Promega Corporation, Madison Wisconsin, USA) as described in **Section 2.10.2**.

2.11 VERIFICATION OF THE INTEGRITY OF THE Y2H CONSTRUCT

2.11.1 Phenotypic assessment of the *S.cerevisiae* strains

The yeast strains used during Y2H analysis have to be assessed phenotypically before they acquire vectors via transformation (Table 2.2). The yeast strains AH109 and Y187 were streaked onto individual SD agar plates, lacking essential amino acids (SD^{-Ade}, SD^{-Trp}, SD^{-His}, SD^{-Leu} and SD^{-Ura}). The viability of the yeast strains was

assessed after four days. Both untransformed AH109 and Y187 are meant to thrive upon only SD^{-Ura} and not on SD^{-Ade} , SD^{-Trp} , SD^{-His} or SD^{-Leu} (Table 2.2). Non-transformed yeast cells that were unable to grow on SD^{-Ade} , SD^{-Trp} , SD^{-His} or SD^{-Leu} , but were able to grow on SD^{-Ura} were then used for the transformations with the bait vector as well as the subsequent Y2H analysis (Section 2.12).

Table 2.2. Phenotypic assessment of the untransformed *S.cerevisiae* strains, grown on specific SD selection media.

Strain	Growth on SD agar plates				
	SD^{-Ade}	SD^{-His}	SD^{-Leu}	SD^{-Trp}	SD^{-Ura}
AH109	-	-	-	-	+
Y187	-	-	-	-	+

Abbreviations: SD, synthetic dropout; - = no growth; + = growth

2.11.2 Test for autonomous reporter gene activation

The *S.cerevisiae* AH109 yeast strain, transformed with the pGBKT7-*TTN* bait construct (Section 2.9.2), was assessed to ensure that the bait construct did not autonomously activate the *ADE2* and Imidazoleglycerolphosphate dehydratase (*HIS3*) reporter genes. Autonomous activation of the reporter genes would result in a very large number of false positive interactions being detected during the Y2H screen and the bait would thus not be able to be used in a library screen. The test was done by means of streaking pGBKT7-*TTN* transformed and untransformed *S.cerevisiae* AH109 yeast onto SD agar plates lacking essential amino acids (SD^{-Ade} , SD^{-Trp} , SD^{-His} , SD^{-Leu} and SD^{-Ura}). pGBKT7-*TTN* transformants should only be able to grow on SD^{-W} and SD^{-Ura} plates (Table 2.3).

Table 2.3. Test for autonomous reporter gene activation by the pGBKT7-*TTN* bait construct.

Strain	Growth on SD agar plates				
	SD ^{-Ade}	SD ^{-His}	SD ^{-Leu}	SD ^{-Trp}	SD ^{-Ura}
AH109	-	-	-	-	+
AH109 transformed with pGBKT7- <i>TTN</i>	-	-	-	+	+

Abbreviations: SD, synthetic dropout; - = no growth; + = growth

2.11.3 Test for toxicity of the bait protein for the transformed *S.cerevisiae*

It is necessary to establish whether the pGBKT7-*TTN* bait construct is toxic to the AH109 yeast strain before beginning with the Y2H screen. To accomplish this, a linearized growth curve that compares the growth of the AH109 host strain containing the pGBKT7-*TTN* bait construct with the growth of AH109 that has been transformed with the empty pGBKT7 vector (non-recombinant vector control) and non-transformed AH109.

The experiments were carried out parallel to one another under the same experimental conditions. The transformed and non-transformed AH109 yeast strains were incubated in 50mL polypropylene centrifuge tubes containing SD^{-Trp} media in a YIH DER model LM-510R shaking incubator (SCILAB Instrument Co. Ltd, Taipei, Taiwan) set to 30°C and 200 rpm. They were grown for 24 hours to stationary phase. A 1:10 dilution of the each primary cultures was then made in SD^{-Trp} and incubated for an additional 24 hours at 30°C and 200 rpm in a YIH DER model LM-510R shaking incubator (SCILAB Instrument Co. Ltd, Taipei, Taiwan). OD₆₀₀ readings

were recorded every two hours for an eight hour period during incubation. One 24 hour reading was also documented.

The data was graphically represented as the log of the OD₆₀₀ readings versus time. The gradient of the graphs for the recombinant and non-recombinant transformants were compared.

2.11.4 Testing of mating efficiency

The purpose of the mating efficiency test is to determine whether the bait construct negatively affects the mating efficiency of AH109. Small scale mating experiments were performed and compared to controlled mating experiments (Table 2.4).

During the test mating experiments, the AH109 transformed with the pGBKT7-*TTN* bait construct was mated with the prey host strain: Y187 transformed with non-recombinant prey vector pACT2 or a control prey vector pTD1.1 (BD Bioscience, Clontech, Paulo Alto, CA, USA). Concurrent control matings were also performed in which the yeast strain AH109 was transformed with non-recombinant pGBKT7 or the control pGBKT7-53 vector (BD Bioscience, Clontech, Paulo Alto, CA, USA) and mated with the prey host strain: Y187 transformed with non-recombinant prey vectors pACT2 or the Clontech pTD1.1 control vector, each encoding an AD/SV40 large T antigen fusion protein.

Table 2.4. Mating efficiency test of *S.cerevisiae* AH109 (pGBKT7-*TTN*).

Category	Mating		
Bait mating (1)	pGBKT7- <i>TTN</i> (bait)	X	pACT2 (prey)
Bait mating (2)	pGBKT7- <i>TTN</i> (bait)	X	pTD1.1 (prey)
Compatible control mating (1)	pGBKT7-53 (bait)	X	pACT2 (prey)
Compatible control mating (2)	pGBKT7-53 (bait)	X	pTD1.1 (prey)

Experimental procedure: The various yeast strains were plated onto the appropriate nutritional selection plates (AH109 pGBKT7-*TTN* bait construct, AH109 pGBKT7 bait vector and pGBKT7-53 were all grown on SD^{-Trp}; Y187 pACT2 and Y187 pTD1.1 were grown on SD^{-Leu}). The plates were then incubated for two to five days in a stationary gravity ventilated incubator (Sanyo, Electronic Company Ltd, Ora-Gun, Japan). A single colony from these plates was used for each of the test mating experiments: the yeast strains were mated in 2mL reaction tubes containing 1mL of YPDA media (**Appendix I**) (**Table 2.4**) and incubated at 30°C in a 311 DS incubator (Labnet International Inc., Edison, NJ, USA), shaking overnight at 150 rpm. Serial dilutions (1:10; 1:100; 1:1000; 1:10 000) of the mating cultures were made the following day and plated onto SD^{-Trp}, SD^{-Leu} and SD^{-Leu/-Trp} and subsequently incubated for four to five days at 30°C in a Sanyo MIR262 stationary gravity ventilated incubator (Sanyo, Electronic Company Ltd, Ora-Gun, Japan). The colonies on each plate were counted after incubation and used to calculate the mating efficiency (**Appendix II**).

2.12 YEAST TWO-HYBRID ANALYSIS

2.12.1 Adult human cardiac cDNA library

Pre-transformed Matchmaker™ human heart cDNA library (BD Biosciences, Clontech, Paulo Alto, CA, USA.), consisting of *S.cerevisiae* Y187 transformed with a human heart cDNA library, was used for the Y2H experiments.

2.12.2 Establishment of the bait culture

A colony of AH109 that was transformed with the pGBKT7-*TTN* bait construct (Section 2.9.2) was streaked onto SD^{-Trp} plates. After the yeast had grown, four single colonies were picked and inoculated into four 500mL Erlenmeyer flasks, each containing 50mL SD^{-W} media. It was necessary to inoculate four flasks to enable pooling of the initial cultures and forming a final bait culture with a titre of at least 1×10^{10} . This translates into a 100 times excess of bait to prey ratio, thus facilitating a high mating efficiency. The cultures were incubated at 30°C overnight in a YIH DER model LM-510R shaking incubator (SCILAB Instrument Co. Ltd, Taipei, Taiwan), shaking at 200 rpm. The cultures were decanted into four separate 50mL polypropylene tubes the following morning and centrifuged at 3000 rpm for ten minutes at room temperature in a Beckman model TJ-6 centrifuge (Beckman Coulter, Scotland, UK). The supernatants were discarded and the pellets combined and then resuspended in 50mL SD^{-Trp} media. The entire culture was then transferred to a 500mL Erlenmeyer flask and incubated for 16 hours in a YIH DER model LM-510R shaking incubator (SCILAB Instrument Co. Ltd, Taipei, Taiwan) at 30°C and 200

rpm. The titre of the bait culture was determined by measuring the OD₆₀₀ reading of 1mL of the culture after incubation. A haemocytometric cell count was also performed so as to confirm the spectrophotometric reading. The Neubauer haemocytometer (Superior, Berlin, Germany) was used for the calculation of the bait culture titre. The following formula was used to determine the number of cells per millilitre:

Number of cells/mL = number of cells x dilution factor x 10⁴ (constant value; the depth of the haemocytometer is 0.1mm)

The final 50mL of bait culture was centrifuged at 3000 rpm for ten minutes in a Beckman model TJ-6 centrifuge (Beckman Coulter, Scotland, UK). The supernatant was removed and the pellet was subsequently resuspended in 1mL SD^{-Trp} media. Ten microlitres of this culture was set aside for the control mating experiment.

2.12.3 The library mating

The pre-transformed adult human heart cDNA library was removed from the -80°C freezer and left for a while to thaw slowly at room temperature. Once thawed, the library tube was vortexed and a 10µL aliquot of the library was set aside for the library titre. The pGBKT7-*TTN* transformed AH109 pellet was added to 45mL of 2xYPDA media (**Appendix I**) in a 2L Erlenmeyer flask. The remaining 990µL of pre-transformed cDNA library was added to the same Erlenmeyer flask. The library mating culture was incubated overnight in a 311 DS incubator (Labnet International Inc., Edison, NJ, USA) set to 30°C and 200 rpm.

The mating culture was transferred to a sterile 50mL polypropylene centrifuge tube the following morning and centrifuged at 3000 rpm for five minutes in a Beckman model TJ-6 centrifuge (Beckman Coulter, Scotland, UK) to pellet the cells. The 2L Erlenmeyer flask used during the mating was rinsed twice with 40mL 2xYPDA media (**Appendix I**) and used to resuspend the mating culture pellet. Each time, the cells were re-pelleted by centrifuging at 3000 rpm for ten minutes. After the final centrifugation step, the supernatant was discarded and the pellet resuspended in 15mL of 0.5xYPDA media (**Appendix I**).

Library mating efficiency was determined by plating serial dilutions of a 100 μ L aliquots (1:10; 1:100; 1:000; 1:10 000) onto SD^{-Leu}, SD^{-Trp}, SD^{-Leu/-Trp} agar plates (**Appendix I**). The rest of the mating culture was plated onto TDO media (lacking leucine, tryptophan and histidine) plates (140mm) in 250 μ L aliquots. The plates were inverted and incubated at 30°C for two weeks in a Sanyo MIR262 stationary gravity ventilated incubator (Sanyo, Electronic Company Ltd, Ora-Gun, Japan).

2.12.4 Establishment of a library titre

To determine the number of library plasmids screened, serial dilutions of the mating culture were plated onto SD^{-Trp}, SD^{-Leu}, SD^{-Leu/-Trp} agar plates, inverted and then incubated in a Sanyo MIR262 stationary gravity ventilated incubator (Sanyo, Electronic Company Ltd, Ora-Gun, Japan) for four days. Colony counts were performed on the different plates in order to calculate the mating efficiency of the library mating as well as to calculate the number of library plasmids screened (**Appendix II**).

2.12.5 Control mating

Control matings were established alongside the library matings so as to assess whether the recombinant pGBKT7-*TTN* bait construct, transformed into the yeast strain AH109, had any negative effects on the yeast's ability to mate with the Y187 library strain. A 10 μ L aliquot of the bait culture and a single prey colony were co-inoculated in 1mL 0.5xYPDA, containing 10 μ g/mL kanamycin, in a 2mL tube. The culture was incubated for 24 hours in a YIH DER model LM-530 shaking incubator, set to 30°C and 200 rpm. Serial dilutions (1:10; 1:100; 1:1000; 1:10 000) were plated onto SD^{-Leu}, SD^{-Trp} and SD^{-Leu/-Trp} agar plates the following day and incubated for four days in a Sanyo MIR262 stationary ventilated incubator. Four days later, the colonies were counted and the mating efficiency was calculated (**Appendix II**). Control preys included non-recombinant pACT2 transformed into Y187 and the pTD1.1 control vector supplied by Clontech.

2.12.6 Detection of the activation of nutritional reporter genes

2.12.6.1 Selection of transformed *S.cerevisiae* colonies

The pGBKT7 bait vector contains the gene for the amino acid tryptophan. Therefore, yeast transformed with the pGBKT7-*TTN* bait construct can be selected for by plating on SD^{-Trp} plates. The plates were incubated in a Sanyo MIR262 stationary gravity ventilated incubator (Sanyo, Electronic Company Ltd, Ora-Gun, Japan) for four to six days. Colonies that grew successfully were selected and used for bait cultures and library matings.

2.12.6.2 Selection of diploid *S.cerevisiae* colonies containing putative interactor peptides

Colonies were plated onto TDO and quadruple dropout (QDO) agar plates in order to identify diploid yeast colonies in which an interaction between *TTN* and a prey protein had taken place. Colony growth on TDO agar plates indicated the activation of the nutritional *HIS3* reporter gene. Growth of colonies on QDO plates indicated the activation of both the *HIS3* and *ADE2* nutritional reporter genes. Activation of these nutritional reporter genes indicates an interaction between the *TTN* bait protein and the prey proteins.

The library mating culture was initially plated onto 140mm TDO plates and incubated for two weeks in a Sanyo MIR262 stationary gravity ventilated incubator (Sanyo, Electronic Company Ltd, Ora-Gun, Japan). The growth of the yeast on the TDO plates was checked regularly (every day) and colonies >2mm were selected and subsequently transferred onto QDO plates (**Appendix I**). The colonies on the QDO plates were incubated for three to six days at 30°C in a Sanyo MIR262 stationary gravity ventilated incubator (Sanyo, Electronic Company Ltd, Ora-Gun, Japan). The colour and growth of the colonies on QDO plates was monitored. Colonies that thrived on the QDO media were selected and subsequently transferred to QDO plates containing X- α -galactose (X- α -Gal). The reporter gene *MEL1* encodes the protein α -galactosidase, which is able to hydrolyse X- α -gal and produce a blue signal. Colonies were incubated on QDO plates containing X-alpha-gal for three to six days in order to check for activation of the *MEL1* reporter gene.

2.12.7 Detection of the activation of colourimetric reporter genes by means of X- α -Galactosidase assay

The activation of the *MEL1* reporter gene indicates the putative interaction between the bait and a prey protein. *MEL1* encodes the enzyme α -galactosidase and its activation can be observed by performing an X- α -galactosidase assay. The α -galactosidase produced from the activation of *MEL1* hydrolyses the X- α -Gal (5-Bromo-4-chloro-3-indolyl- α -D-galactopyranoside) in the plates, causing the yeast colonies to turn a distinctive blue colour.

Colonies that showed activation of *HIS3* and *ADE2* reporter genes on QDO agar plates (lacking histidine and adenine) were transferred to QDO plates containing 20mg/mL of X- α -GAL solution (BD biosciences, Clontech, Palo Alto, CA, USA). The plates were incubated at 30°C in a Sanyo MIR262 stationary gravity ventilated incubator (Sanyo, Electronic Company Ltd, Ora-Gun, Japan) for three to five days. After the incubation, the intensity of the blue colour in the yeast colonies that had been able to activate the *MEL1* reporter gene was assessed visually.

2.12.8 Rescuing of prey plasmids from diploid colonies

From the diploid (pGBKT7-*TTN* and prey pACT2 plasmids) yeast colonies that activated all three reporter genes (*HIS3*, *ADE2* and *MEL1*), the individual preys had to be isolated. The plasmid isolation facilitates the identification of the interactor proteins as well as to allow for the assessment of the specificity of the protein-protein interactions (**Section 2.12.9**).

Plasmid DNA was isolated from the yeast using the yeast plasmid purification method described in **Section 2.10.3** and subsequently transformed into competent *E.coli* DH5 α cells, as described in **Section 2.9.1**. The transformed *E.coli* were inoculated overnight in LB/Amp liquid medium (prey vector contains ampicillin resistance gene) (**Section 2.12.8**). Only the *E.coli* transformed with the prey plasmid would survive and grow in the LB/Amp liquid medium culture. The isolated prey plasmids were purified from the *E.coli* (**Section 2.10.1**) and transformed into the Y187 yeast strain as described in **Section 2.9.2**.

2.12.9 Interaction specificity testing - exclusion of non-specific bait and prey interactions

Interaction specificity tests were performed to determine whether the interaction detected by the Y2H analysis was specific between the pGBKT7-*TTN* bait construct and a particular prey peptide. The Y187 yeast, transformed with the isolated prey plasmids were individually mated with: yeast strain AH109 transformed with the pGBKT7-*TTN* construct; AH109 transformed with non-recombinant pGBKT7; AH109 transformed with the pGBKT7-53 control bait-plasmid, encoding murine p53 tumour suppressor protein (BD Bioscience, Clontech, Palo Alto, CA, USA), as well as AH109 transformed with a heterologous bait, namely SLITRK. SLITRK is expressed primarily in the brain, but may also show differential expression in other normal tissues and nervous system-derived tumours, thus it was a good control because it is not expressed in the heart. After selection for the expression of both bait and prey proteins, the diploid clones were plated onto TDO and QDO plates to test for the activation of nutritional reporter genes. The interaction specificity test determines

whether the prey peptides interacted with some or all of the heterologous baits or only with the *TTN* bait. Clones that only interacted with the *TTN* bait were considered to be possible putative interactors. These clones were thus sequenced so as to determine their identities.

2.13 COLOCALISATION

Colocalisation experiments were performed in order to confirm that two proteins (the bait protein and the various preys that were identified) are indeed localised to the same subcellular compartment, under representative cellular conditions. Proteins of interest were labelled with antibodies directed against each specific protein and fluorescently conjugated secondary antibodies were used for visualisation.

2.13.1 Immunostaining procedure

H9C2 cells were grown on sterile glass coverslips by seeding 40 000 cells per coverslip, placed inside 30mm culture dishes (Greiner Bio One, Cellstar, North Carolina, USA). The cells were maintained at 37°C and 5% CO₂ in Dulbecco's modified Eagle's medium (DMEM) (Lonza Walkerville Inc., Maryland, USA) supplemented with 10% fetal calf serum (Gibco, Invitrogen Corporation, Carlsbad, CA, USA), 4% glutamine and 1% penicillin/streptomycin (Gibco, Invitrogen Corporation, Carlsbad, CA, USA). One day later, or after the cells had grown to a confluency of 80%, the media was changed to differentiation media, containing DMEM with added 1% horse serum as well as 1% penicillin/streptomycin antibiotic. They subsequently were differentiated for seven to ten days in the same

differentiation media. The differentiation media was changed on the seventh day, in the event that the cells needed to be differentiated for longer. This differentiation was performed so that the cells could develop sarcomeric structures and express the protein titin, as well as other possible proteins of interest. The media was monitored to prevent contamination by means of checking daily under a light microscope and was changed during this time if necessary. After the cells had been differentiated, the media was removed and they were washed with PBS (**Appendix I**).

The cells were alcohol fixed/permeabilized by immersing the coverslips carrying the H9C2 cells in absolute methanol for five minutes at -20°C . The methanol was removed and a second fixation step performed by immersing the coverslips in 4% formaldehyde, made up in PBS (2.7mL of 37% formaldehyde in 22.3mL of PBS) for five minutes at room temperature. The cultures were then washed in PBS three times, each time for ten minutes at room temperature (removing the PBS between each step). The coverslips were removed from the culture dishes and placed with the cells facing upward onto pre-labelled temporary glass slides that had been covered with Parafilm M laboratory film (Pechiney Plastic Packaging, Chicago, IL. 60631) (prevents the liquid on each coverslip from running off). The cells were then incubated with a blocking solution of normal donkey serum (Santa Cruz Biotechnology, CA. USA), diluted 1:9 donkey serum:PBS, to reduce non-specific staining, for one hour at room temperature in a humidified chamber (to prevent coverslips from drying). The donkey serum was subsequently drained. Thereafter, the cells were incubated overnight with the appropriate pair of primary antibodies, diluted in PBS (**Table 2.5**) and sealed in a humidified chamber at 4°C . These pairs of antibodies were combinations of bait and

prey antibodies. Primary antibody concentrations needed to be optimised, but the ratios in **Table 2.5** were the ones used during the final colocalisation experiments.

Table 2.5. Antibody properties of the primary bait and prey antibodies used during the colocalisation analysis.

Protein	Concentration	Isotype	Dilution used and (amount of antibody)	Supplier and catalogue number	Monoclonal or polyclonal
TTN	3.5mg/mL	Mouse IgG2b	1:10 (73.15 μ L)	Abcam Inc. ab7034	Monoclonal
FLNC	0.12mg/mL	Rabbit IgG1	1:20 (13.31 μ L)	Sigma-Aldrich (Pty.) Ltd. HPA006135	Polyclonal
PEBP4	0.2mg/mL	Rabbit IgG1	1:30 (8.87 μ L)	Sigma-Aldrich (Pty.) Ltd. HPA025064	Polyclonal
H-FABP3	0.5mg/mL	Rabbit IgG1	1:15 (17.74 μ L)	Abcam Inc. ab46185	Polyclonal
MYOM2	0.09mg/mL	Rabbit IgG1	1:50 (4.0 μ L)	Sigma-Aldrich (Pty.) Ltd. HPA001765	Polyclonal
MYOM1	1.0mg/mL	Rabbit IgG1	1:50 (5.32 μ L)	Abcam Inc. ab111433	Polyclonal

Abbreviations: TTN, titin; FLNC, filamin C; PEBP4, phosphatidylethanolamine-binding protein 4; H-FABP3, heart-type fatty acid binding protein 3; MYOM2, myomesin 2; MYOM1, myomesin 1.

Table 2.6. Excitation and emission spectra of the secondary antibodies used during the colocalisation analysis.

Proteins	Secondary antibody	Excitation	Emission	Colour
TTN	Donkey-anti-mouse Alexa 488	495nm	519nm	Cyan-green
FLNC PEBP4 H-FABP3 MYOM2 MYOM1	Donkey-anti-rabbit Cy3	550nm	570nm	Red

Abbreviations: nm, nanometre; TTN, titin; FLNC, filamin C; PEBP4, phosphatidylethanolamine-binding protein 4; H-FABP3, heart-type fatty acid binding protein 3; MYOM2, myomesin 2; MYOM1, myomesin 1.

The following morning, the cells were washed with PBS three times, each time for ten minutes at room temperature (draining the PBS between each step). The cells were incubated with light sensitive secondary antibodies for 90 minutes at room temperature in a humidified chamber in the dark. Donkey-anti-mouse Alexa 488 was used for the titin bait antibody and donkey-anti-rabbit Cy3 was used for the preys (Table 2.6). Both secondary antibodies were diluted 1:500 in PBS. The cells were washed again with PBS three times, each time for ten minutes at room temperature (draining the PBS between each step), whilst being kept in the humidified chamber in the dark. Counterstaining for ten minutes with 10mg/mL Hoechst 33342, trihydrochloride, trihydrate (molecular weight: 615.99; catalogue number: H1399) (Invitrogen™ Life Technologies, South Africa) nuclear stain, diluted 1:200 in PBS, was then performed in a humidified chamber in the dark. The fluorescence

excitation/emission when the Hoechst is bound to double stranded DNA: 350/461nm. The coverslips were washed one final time with PBS at room temperature in the humidified chamber. The coverslips were subsequently mounted with the cells facing downward onto pre-labelled, ethanol cleaned glass slides. Mowiol (containing n-propylgallate as anti-fading agent), that had been centrifuged at maximum speed for one minute so as to spin down the anti-fading agent, was used as mounting media and sealant. The slides were then stored at room temperature in the dark for an hour so that the Mowiol could set. Thereafter, the slides were stored at 4°C until viewing.

The cells were observed at the University of Cape Town's department of Human Biology by means of the LSM 510 META with NLO (NLO = two photon laser) confocal microscope (Carl Zeiss, Germany) system. The confocal microscope is completely different from wide-field fluorescence microscopes. There is no camera involved, but the confocal microscope has photomultiplier tubes (PMTs) that detect the signals. The confocal microscope is a laser scanning microscope with a spectral detector and a pin hole that allows only the light that is in focus to be detected. It is therefore much better than a normal fluorescence microscope, which is a wide-field system, where the out of focus light blurs the image. This is thus eliminated with the confocal system.

The protein interactions were observed using the following lasers: Argon gas laser for the green emission (488nm line), solid state red laser at 561nm for red Cy3 phlorophore detection and MaiTai DeepSee 2 photon (infrared pulsed in femto seconds) laser at 750nm for acquiring the blue nuclear images. Emission was collected using a 63x/1.4 DIC (numerical aperture: 1.4; DIC = differential

interference contrast white light image) objective. The Zeiss LSM and ZEN 2009 software programmes were used for the image acquisition and analysis. Colocalised images were produced and based on the image data; colocalisation was calculated using the ZEN 2009 colocalisation analysis tool. The two fluorescent signals (bait and prey) to be measured were activated, the threshold was set and colocalisation was displayed as a new false colour image so as to determine whether the bait and various prey signals were indeed colocalised to the same subcellular compartment. Images were exported as 8 bit TIFFs with no compression.

CHAPTER 3**RESULTS****INDEX**

	PAGE
3.1 YEAST TWO-HYBRID ANALYSIS	91
3.1.1 Generation of Y2H construct	91
3.1.1.1 Sequence analysis of pGBKT7-<i>TTN</i> bait construct	91
3.1.2 Verification of the integrity of the Y2H construct by assessment of <i>S.cerevisiae</i> AH109 bait strain	91
3.1.2.1 Auto-activation test	92
3.1.2.2 Toxicity test	92
3.1.2.3 Mating efficiency of <i>S.cerevisiae</i> AH109 transformed with the Y2H construct	93
3.1.3 Y2H screening of pre-transformed cardiac cDNA library	95
3.1.3.1 <i>TTN</i> bait culture titre	95
3.1.3.2 Library titre	95
3.1.3.3 Library mating efficiency and number of clones screened	96
3.1.3.4 Nutritional selection of diploid <i>S.cerevisiae</i> colonies containing putative interactor peptides	97
3.1.3.5 X-α-Galactosidase assay	98
3.1.3.6 Heterologous mating – interaction specificity test	99
3.1.3.7 Sequence analysis	99

3.2 COLOCALISATION 101

3.2.1 Colocalisation of titin and FLNC, PEBP4, H-FABP3, MYOM2 and MYOM1 101

CHAPTER 3: RESULTS

3.1 YEAST TWO-HYBRID ANALYSIS

3.1.1 Generation of Y2H construct

3.1.1.1 Sequence analysis of pGBKT7-*TTN* bait construct

The sequence integrity of the pGBKT7-*TTN* clone obtained from ImaGenes was assessed by automated sequencing. Analysis of the sequence showed that the pGBKT7-*TTN* construct was in the correct reading frame and the nucleotide sequence was intact.

3.1.2 Verification of the integrity of the Y2H construct by assessment of *S.cerevisiae* AH109 bait strain

The pGBKT7-*TTN* bait construct was transformed into the *S.cerevisiae* yeast strain AH109 (Section 2.9.2), to be used during the yeast two-hybrid library screen. Successful transformants were identified by their ability to grow on SD^{-Trp} agar plates. The pGBKT7-*TTN* bait construct was subsequently assessed to determine whether it was able to autonomously activate the reporter genes, as well as to determine whether it was toxic to the *S.cerevisiae* cells.

3.1.2.1 Auto-activation test

The pGBKT7-*TTN* bait construct did not autonomously activate expression of the reporter genes. This was indicated by the lack of growth on SD^{-Ade}, SD^{-His} and SD^{-Leu} agar plates. The presence of growth of transformed *S.cerevisiae* AH109 cells on SD^{-Ura} indicated that the phenotype of the *S.cerevisiae* AH109 yeast strain remained intact after the transformation with pGBKT7-*TTN* bait construct. Thus, the activation of reporter genes during the library screen would be indicative of a putative bait-prey interaction.

3.1.2.2 Toxicity test

Growth curves of *S.cerevisiae* AH109 transformed with a) pGBKT7-*TTN* bait construct (AH109-pGBKT7-*TTN*) and b) non-recombinant pGBKT7 vector (AH109-pGBKT7) were created from OD₆₀₀ readings taken over a period of 24 hours (**Section 2.11.3**). The growth curves were compared alongside one another in order to determine whether the pGBKT7-*TTN* bait construct was toxic to *S.cerevisiae* strain AH109 (**Figure 3.1**). The empty pGBKT7 vector, when transformed into *S.cerevisiae* strain AH109, is non-toxic to the *S.cerevisiae* cells and was thus used as a positive growth control. The rate of growth of the AH109-pGBKT7-*TTN* bait strain, shown by the gradient of the linearized growth curve, is similar to that of the AH109-pGBKT7 positive control. This indicated that the pGBKT7-*TTN* bait construct did not inhibit the growth of *S.cerevisiae* AH109 and was thus non-toxic to the *S.cerevisiae* strain.

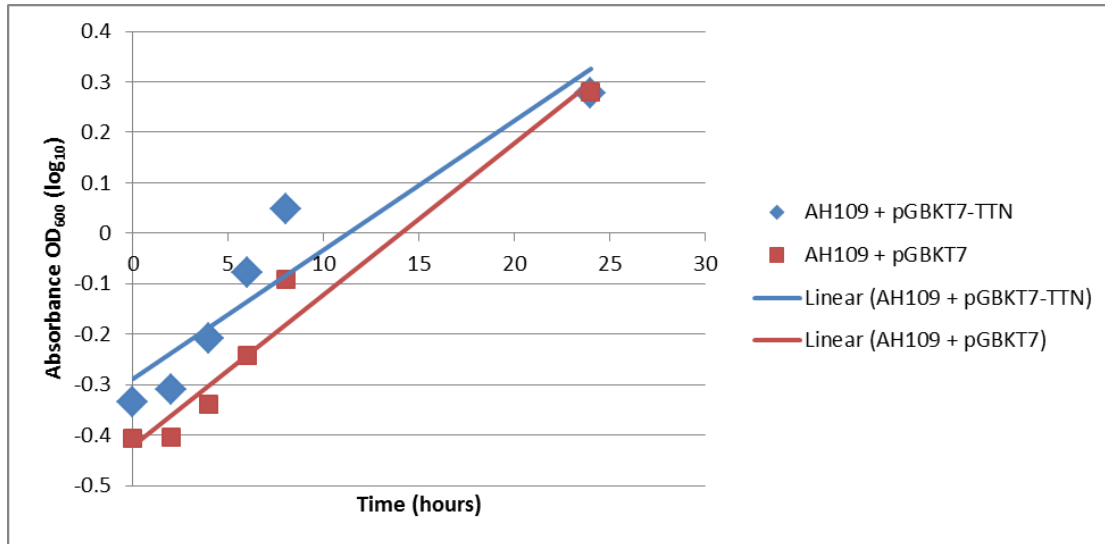


Figure 3.1. Linear growth curves of untransformed *S.cerevisiae* AH109 strain transformed with either non-recombinant pGBKT7 or pGBKT7-*TTN* bait constructs. Both the non-recombinant pGBKT7 and the pGBKT7-*TTN* bait construct grew at a similar rate, as indicated by the comparable gradients of the linearized growth curves. These results indicated that the bait construct did not impede the growth of the host *S.cerevisiae* AH109 strain.

3.1.2.3 Mating efficiency of *S.cerevisiae* AH109 transformed with the Y2H construct

Small-scale yeast mating experiments were conducted to evaluate whether the *TTN* bait construct affected the mating efficiency of the host *S.cerevisiae* AH109 strain. The mating efficiency of the *TTN* bait construct (transformed into AH109) mated with the standard prey transformants, namely pACT2 and pTD1.1 (in Y187) was compared to the mating efficiency of a control plasmid, namely pGBKT7-53 (in AH109) mated with the same standard prey transformants (pACT2 and pTD1.1 in Y187) (**Section 2.11.4**). The results of the mating efficiency tests are indicated in **Table 3.1**

and **Table 3.2** and the calculations are given in detail in **Appendix II**. The mating efficiency percentage recommended by the manufacturer of the MATCHMAKER™ Y2H system (BD Biosciences, Clontech, Paulo Alto, CA, USA.) is a minimum of 2%.

Library mating efficiency was calculated by using the results of the growth of library mating progeny *S.cerevisiae* colonies on SD agar plates (**Section 3.1.2.3**) as shown in **Table 3.1**. Calculations designated that the test library mating efficiency was 3.87%, which was higher than the recommended minimum of 2% and therefore showed that the library mating efficiency was within acceptable limits to continue with Y2H analysis. The calculations indicated that at least the minimum number of 10^6 pretransformed cardiac cDNA library clones would be screened using the pGBKT7-*TTN* construct.

Table 3.1. Mating efficiency of AH109 pGBKT7-*TTN* as determined by growth of colonies on selection media.

	Bait mating (1)	Control mating (1)	Bait mating (2)	Control mating (2)
	pGBKT7- <i>TTN</i> x pACT2	pGBKT7-53 x pACT2	pGBKT7- <i>TTN</i> x pTD1.1	pGBKT7-53 x pTD1.1
Mating efficiency (%)	3.87	22.22	9.36	8.42

3.1.3 Y2H screening of pre-transformed cardiac cDNA library

Following all the verification tests performed in **Section 3.1.2**, the AH109 pGBKT7-*TTN* bait strain was used to screen a cardiac cDNA library as described in **Section 2.12**.

3.1.3.1 *TTN* bait culture titre

The bait culture titre prior to the library mating was established by performing a haemocytometric cell count (**Appendix II**). The total number of cells counted in five of the 25 squares was 131. According to the calculation in **Appendix II**, the titre of the bait culture was equal to 1.31×10^9 colony forming units per millilitre (cfu/mL).

3.1.3.2 Library titre

The library titre was also determined prior to the library mating (**Section 2.12.4**). After four days of growth, 1068 colony forming units (cfu) were counted on the SD^{-Leu} agar plates onto which 100 μ L of 1:10 000 dilution of the library had been plated. The library titre was calculated according to the calculation shown in **Appendix II**. A library titre of 1.068×10^8 cfu/mL was calculated (**Appendix II**), which was confirmation of the expected titre specified by the manufacturer.

3.1.3.3 Library mating efficiency and number of clones screened

The library mating efficiency (**Section 2.12.3**) was calculated according to the calculation given in **Appendix II** by counting the number of progeny *S.cerevisiae* cells that were on the SD^{-Leu}, SD^{-Trp} and SD^{-Leu-Trp} agar plates (**Table 3.2**). The library mating efficiency was calculated as 25%. This was in accordance with the test mating efficiency of 3.87% (pGBKT7-*TTN* x pACT2). The library mating was carried out under the same conditions as the test mating and the bait titre as well as the library titre was at acceptable levels. Based on the results of the library mating efficiency, the number of pretransformed heart cDNA clones that were screened using the pGBKT7-*TTN* construct was calculated (**Appendix II**) as 1.35×10^6 independent clones (final resuspension volume = 13.5mL). It is, however, still possible that more putative interactors for the C-terminal region of *TTN* could be identified during future Y2H screens, even though there were more than the recommended number of clones screened.

Table 3.2. Mating efficiency of library mating (pACT2 heart cDNA in Y187 x pGBKT7-bait construct in AH109).

Mating culture dilution	Library mating: pGBKT7- <i>TTN</i> x pACT2			
	1:10	1:100	1:1000	1:10000
SD ^{-Leu}	*	*	*	4
SD ^{-Trp}	*	*	*	1160
SD ^{-Leu-Trp}	*	*	*	1
Mating efficiency (%)	25			

* = uncountable number of colonies

3.1.3.4 Nutritional selection of diploid *S.cerevisiae* colonies containing putative interactor peptides

The first nutritional selection stage was used to select diploid yeast colonies with the ability to activate expression of the *HIS3* reporter gene, using TDO plates. A total of 65 colonies were able to activate the *HIS3* expression.

During the second nutritional selection stage, QDO agar plates (SD^{-Trp/-Leu/-His/-Ade}) were used to select for diploid yeast colonies with the ability to activate the expression of both *HIS3* and *ADE2* reporter genes. From the 65 colonies that were able to activate the *HIS3* reporter gene, only 49 were able to additionally activate the *ADE2* reporter gene.

3.1.3.5 X- α -Galactosidase assay

The 49 yeast colonies that showed expression of *HIS3* and *ADE2* were then assessed for the ability to activate the *MEL1* reporter gene. The presence of α -galactosidase, which is the enzyme encoded by *MEL1*, caused the X- α -gal on the QDO X- α -gal indicator agar plates to hydrolyse and thus produced blue colonies. Colonies were scored as blue, white/blue or white/pink/blue. Eleven of the 49 colonies that had passed the nutritional selection were able to activate the *MEL1* reporter gene (**Table 3.3**).

Table 3.3. Activation of the *HIS3* & *ADE2* and *MEL1* reporter genes by prey-*TTN* interactions.

Colony Number	Growth on QDO	X- α -Galactosidase assay
	(<i>HIS3</i> & <i>ADE2</i> activation)	(<i>MEL1</i> activation)
10	+++	++ (very light blue)
15	+++	+++ (blue)
29	++++	+++ (blue)
32	+++	++ (very light blue)
35	+++	++ (very light blue)
44	++++	+++ (blue)
74	++++	++++ (very blue)
84	++++	++++ (very blue)
99	++++	+++ (blue)
100	++++	+++ (blue)
109	+++	+++ (blue)

Abbreviations: QDO, solid media lacking leucine, tryptophan, histidine and adenine. Growth of clones on solid media: +++++, very good; +++, good; ++, weak; +, very weak.

3.1.3.6 Heterologous mating – interaction specificity test

The prey plasmids of the eleven colonies that were able to activate all three of the reporter genes were salvaged from their diploid colonies by means of the protocol described in **Section 2.12.8**. Each of the preys was used in heterologous mating experiments to test the specificity of the various bait-prey interactions. The interaction specificity test was performed, as explained in **Section 2.12.9**. Prey colonies that grew when they had been mated with pGBKT7 were excluded. Any activation of the Gal4-responsive reporters, with the lack of the bait protein, was considered to be a false positive interaction. The results indicated that from the initial eleven prey colonies that were able to activate all three of the reporter genes, just five showed binding specificity towards the titin bait protein. These five colonies were subsequently sequenced to classify the putative interacting proteins.

3.1.3.7 Sequence analysis

The five colonies that passed the nutritional selection levels, the α -galactosidase assay as well as the heterologous mating experiment were sequenced to ascertain the protein coded for by the prey insert. The sequence data was BLAST searched against the Genbank DNA database using the BLASTn (genomic hit) and BLASTp (in-frame hit) (<http://www.ncbi.nlm.nih.gov/Entrez>). The five prey plasmids encoded in-frame proteins namely filamin C (FLNC), phosphatidylethanolamine-binding protein 4 (PEBP4), heart-type fatty acid binding protein 3 (H-FABP3), myomesin 2 (MYOM2) and myomesin 1 (MYOM1). The interactions were then subjected to further verification in mammalian cells.

Table 3.4. Identification of plausible TTN interacting clones from the Y2H screen.

Colony Number	GENOMIC HIT		Location	Function
	BLASTn Acc# (e-value)	Identity		
29 and 44	NG_011807.1	Homo sapiens filamin C, gamma (FLNC), RefSeqGene on chromosome 7	Cortical cytoplasm	Crosslink actin filaments into orthogonal networks and participate in the anchoring of membrane proteins for the actin cytoskeleton.
32 and 99	NM_144962.2	Homo sapiens phosphatidyl ethanolamine -binding protein 4 (PEBP4), mRNA	Within most human tissues, especially tumour cells	Lipid binding and inhibition of serine proteases.
84 and 109	NM_004102.3	Homo sapiens fatty acid binding protein 3, muscle and heart (H-FABP3), mRNA	Cytoplasm	Participate in the uptake, intracellular metabolism and/or transport of long-chain fatty acids. May also be responsible in the modulation of cell growth and proliferation.
74 and 100	NM_003970.2	Homo sapiens myomesin 2 (MYOM2), mRNA	Major component of the vertebrate myofibrillar M band	MYOM2 has a unique N-terminal domain followed by 12 repeat domains with strong homology to either fibronectin type III or immunoglobulin C2 domains.
10	NG_032120.1	Homo sapiens myomesin 1 (MYOM1), RefSeqGene on chromosome 18	Major component of the vertebrate myofibrillar M band	Binds myosin, titin, and light meromyosin. This binding is dose dependent.

Abbreviation: Acc#; accession number.

3.2 COLOCALISATION

3.2.1 Colocalisation of titin and FLNC, PEBP4, H-FABP3, MYOM2 and MYOM1

Colocalisation by means of confocal microscopy was used to determine whether titin colocalises with FLNC, PEBP4, H-FABP3, MYOM2 and MYOM1 within the mammalian cell (**Figure 3.2, Figure 3.3, Figure 3.4, Figure 3.5** and **Figure 3.6**). In the images below, the single colour channels (A, C and D), cells' structures (B), overlay (E) of the three single colour channels as well as the colocalisation (F) of titin and each prey protein are displayed. The results acquired from the colocalisation indicate a significant degree of colocalisation of titin with FLNC, PEBP4 and H-FABP3 in H9C2 cells. Although a moderate degree of colocalisation can be seen in the images of titin with MYOM2 and MYOM1, they were not significant and can thus not be recorded as true interactors in this study. This was contrary to what was expected and is discussed further in **Section 4.5.3**.

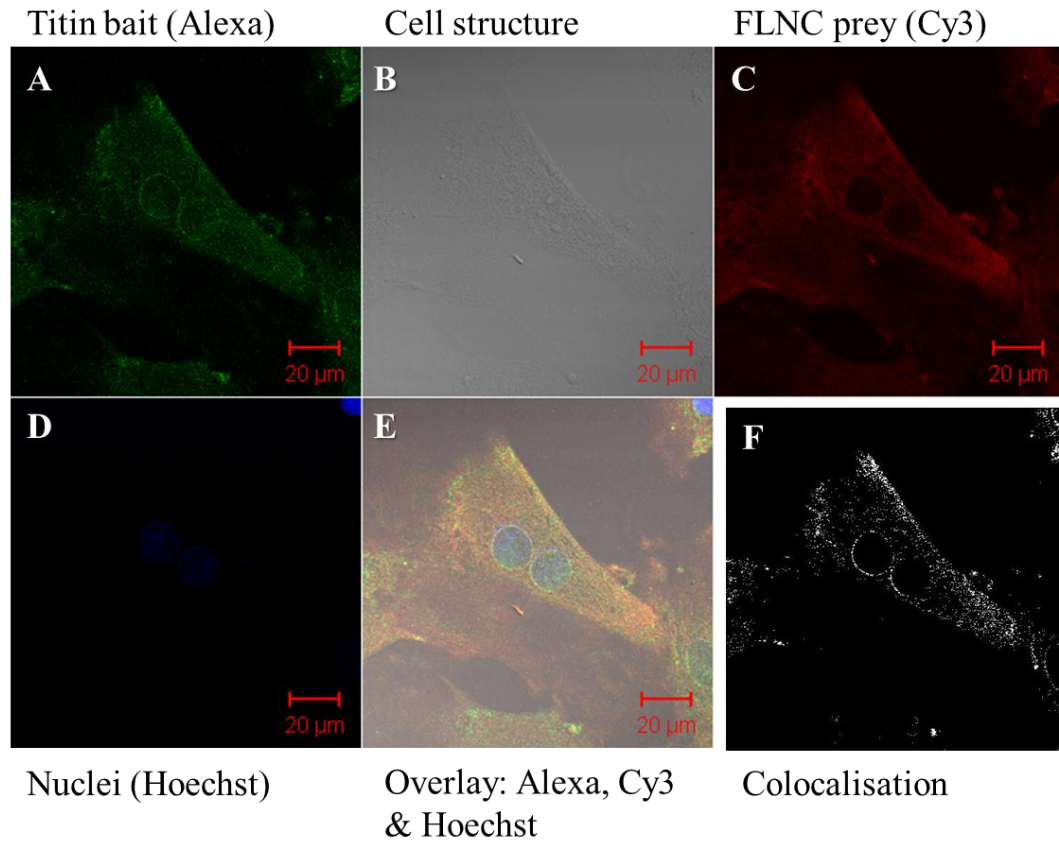


Figure 3.2. Confocal imaging of titin and FLNC. (A) Titin antibody labelled with Alexa 488 (green). (B) Cellular structure. (C) FLNC antibody labelled with Cy3 (red). (D) Nuclei labelled with Hoechst. (E) Overlay of images A, C and D. (F) Colocalisation of titin and FLNC (white).

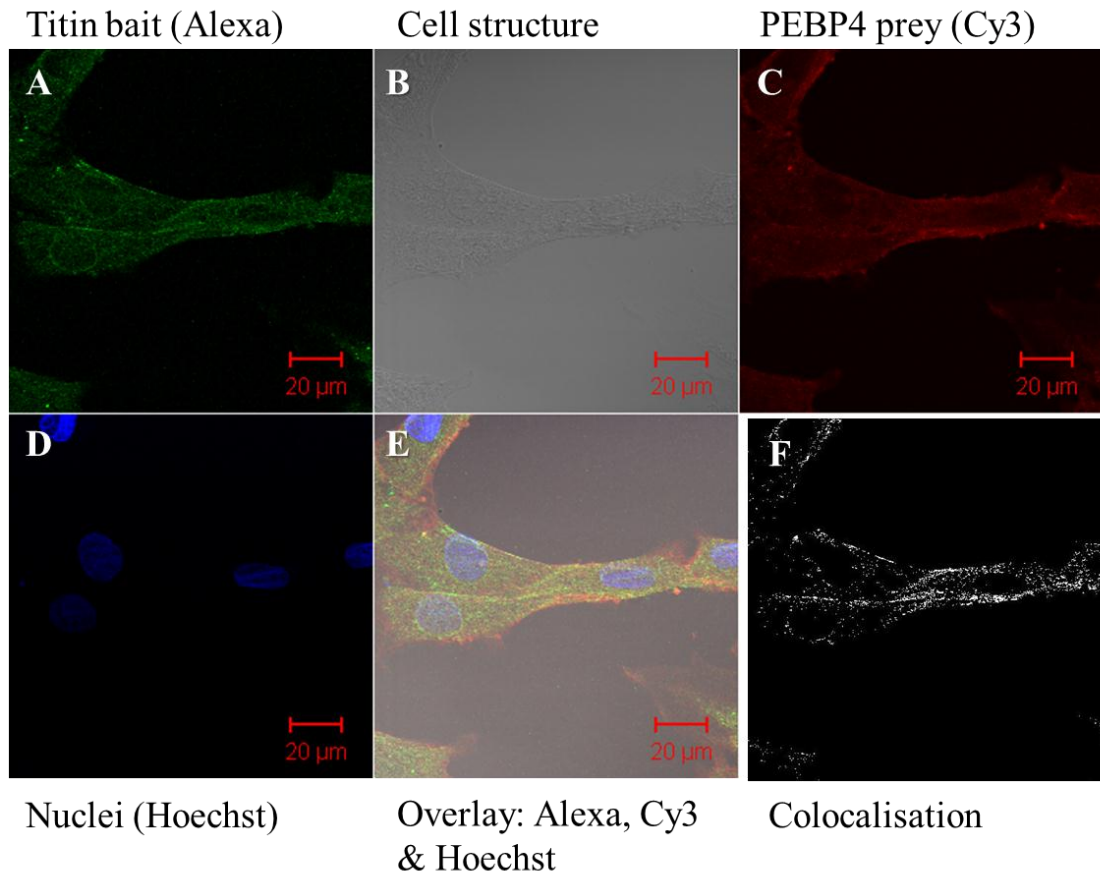


Figure 3.3. Confocal imaging of titin and PEBP4. (A) Titin antibody labelled with Alexa 488 (green). (B) Cellular structure. (C) PEBP4 antibody labelled with Cy3 (red). (D) Nuclei labelled with Hoechst. (E) Overlay of images A, C and D. (F) Colocalisation of titin and PEBP4 (white).

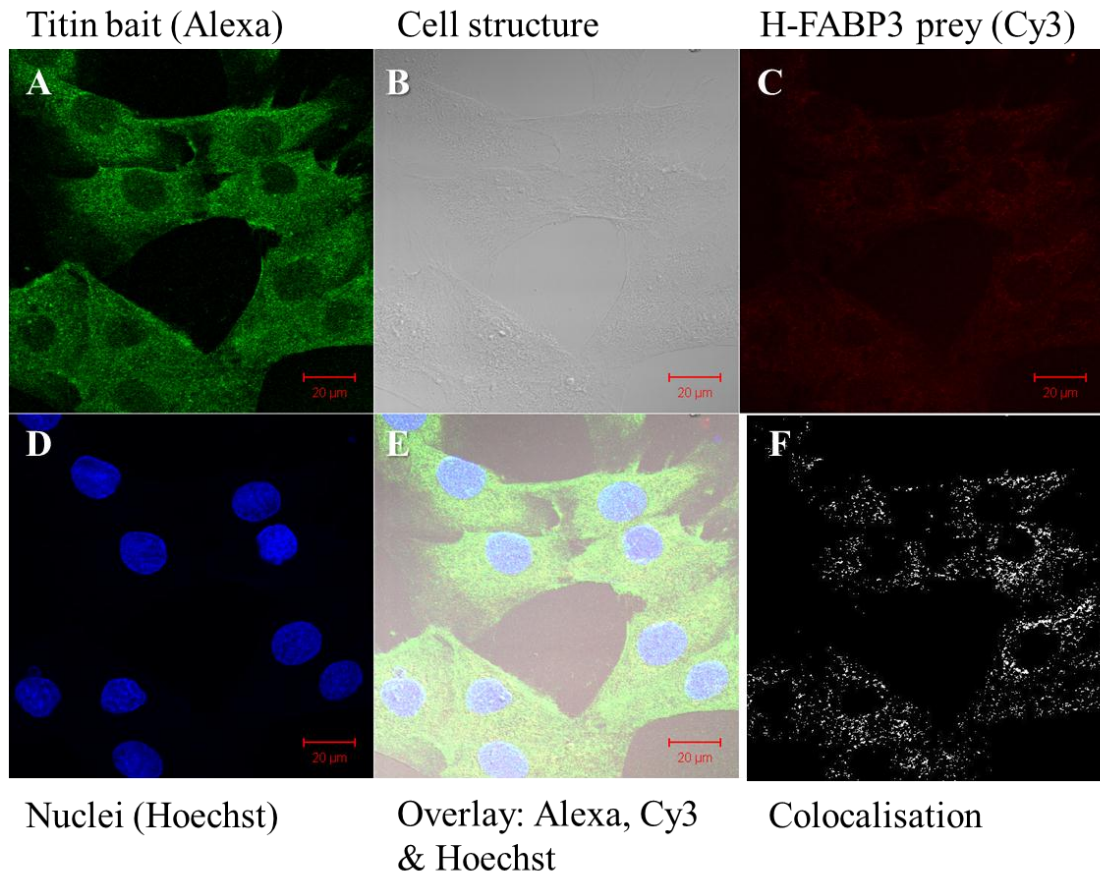


Figure 3.4. Confocal imaging of titin and H-FABP3. (A) Titin antibody labelled with Alexa 488 (green). (B) Cellular structure. (C) H-FABP3 antibody labelled with Cy3 (red). (D) Nuclei labelled with Hoechst. (E) Overlay of images A, C and D. (F) Colocalisation of titin and H-FABP3 (white).

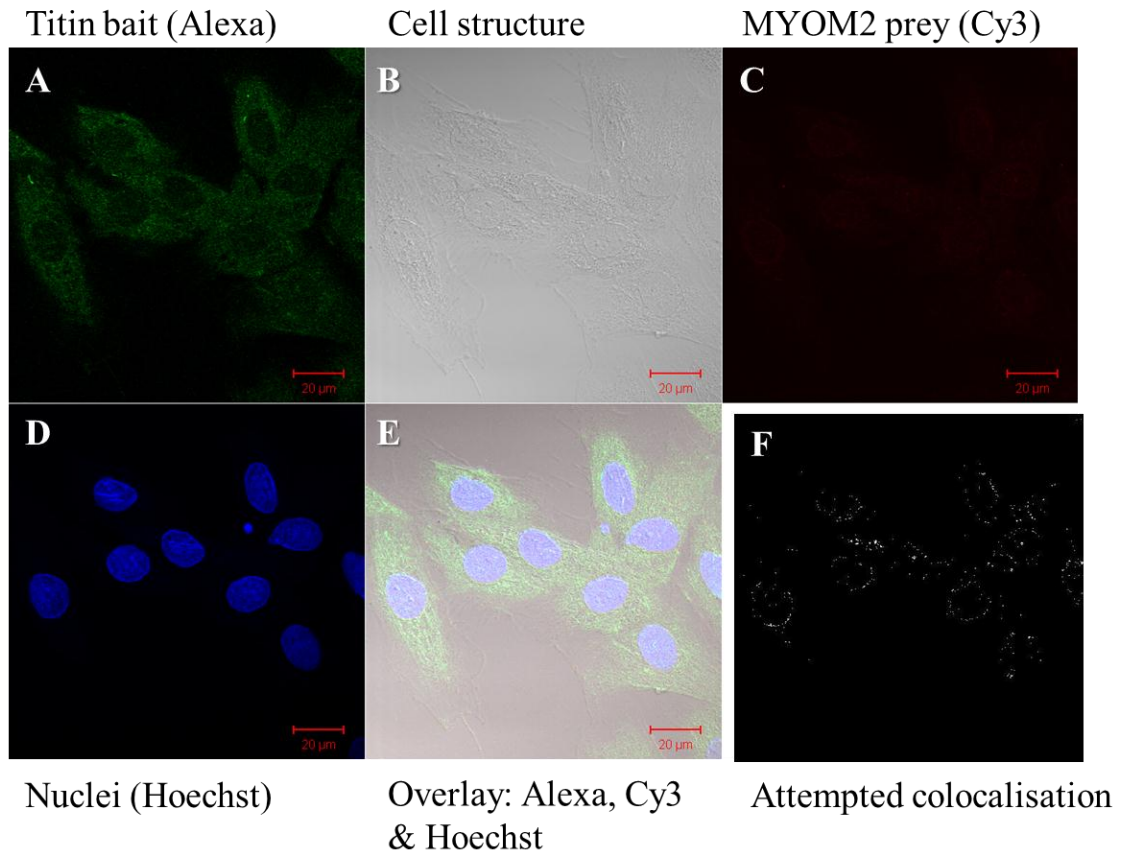


Figure 3.5. Confocal imaging of titin and MYOM2. (A) Titin antibody labelled with Alexa 488 (green). (B) Cellular structure. (C) MYOM2 antibody labelled with Cy3 (red). (D) Nuclei labelled with Hoechst. (E) Overlay of images A, C and D. (F) Attempted colocalisation of titin and MYOM2 (white).

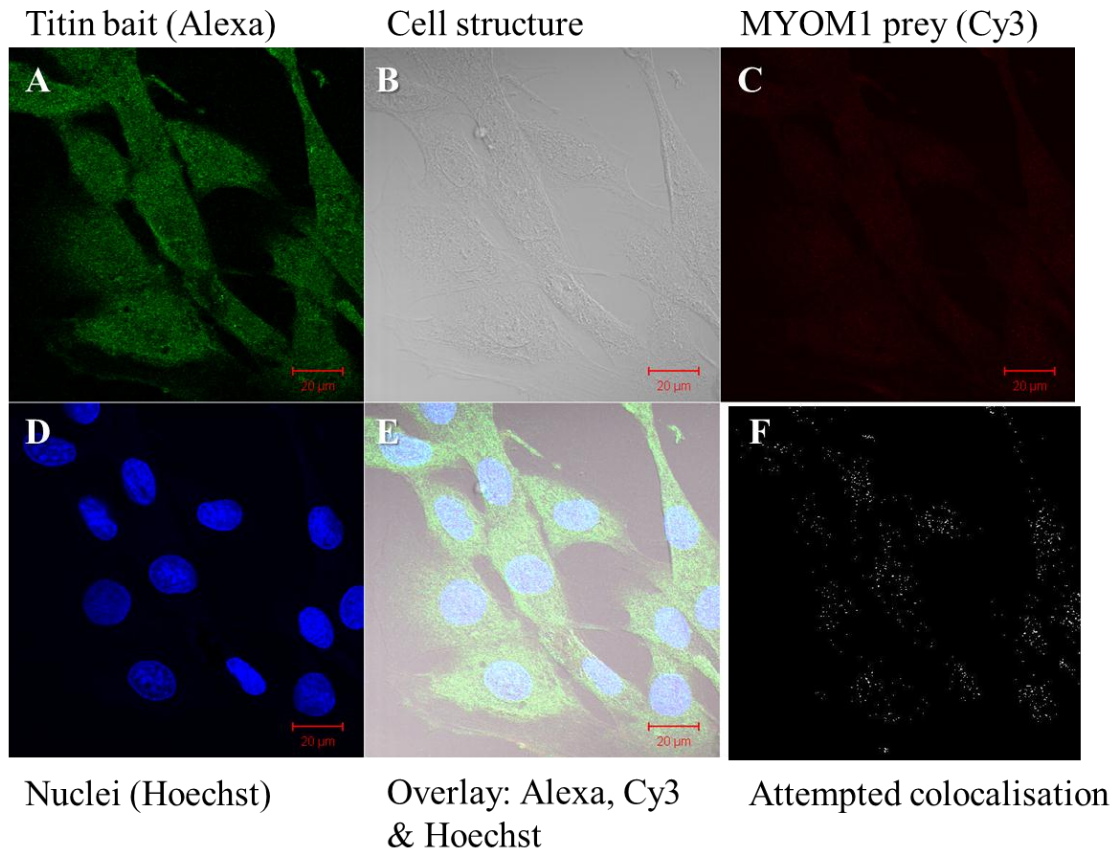


Figure 3.6. Confocal imaging of titin and MYOM1. (A) Titin antibody labelled with Alexa 488 (green). (B) Cellular structure. (C) MYOM1 antibody labelled with Cy3 (red). (D) Nuclei labelled with Hoechst. (E) Overlay of images A, C and D. (F) Attempted colocalisation of titin and MYOM1 (white).

Table 3.5. Colocalisation of titin and FLNC.

Scatter Region	Number Pixels	Area ($\mu\text{m} \times \mu\text{m}$)	Relative Area (%)	Mean Intensity Ch2-T1	Mean Intensity Ch3-T2	Standard Deviation Ch2-T1	Standard Deviation Ch3-T2	Colocalisation Coefficient Ch2-T1	Colocalisation Coefficient Ch3-T2	Weighted Coloc. Coefficient Ch2-T1	Weighted Coloc. Coefficient Ch3-T2	Overlap Coefficient	Correlation R	Correlation R x R
1	2785	216.81	1.1	72	36	16	8							
2	31231	2431.36	11.9	28	63	13	13							
3	4257	331.41	1.6	74	70	18	17	0.605	0.120	0.611	0.132	0.9	0.05	0.00

Abbreviations: Ch2 T1, image channel for green; Ch3 T2, image channel for red; Coloc., Colocalisation; R, correlation coefficient.

Table 3.6. Colocalisation of titin and PEBP4.

Scatter Region	Number Pixels	Area ($\mu\text{m} \times \mu\text{m}$)	Relative Area (%)	Mean Intensity Ch2-T1	Mean Intensity Ch3-T2	Standard Deviation Ch2-T1	Standard Deviation Ch3-T2	Colocalisation Coefficient Ch2-T1	Colocalisation Coefficient Ch3-T2	Weighted Coloc. Coefficient Ch2-T1	Weighted Coloc. Coefficient Ch3-T2	Overlap Coefficient	Correlation R	Correlation R x R
1	3235	251.85	1.2	76	40	21	7							
2	16443	1280.10	6.3	30	65	15	16							
3	3181	247.64	1.2	79	68	20	17	0.496	0.162	0.503	0.168	0.9	0.09	0.01

Abbreviations: Ch2 T1, image channel for green; Ch3 T2, image channel for red; Coloc., Colocalisation; R, correlation coefficient.

Table 3.7. Colocalisation of titin and H-FABP3.

Scatter Region	Number Pixels	Area ($\mu\text{m} \times \mu\text{m}$)	Relative Area (%)	Mean Intensity Ch2-T1	Mean Intensity Ch3-T2	Standard Deviation Ch2-T1	Standard Deviation Ch3-T2	Colocalisation Coefficient Ch2-T1	Colocalisation Coefficient Ch3-T2	Weighted Coloc. Coefficient Ch2-T1	Weighted Coloc. Coefficient Ch3-T2	Overlap Coefficient	Correlation R	Correlation R x R
1	96771	7533.72	36.9	83	31	29	8							
2	552	42.97	0.2	36	59	10	9							
3	5252	408.87	2.0	100	60	34	8	0.051	0.905	0.061	0.907	0.9	0.11	0.01

Abbreviations: Ch2 T1, image channel for green; Ch3 T2, image channel for red; Coloc., Colocalisation; R, correlation coefficient.

Table 3.8. Colocalisation of titin and MYOM2.

Scatter Region	Number Pixels	Area ($\mu\text{m} \times \mu\text{m}$)	Relative Area (%)	Mean Intensity Ch2-T1	Mean Intensity Ch3-T2	Standard Deviation Ch2-T1	Standard Deviation Ch3-T2	Colocalisation Coefficient Ch2-T1	Colocalisation Coefficient Ch3-T2	Weighted Coloc. Coefficient Ch2-T1	Weighted Coloc. Coefficient Ch3-T2	Overlap Coefficient	Correlation R	Correlation R x R
1	26911	2095.05	10.3	52	19	16	5							
2	964	75.05	0.4	21	38	9	6							
3	543	42.27	0.2	57	40	20	12	0.020	0.360	0.022	0.369	0.9	-0.01	0.00

Abbreviations: Ch2 T1, image channel for green; Ch3 T2, image channel for red; Coloc., Colocalisation; R, correlation coefficient.

Table 3.9. Colocalisation of titin and MYOM1.

Scatter Region	Number Pixels	Area ($\mu\text{m} \times \mu\text{m}$)	Relative Area (%)	Mean Intensity Ch2-T1	Mean Intensity Ch3-T2	Standard Deviation Ch2-T1	Standard Deviation Ch3-T2	Colocalisation Coefficient Ch2-T1	Colocalisation Coefficient Ch3-T2	Weighted Coloc. Coefficient Ch2-T1	Weighted Coloc. Coefficient Ch3-T2	Overlap Coefficient	Correlation R	Correlation R x R
1	72371	5634.15	27.6	69	24	22	6							
2	353	27.48	0.1	32	50	8	7							
3	937	72.95	0.4	72	50	24	8	0.013	0.726	0.013	0.727	0.9	-0.01	0.00

Abbreviations: Ch2 T1, image channel for green; Ch3 T2, image channel for red; Coloc., Colocalisation; R, correlation coefficient.

CHAPTER 4
DISCUSSION

INDEX

	PAGE
4.1 YEAST TWO-HYBRID STUDY TO IDENTIFY INTERACTORS OF TITIN	112
4.2 TITIN-FLNC INTERACTION	114
4.2.1 The functions of FLNC	114
4.2.2 The functional significance of the titin-FLNC interaction	115
4.3 TITIN-PEBP4 INTERACTION	116
4.3.1 The functions of PEBP4	117
4.3.2 The functional significance of the titin-PEBP4 interaction	118
4.4 TITIN-H-FABP3 INTERACTION	119
4.4.1 The functions of H-FABP3	119
4.4.2 The potential role of H-FABP3 in hypertrophic cardiomyopathy and heart disease	120
4.4.3 The functional significance of the titin-H-FABP3 interaction	123
4.5 TITIN-MYOM2 AND TITIN-MYOM1 INTERACTIONS	124

	111
4.5.1 The functions of MYOM2 and MYOM1	125
4.5.2 The potential role of MYOM2 and MYOM1 in hypertrophy or hypertrophic cardiomyopathy	128
4.5.3 The functional significance of the titin-MYOM2 and titin-MYOM1 interactions	130
4.6 LIMITATIONS OF THE PRESENT STUDY	132
4.7 LIMITATIONS OF Y2H ANALYSIS	132
4.8 LIMITATIONS OF COLOCALISATION	134
4.9 THE FUTURE OF THIS RESEARCH	135
4.10 CONCLUSION	136

CHAPTER 4: DISCUSSION

4.1 YEAST TWO-HYBRID STUDY TO IDENTIFY INTERACTORS OF TITIN

Titin (*TTN*) is a known HCM susceptibility gene (Satoh *et al.*, 1999), thus the protein titin was a good candidate to include in an investigation into the pathophysiology and molecular aetiology of HCM.

Titin has a number of functions related to muscle assembly and passive resting tension (Maruyama, 1997) as well as myofibril elasticity and structural integrity (Bang *et al.*, 2001b). Granzier and Labeit hypothesised in 2002 that titin may play a role in the modulation of actomyosin interactions and that titin has been linked to membrane channels, protein turnover as well as gene expression (Granzier and Labeit, 2002). Titin also has been shown to have significant functions in both passive and contracting myocardium (Granzier and Labeit, 2002). Furthermore, Linke showed in 2007 that titin plays an important role in myocardial stress-sensing and mechanical dysfunction (Linke, 2008).

In the present study, we hypothesised that since titin is known to play a role in the development of hypertrophy, any protein interacting with it may also play a role in the development of hypertrophy. We therefore set out to identify novel protein interactors of the 11-domain super-repeat region of titin.

A pre-transformed adult heart cDNA library was screened using a bait containing the scaffold region of titin, located within the C-zone of the sarcomere, to identify potential interactors using yeast two-hybrid (Y2H) methodology.

Interacting partners of other regions of titin have been identified by previous studies such as myomesin (Wang *et al.*, 1998; Auerbach *et al.*, 1999; Schoenauer *et al.*, 2005) filamin (Linke, 2008), obscurin (Granzier and Labeit, 2007), actin (Linke, 2008) and myosin (Linke, 2008) among others; however, no published data is available for interacting partners of the scaffold region. Five putative interactors of the scaffold region of titin were identified in this study. These interactions were subsequently verified in mammalian cells using colocalisation in H9C2 rat cardiomyocytes, providing further evidence for possible interactions between titin and these proteins.

As can be seen from the colocalisation experiments, titin localises with filamin C (FLNC), phosphatidylethanolamine-binding protein 4 (PEBP4), heart-type fatty acid binding protein 3 (H-FABP3), myomesin 2 (MYOM2) and myomesin 1 (MYOM1). It should be noted that, while the colocalisation experiments are not able to verify physical interactions, they do indicate that two or more proteins occupy the same cellular space which makes a physical interaction probable. Based on this limitation, these identified interactions need to be further verified by means of other techniques such as Western blotting and co-immunoprecipitation (co-IP); phage display; or mass-spectrometry, but this would only indicate a complex of interacting proteins and not specific proteins that interact with one another. For the purpose of this study, speculations of the functional role that these interactions could play in HCM will be made. The following section will discuss the results of the present study.

4.2 TITIN-FLNC INTERACTION

The filamin C protein (FLNC) was identified and verified as an interactor of the scaffold region of titin. The characteristics and functions of FLNC will be discussed and a possible functional role for the interaction between FLNC and titin will be proposed.

4.2.1 The functions of FLNC

Human filamins are a family of large cytoskeletal proteins consisting of three isoforms, namely filamins A, B and C (Kley *et al.*, 2007). One of their most important functions is to crosslink F-actin filaments into a dynamic three dimensional meshwork, or alternatively into parallel bundles (Kley *et al.*, 2007).

Filamin C is the most expressed filamin isoform in striated muscles (Van der Ven *et al.*, 2006). It is found in myofibrillar Z-discs binding to γ -filamin/ABP-L, α -actinin and telethonin binding protein of the Z-disk (FATZ) and myotilin, as well as in myotendinous junctions and intercalated discs (Van der Ven *et al.*, 2006).

Filamin C plays an essential role in the maintenance of the structural integrity of cardiac and skeletal muscles during contraction (Fujita *et al.*, 2012). The expression of FLNC starts at the onset of somitogenesis and is specifically expressed in cardiac and skeletal muscles where it plays a role in actin crosslinking (Fujita *et al.*, 2012). The *in vivo* function of FLNC is not fully understood; however, mutations in the FLNC gene (*FLNC*) have been shown to cause a myofibrillar myopathy which is

morphologically categorised by the focal destruction of myofibrils, altered myofibril organization as well as the abnormal accumulation of several proteins in skeletal (Kley *et al.*, 2007) and cardiac muscle fibres (Fujita *et al.*, 2012). This could be of importance in HCM, as abnormal myofibrillar organisation is observed in the hearts of patients with HCM (McLeod *et al.*, 2009).

Furthermore, FLNC has been shown to work together with Ras GTPase-activating protein (RasGAP) and RasGAP SH3 domain-binding protein to regulate myocyte growth (Lypowy *et al.*, 2005). Moreover, FLNC and RasGAP have been shown to be linked to mRNA stabilization as well as localization and were found to be up-regulated in various hypertrophy models (Lypowy *et al.*, 2005).

4.2.2 The functional significance of the titin-FLNC interaction

Previous studies have demonstrated that the N-terminal of smooth muscle titin contains both filamin as well as α -actinin binding sites (Luther and Squire, 2002; Linke, 2008), while myosin binding sites have been identified at the C-terminal end (**Figure 1.9**) (Granzier and Labeit, 2007; Tskhovrebova and Trinick, 2010; Czajlik *et al.*, 2012). Due to titin's N-terminal seven-domain and C-terminal 11-domain super-repeats being structurally similar, it is thus possible that the C-terminal end of titin could also interact with FLNC, as this study has showed.

Smooth muscle titin is able to provide physical integrity and passive elasticity to smooth muscles by linking dense bodies to thick filaments (Granzier and Labeit, 2007). It is possible that the *FLNC* gene could be a candidate for cardiac diseases,

especially cardiomyopathies that are associated with hypertrophy or developmental defects (Van der Ven *et al.*, 2006).

Protein kinase B (PKB) plays an important role in mediating some of the metabolic actions of insulin as well as the anti-apoptotic effects of survival factors (Murray *et al.*, 2004). Interestingly, FLNC has been identified as a new physiological substrate of PKB α using kinase substrate tracking and elucidation (KESTREL) (Murray *et al.*, 2004). Insulin was shown to induce the phosphorylation of FLNC in cardiac muscle, but only in cardiac muscle that expresses 3-phosphoinositide-dependent kinase 1 (PDK1) which is the upstream activator of PKB α (Murray *et al.*, 2004). This anti-apoptotic link to FLNC could play a role in the pathogenesis of HCM because many HCM patients progress to heart failure due to cardiomyocyte apoptosis (Arad *et al.*, 2002). It is therefore possible that the titin-FLNC interaction could indirectly influence anti-apoptotic pathways within the heart and therefore play a role in the regulation of cardiac hypertrophy.

4.3 TITIN-PEBP4 INTERACTION

Phosphatidylethanolamine-binding protein 4 was identified and verified as an interactor of titin. The characteristics and functions of PEBP4 will be discussed in the following sections and a potential functional role for the interaction between PEBP4 and titin will be suggested.

4.3.1 The functions of PEBP4

The phosphatidylethanolamine-binding proteins, which include PEBP4, are a family of evolutionarily conserved serine protease inhibitors and lipid binding proteins (Hengst *et al.*, 2001). Furthermore, the crystal structure of human phosphatidylethanolamine-binding protein suggests that it plays a role in membrane signal transduction (Banfield *et al.*, 1998).

Phosphatidylethanolamine-binding protein 4 is a 227 amino acid lysosomal protein, with a molecular mass of 25.7kDa, identified by Wang and co-workers in 2004 (Wang *et al.*, 2004). It was found to be expressed within most human tissues and exceedingly expressed within tumour cells (Wang *et al.*, 2004). Phosphatidylethanolamine-binding protein 4 is an anti-apoptotic molecule and the silencing of PEBP4 expression was shown to sensitize breast cancer cells to tumour necrosis factor- α -induced apoptosis as well as cell growth arrest, which was caused by the increased mitogen-activated protein kinase activation and the enhanced phosphatidylethanolamine externalization (Wang *et al.*, 2004; Wang *et al.*, 2005).

Phosphatidylethanolamine-binding protein 4 plays an important role in the regulation of human myoblast differentiation by acting as a scaffold protein for proto-oncogene serine/threonine-protein kinase1-mitogen-activated protein kinase/extracellular-signal-regulated kinase (RAF1-MEK) interactions (Garcia *et al.*, 2009). The RAF-MEK-ERK pathway plays a role in the regulation of differentiation and proliferation and PEBP4 contributes to the control of muscle cell differentiation by means of modulating MEK and ERK activity (Garcia *et al.*, 2009).

4.3.2 The functional significance of the titin-PEBP4 interaction

The literature suggests that PEBP4 may play a role in regulating human myoblast differentiation because the expression of PEBP4 is induced during primary human myoblast differentiation (Garcia *et al.*, 2009). Garcia and colleagues (2009) performed fluorescence-activated cell sorting (FACS) analysis where sorted cells were induced to differentiate (Garcia *et al.*, 2009). The cells were then examined to determine if there was formation of multinucleated myotubes as well as expression of myosin heavy chains (myHCs), which would act as morphological and biochemical markers for terminal differentiation (Garcia *et al.*, 2009). The findings were that PEBP4 enhanced the RAF1-MEK interaction as well as the activation of MEK at low expression levels, but inhibited them during elevated expression levels (Garcia *et al.*, 2009). Furthermore, a downregulation of PEBP4 by means of short hairpin RNA within the human myoblasts resulted in increased MEK signalling and subsequent inhibition of differentiation (Garcia *et al.*, 2009). Additionally, the overexpression of PEBP4 resulted in increased differentiation (Garcia *et al.*, 2009). The activity of MEK and ERK are therefore modulated by PEBP4 as it plays an important role in the control of myocyte differentiation (Garcia *et al.*, 2009).

As titin is known to play a functional role in muscle assembly as well as passive resting tension (Maruyama, 1997) and PEBP4 has been shown to be a crucial scaffolding protein during myocyte differentiation, it is tempting to speculate that disruption of this interaction could lead to impaired myocyte differentiation and development. The myocytes may remain in the myoblast phase, as opposed to

differentiating further into myotubes. The result would be a lack of sarcomeric structure formation, which could result in pathologies such as HCM.

4.4 TITIN-H-FABP3 INTERACTION

The heart-type fatty acid binding protein 3 protein was identified and verified as an interactor of titin. The characteristics and functions of H-FABP3 will be discussed and a likely functional role for the interaction between H-FABP3 and titin will be offered.

4.4.1 The functions of H-FABP3

Heart-type fatty acid-binding protein 3 is a 15kDa low molecular weight cytoplasmic protein that plays a role in intracellular transportation of free fatty acids in the cardiomyocyte (Kim and Storch, 1992; Morioka *et al.*, 2005). Since H-FABP3 is released from the cardiomyocyte into circulation after myocardial damage, it is considered a sensitive biochemical marker of myocardial damage (Morioka *et al.*, 2005). Unbound free fatty acids as well as H-FABP3, their intracellular binding protein, could prove useful as clinical indicators of cardiac ischemia and necrosis, respectively (Azzazy *et al.*, 2006).

Fatty acid binding proteins bind reversibly and noncovalently to long-chain fatty acids and consist of 126-137 amino acids (Azzazy *et al.*, 2006). Nine different fatty acid binding protein types have been identified thus far and each type has its own pattern of tissue distribution with a constant intracellular half-life of two to three days (Glatz

and Van der Vusse, 1996). The human H-FABP3 isoform comprises of 132 amino acid residues and is an acidic protein (Schreiber *et al.*, 1998).

The very low solubility of long-chain fatty acids in aqueous solutions impairs their intracellular translocation, which is facilitated by fatty acid binding proteins such as H-FABP3 (Glatz and Van der Vusse, 1996). Heart-type fatty acid-binding protein 3 is the cytoplasmic counterpart of plasma albumin (Azzazy *et al.*, 2006). Albumin is the main transporter of free fatty acids in blood plasma as well as in interstitial fluid (Glatz and Van der Vusse, 1996). Heart-type fatty acid-binding protein 3 is therefore the protein responsible for free fatty acid translocation within the cytoplasm (Azzazy *et al.*, 2006).

Heart-type fatty acid-binding protein 3 takes part in signal transduction pathways, for example the regulation of gene expression by means of facilitating fatty acid signal translocation to peroxisome proliferator-activated receptors (Wolfrum *et al.*, 2001). Heart-type fatty acid-binding protein 3 is also responsible for the protection of cardiomyocytes against the detergent-like effects of locally elevated concentrations of long-chain fatty acids, predominantly during ischemic conditions (Glatz and Van der Vusse, 1996; Glatz and Storch, 2001).

4.4.2 The potential role of H-FABP3 in hypertrophic cardiomyopathy and heart disease

Elevated H-FABP3 levels are used as an indicator of ongoing myocardial damage in patients with HCM and heart failure and could thus result in the clinical deterioration

of these patients (Morioka *et al.*, 2005). The measurement of serum H-FABP3 levels in combination with myoglobin levels can be used as a means of discerning between myocardial damage and skeletal muscle injury due to the composition of cardiomyocytes and skeletal muscles that differ with regards to H-FABP3 and myoglobin content (Van Nieuwenhoven *et al.*, 1995; Morioka *et al.*, 2005). The average serum level of H-FABP3 has been shown to be significantly higher in patients with HCM than in controls (Morioka *et al.*, 2005). However, there appears to be no significant difference in myoglobin levels of patients with HCM (Morioka *et al.*, 2005).

The exact mechanisms of myocardial damage in HCM are still unknown, however, myocardial ischemia has been proposed as a possible explanation (Morioka *et al.*, 2005). Serum H-FABP3 levels could point to myocardial damage that advances progressively according to the severity of the heart failure in HCM patients (Morioka *et al.*, 2005). Heart failure results in myocardial changes such as myocardial ischemia, apoptosis, neurohormonal activation and an increase in collagen activation; as well as myocardial load which could all lead to the contribution to myocardial damage in HCM patients (Morioka *et al.*, 2005).

Fatty acid binding proteins, including H-FABP3, are found in many tissues that actively utilize free fatty acids and thus have an essential role in the heart, where more than 80 percent of the organ's energy requirements are derived from the oxidation of long chain fatty acids (Kim and Storch, 1992). The heart has high energy demands and primarily uses fatty acids and carbohydrates in the form of glucose as substrates for energy production in the form of ATP (Lopaschuk, 2004; Lopaschuk *et al.*, 2010).

The predominant physiological energy source is thus derived from circulating fatty acids, as they are capable of significantly inhibiting the oxidation of glucose (Gambert *et al.*, 2006). Fatty acids are able to damage myocardium during pathological conditions and therefore cause the impairment of myocardial mechanical function, enhance enzyme release as well as provoke arrhythmias (Gambert *et al.*, 2006). The post-ischemic reperfusion period is when the negative effects of fatty acids are most notable (Gambert *et al.*, 2006).

Compensated cardiac hypertrophy induced by the proto-oncogene C-Myc leads to an increase in fatty acid utilization for the citric acid cycle (Olson *et al.*, 2012). Since H-FABP3 is responsible for the transportation of free fatty acids in the cytoplasm, elevated levels of H-FABP3 will be found in the heart during the hypertrophic process. C-Myc regulates cardiac hypertrophy by promoting compensated cardiac function, indicating that the mechanisms at work are different from those leading to heart failure (Olson *et al.*, 2012). The literature suggests that C-Myc induces shifts in substrate utilization signals, but that the substrate utilization changes for the citric acid cycle do not precede hypertrophy and are thus not the primary signal for cardiac growth (Olson *et al.*, 2012). Free fatty acid utilization as well as oxidation has been shown to increase when hypertrophy is established and the understanding of the mechanisms involved in maintaining the compensated function could lead to the development of a novel metabolic therapy for the treatment of heart failure (Olson *et al.*, 2012).

Free fatty acids exert a number of detrimental effects on the myocardium and may contribute to SCD, which is the most common fatal cardiovascular event (Pilz *et al.*,

2007). An increase in the concentration of fasting plasma free fatty acids; and subsequently of H-FABP3, has been shown to be an independent risk factor for SCD in patients requiring coronary angiography (Pilz *et al.*, 2007). Besides predicting SCD with high accuracy, the prevention of all causes of cardiovascular mortality can benefit from the knowledge of the risks of elevated H-FABP3 and free fatty acids levels (Pilz *et al.*, 2007). Free fatty acids and H-FABP3 can thus be used as markers to identify patients at risk for SCD as well as other fatal cardiovascular events (Pilz *et al.*, 2007). Arrhythmias arising at the beginning of ischemia and reperfusion can lead to SCD if left untreated so their prevention is extremely important (Nair *et al.*, 1996). It remains unknown if elevated free fatty acids are the cause of pathogenesis or if they are increased due to other pathological processes contributing to these fatal cardiovascular events (Pilz *et al.*, 2007).

Since H-FABP3 levels have been shown to indicate myocardial damage in HCM patients; and the subsequent heart failure results in apoptosis as well as myocardial load, H-FABP3 could in turn indirectly contribute to HCM pathogenesis (Morioka *et al.*, 2005).

4.4.3 The functional significance of the titin-H-FABP3 interaction

Heart-type fatty acid-binding protein 3 has a number of clinical applications. Heart-type fatty acid-binding protein 3 has prognostic value to predict recurrent cardiac events and is used as an early marker for acute myocardial infarction; to differentiate between cardiac and skeletal muscle injuries; the estimation of

myocardial infarct size; the clinical assessment of congestive heart failure and as a potential biomarker of cardiac ischemia (Azzazy *et al.*, 2006).

Heart-type fatty acid-binding protein 3 takes part in signal transduction pathways. It can be speculated that an interruption in these pathways could be caused by the titin-H-FABP3 interaction because H-FABP3 is a low molecular weight small protein and could therefore be weighed down by the giant protein titin. Heart-type fatty acid-binding protein 3 would no longer be able to perform its function properly and this interaction could thus play a role in HCM modulation due to its signal transduction pathways being interrupted. Titin could also inhibit the transportation of free fatty acids when bound to H-FABP3 due to its size.

4.5 TITIN-MYOM2 AND TITIN-MYOM1 INTERACTIONS

Myomesin 2 and myomesin 1 were identified and verified as interactors of titin's scaffold region. The characteristics and functions of MYOM2 and MYOM1 will be discussed and a probable functional role for the interaction between MYOM2 and titin as well as MYOM1 and titin will be put forward. Myomesin 2 and MYOM1 are structurally very similar and will thus be discussed together. To uncomplicate the following section: when referring to myomesin in general, it is meant that both MYOM2 as well as MYOM1 are collectively involved. However, if only MYOM2 or MYOM1 are mentioned then the information is only applicable to one of the proteins.

4.5.1 The functions of MYOM2 and MYOM1

Myomesin is a myosin-binding protein (Linke, 2008) that is located in the M-band of striated muscles and may play a functional role in connecting thick filaments to the third filament system (Auerbach *et al.*, 1999). Myomesin's principal function is the preservation of the thick filament lattice and its anchoring to the elastic filament system, comprising of titin (Agarkova *et al.*, 2000).

Myomesin 2 is a 165kDa protein (Van der Ven and Fürst, 1997; Ashbaugh *et al.*, 1998; Hornemann *et al.*, 2003; Herwald *et al.*, 2004) while MYOM1 is a 190kDa protein (Eppenberger *et al.*, 1981; Obermann *et al.*, 1997; Van der Ven and Fürst, 1997; Agarkova and Perriard, 2005; Schoenauer *et al.*, 2005). Myomesin 2 and MYOM1 are major components of vertebrate myofibrillar M bands and are associated with titin, myosin and connectin (Auerbach *et al.*, 1999). Myomesin 1 is known to bind to myosin, titin as well as light meromyosin in a dose dependent manner (Obermann *et al.*, 1996). Myomesin 2 is jointly responsible with MYOM1 for the creation of a head structure on one end of the titin string, connecting the Z and M bands of the sarcomere to each other (See **Figure 1.8** and **Figure 1.14**) (Fürst *et al.*, 1999). Myomesin 2 and MYOM1 have unique N-terminal domains that vary between isoforms (Tskhovrebova and Trinick, 2012). The gene encoding human MYOM2 and MYOM1 has been shown to map to the chromosomal region: 18p11.31-p11.32 (<http://www.acris-antibodies.com>).

Myomesin 2 and MYOM1 are the major prominent structural elements of the sarcomeric M-line (Porter *et al.*, 2003) and they are expressed in both cardiac and

striated skeletal muscle, but predominantly in skeletal muscle (Agarkova *et al.*, 2000; Bertoncini *et al.*, 2005). Myomesin is able to form antiparallel dimers that could play a role in cross-linking the adjacent thick filaments (Schoenauer *et al.*, 2005). Myomesin has been proposed to be comparable to titin in that they both function as molecular springs with their elasticity controlled by means of alternative splicing (Schoenauer *et al.*, 2005). Myomesin has a number of different isoforms (Grove *et al.*, 1985) which have expression patterns that are regulated both spatially as well as temporally (Agarkova *et al.*, 2000; Bertoncini *et al.*, 2005).

The key components of myomesin are immunoglobulin-like (Ig) and fibronectin type III (Fn) domains (Auerbach *et al.*, 1999; Bertoncini *et al.*, 2005; Schoenauer *et al.*, 2005), both of which have approximately 100 residues (Tskhovrebova and Trinick, 2012). When there are exceedingly great or extended sustained stretching forces, the Ig and Fn domains could function as adjustable “shock absorbers” by means of sequential unfolding (Schoenauer *et al.*, 2005). The multifaceted visco-elastic mechanical properties of myomesin molecules depend upon the contractile parameters found in different muscle types (Bertoncini *et al.*, 2005) and may be essential for maintaining the stability of the sarcomeric cytoskeleton during muscular contraction (Schoenauer *et al.*, 2005).

Myomesin is an intracellular member of the immunoglobulin superfamily (Bantle *et al.*, 1996) which has a flexible filamentous structure (Bertoncini *et al.*, 2005). A number of other myosin-binding proteins have a place in this family, for example M-protein (Noguchi *et al.*, 1992; Vinkemeier *et al.*, 1993), myosin binding protein C (Offer *et al.*, 1973; Einheber and Fischman, 1990), H-protein (Bähler *et al.*, 1985) as

well as titin (Labeit and Kolmerer, 1995). Several thick filament-associated proteins also comprise of Ig and Fn domains (Auerbach *et al.*, 1999). This could indicate a possible function of these domains in facilitating interactions with myosin (Fürst and Gautel, 1995; Bantle *et al.*, 1996). It has been shown by means of Western blotting biochemical assays that myomesin interacts with myosin as well as titin (Wang *et al.*, 1998), however, it remains unclear how these interactions are able to direct myomesin to its assembly site within the M-band in vivo (Auerbach *et al.*, 1999).

M-protein is a splice variant encoded by the same gene as myomesin (Fürst *et al.*, 1999; Steiner *et al.*, 1999). Myomesin and M-protein both have an affinity for myosin (Mani and Kay, 1978; Grove *et al.*, 1985; Obermann *et al.*, 1996) and titin (Nave *et al.*, 1989; Obermann *et al.*, 1997). They are thus involved in anchoring thick filaments to the elastic third filament system (Auerbach *et al.*, 1999). Myomesin is found in all types of adult striated muscle (Grove *et al.*, 1989), as opposed to M-protein which can only be found in cardiac and fast skeletal fibres (Eppenberger *et al.*, 1981). Myomesin could therefore be the primary link between thick and elastic filaments (Auerbach *et al.*, 1999).

Tissue- and developmental-stage-specific alternative splicing is displayed by MYOM1 (Porter *et al.*, 2003). Myomesins have an important organizational role in developing sarcomeres and function as structural components in adult striated muscle (Ehler *et al.*, 1999; Grove *et al.*, 1985; Wang *et al.*, 1998). A distinct M-line forms during myogenesis, but it is repressed during the early postnatal period (Agarkova *et al.*, 2000; Porter *et al.*, 2003). Both MYOM2 and MYOM1 transcripts show the

M-line pattern of developmental down-regulation (Agarkova *et al.*, 2000; Porter *et al.*, 2003).

There are multiple myomesin isoforms that are expressed in striated muscles; however, MYOM2 has only one isoform (Porter *et al.*, 2003). The separate functions of the different myomesin isoforms are not yet understood entirely (Porter *et al.*, 2003). The My1 amino-terminal domain of MYOM1 binds to the light meromyosin section of myosin and My4-My6 have been found to bind to titin (Obermann *et al.*, 1997) (see **Figure 1.14**). Embryonic heart-specific MYOM1 most likely has comparable binding capabilities (the embryonic heart-specific insert lies between domains My6 and My7), which can be deduced from its primary structure (Agarkova *et al.*, 2000). It is, however, interesting that the formation of M-lines is not able to be supported by the expression of embryonic heart-specific MYOM1 on its own (Agarkova *et al.*, 2000).

4.5.2 The potential role of MYOM2 and MYOM1 in hypertrophy or hypertrophic cardiomyopathy

Previous studies by Komuro and Yazaki (1993) showed that the re-expression of embryonic or fetal genes could be utilized as a molecular marker for hypertrophy (Agarkova *et al.*, 2000). Cardiomyocytes obtained from hypertrophic hearts can commonly be characterized by myofibril disarray (Agarkova *et al.*, 2000). The organization of the sarcomeres is not as uniform as they are in healthy hearts (Agarkova *et al.*, 2000). This could indicate a return to more embryonic sarcomeric structures during hypertrophy development (Agarkova *et al.*, 2000). Studies by

Agarkova and co-workers (2000) indicated the presence of re-expression of embryonic heart-specific myomesin in cardiomyocytes from muscle LIM protein knock-out mice as well as from tropomodulin-overexpressing mice (Agarkova *et al.*, 2000). The two mouse strains both displayed a phenotype of dilated cardiomyopathy (Arber *et al.*, 1997; Sussman *et al.*, 1998; Agarkova *et al.*, 2000). It still remains unknown to what extent the re-expression of embryonic heart-specific myomesin can be connected to myofibrillar disarray during other types of pathological hypertrophy (Agarkova *et al.*, 2000).

Agarkova and Perriard (2005) described the M-band as a dynamic component of the sarcomeric cytoskeleton which is able to adapt to the contractile command of an individual muscle by means of varying the type and number of different myomesin molecules that cross-link the thick filaments (Schoenauer *et al.*, 2011). Myosin and titin filaments are cross-linked in the middle of the sarcomere by the prominent cytoskeletal structure of the M-band (Schoenauer *et al.*, 2011). The expression of the M-band's key constituents, namely proteins of the myomesin family, were analysed by Schoenauer and colleagues in 2011 to investigate M-band alterations in heart disease in both mouse and human cardiomyopathies (Schoenauer *et al.*, 2011).

Embryonic heart-specific myomesin, which is the dominant splice isoform found within the embryonic heart, was shown to be significantly up-regulated in the failing heart of DCM patients and correlated with a reduction in cardiac functioning (Schoenauer *et al.*, 2011). Schoenauer and colleagues (2011) demonstrated that embryonic heart-specific myomesin was up-regulated in a cell-specific way, which lead to an increased heterogeneity of the myocytes' cytoskeletons through the

myocardial wall. An adaptive remodelling of the sarcomeric cytoskeleton could be indicated by up-regulation of embryonic heart-specific myomesin in the dilated heart (Schoenauer *et al.*, 2011). This up-regulation of embryonic heart-specific myomesin may assist as a potential marker for DCM in mouse and human myocardium (Schoenauer *et al.*, 2011). New insights into the understanding of progressive ventricular dilation on an organisational level could be obtained from the information that the embryonic heart-specific myomesin isoform is associated with an increased degree of M-band elasticity (Schoenauer *et al.*, 2005). This could lead to a better characterization of DCM in human patients because of the up-regulation of embryonic heart-specific myomesin at early stages of the disease and its relationship to the impairment of ventricular function (Schoenauer *et al.*, 2011).

4.5.3 The functional significance of the titin-MYOM2 and titin-MYOM1 interactions

Titin is known to interact with myomesin (Wang *et al.*, 1998), which has the function of cross-linking the thick filaments and titin's COOH-terminus in an elastic way (Linke, 2008). The elasticity of myomesin could be significant in correcting force imbalances found between parallel thick filaments in the course of active muscle contraction (Linke, 2008). Myomesin has been shown to associate with creatine-kinase as well as myofibrillogenesis-regulator-1 and is controlled in its affinity to titin by means of phosphorylation (Linke, 2008). The myomesin-titin-myosin complex is an essential structure that retains the stability of the M-band (Linke, 2008). The relationship of titin's COOH-terminus to signalling and structural molecules associates the COOH-terminus of titin with thick filament

assembly or turnover, thus conferring flexibility as well as mechanical stability to the M-band (Linke, 2008).

Myomesin is, however, not found in the C-zone of the sarcomere as the section of titin that was under investigation, but due to the structural similarities of titin's large repeat regions, this interaction could still be valid. This is because the titin domains that were under investigation are structurally similar to the domains found at the M-line where myomesin is located. The interactions were made possible because the experiments put the proteins together and they were then able to interact. The colocalisation therefore merely showed that the proteins are capable of interacting, even though the colocalisations were not necessarily statistically significant. This was not the expected result since the literature states that titin and myomesin are known to interact (Mayans *et al.*, 1998; Nave *et al.*, 1989; Vinkemeier *et al.*, 1993; Obermann *et al.*, 1996; Wang *et al.*, 1998; Fürst *et al.*, 1999).

The fact that the H9C2 cells were already differentiated could be the reason that a stronger interaction was not detected between titin and MYOM2 and MYOM1 in this study. Titin and myomesin are known to interact biochemically during sarcomerogenesis, as they are simultaneously assembled (Wang *et al.*, 1998). However, the H9C2 cells were no longer developing and MYOM2 and MYOM1 could thus have been expressed to a lesser degree when the colocalisation experiments were performed. It is also a possibility that not all the binding sites were accessible for titin in the differentiated cells, as was the case with Auerbach and co-workers in 1999 (Auerbach *et al.*, 1999). Phosphorylation also plays a role in the interactions between titin and MYOM2 and MYOM1, as previous studies have shown that the

phosphorylation of a linker that connects two of the Fn3 domains was able to disrupt their interactions (Oberman *et al.*, 1997; Auerbach *et al.*, 1999). It is therefore also a possibility that the phosphorylation state was not optimal for interaction at the time of the experiments being performed. These factors could be linked to a developmental error resulting in a defect in sarcomeric structure formation, which could result in various pathologies, including HCM.

The titin-MYOM2 and titin-MYOM1 interactions are therefore likely to reflect the results obtained by Gotthardt and colleagues in 2003 when they found that mice that had a conditional knockout for the M-band region of titin – including the myomesin binding site – displayed progressive sarcomere disassembly with associated muscle weakness (Gotthardt *et al.*, 2003; Schoenauer *et al.*, 2005).

4.6 LIMITATIONS OF THE PRESENT STUDY

Further verification (**Section 4.9**) of the identified interactors is required before the proteins can be stated unequivocally as interactors of titin. It is also possible that additional putative interactors for the scaffold region of titin could still be identified in future Y2H screens. However, five putative interactors were successfully identified and subsequently verified using an independent molecular biological method.

4.7 LIMITATIONS OF Y2H ANALYSIS

Although the Y2H system is a useful tool in the detection of protein-protein interactions, a number of intrinsic limitations do exist.

Yeast is a better candidate than bacterial hosts for this type of analysis, as it is closer to higher eukaryotes and is more illustrative than conducting *in vitro* experiments (Van Crielinge and Beyaert, 1999). However, a large disadvantage in using a heterologous system is that many protein-protein interactions are subject to the post-translational modification of proteins such as disulfide bridges, glycosylation and phosphorylation (Van Crielinge and Beyaert, 1999). These modifications might not take place properly in yeast cells due to a lack of the enzymes required for these developments and may therefore affect the binding affinity of the interacting proteins (Van Crielinge and Beyaert, 1999).

The principle of the Y2H system is dependent on a transcriptional event to regulate the interaction of two proteins. It is thus vital that auto-activation of the bait protein must be assessed prior to performing the Y2H screen (Van Crielinge and Beyaert, 1999; Sobhanifar, 2003). A protein of interest that is able to auto-activate the reporter genes is not suitable for Y2H analysis, therefore limiting bait selection. In the present study, it has been shown that the bait construct was unable to auto-activate the reporter genes (**Section 2.11.2**). The fusion proteins are required to be targeted to the yeast nucleus, which could be challenging for proteins that have strong targeting signals to compartments other than the nucleus (Sobhanifar, 2003). The expression of certain proteins may also become toxic upon expression in yeast (Van Crielinge and Beyaert, 1999). Some proteins might proteolyse essential yeast proteins or may affect the DNA binding domain or activation domain – the critical transcription system that forms the foundation of the Y2H method (Van Crielinge and Beyaert, 1999). The generation of fusion proteins may change the conformation or protein folding of the bait and prey proteins. This could result in the incorrect folding of proteins so as to

render them inactive or could potentially block possible binding sites (Van Crielinge and Beyaert, 1999).

The likelihood exists that a third protein plays a linking role between the two interacting proteins and this must be taken into account when interpreting interaction data (Sobhanifar, 2003). Cellular processes often rely upon the formation of complexes between several proteins; thus it is possible that interactions may be overlooked in the two-hybrid system if the presence of a third protein is a prerequisite for the interaction between two proteins (Causier and Davies, 2002).

4.8 LIMITATIONS OF COLOCALISATION

Colocalisation is a valuable technique to determine whether two proteins occur in the same physical location within a cell. The technique can, however, not provide direct evidence of an interaction, so the use of colocalisation to verify interacting proteins is limited. There are also limitations when using microscopy, such as the image resolution. The resolution of a microscope is defined as the smallest distance between two points that can be clearly distinguished from one another. The resolution is dependent upon the wavelength of the light imaged and the numerical aperture of the objective. The resolution of the highest objective of the LSM 510 META with NLO (NLO = two photon laser) confocal microscope (Carl Zeiss, Germany) system is 200nm implying that objects located closer together than 200nm appear as one colocalised object. Within the area of the colocalisation, proteins are able to appear as if to colocalise without physically interacting.

To overcome the limitations of colocalisation, other molecular biological methods such as *in vivo* co-IP experiments can be conducted to provide proof of direct protein-protein interactions. However, co-IP assays are very expensive, time consuming and require optimisation. The cell environment is also multifaceted and proteins may only interact under particular conditions, which might not always be apparent.

4.9 THE FUTURE OF THIS RESEARCH

The present study has identified and verified the interactions between titin and filamin C (FLNC), phosphatidylethanolamine-binding protein 4 (PEBP4), heart-type fatty acid binding protein 3 (H-FABP3), myomesin 2 (MYOM2) and myomesin 1 (MYOM1). These findings could link the functions of the interactors with titin to the development of HCM.

Future directions include: validation of putative interactors using independent biochemical analyses. These experiments will provide researchers with more insight into the functional significance of the interactions with titin and may also be helpful in determining the role that the interactions may play in the development of HCM.

Further research could be conducted into elucidating the functional role of these interactors so as to investigate why these proteins interact with titin. Verified interactors of C-zone scaffold regions could be prioritized as candidate modifiers by whether biological function relates to hypertrophy. The genes encoding these proteins could also be considered candidate genes for HCM-causing mutations. This could be

tested by means of high resolution melt (HRM) analysis or target next generation sequencing. To test whether the identified interactor would have any effect on modulating hypertrophy, single nucleotide polymorphisms in the genes encoding these interactors could be genotyped in a panel of HCM patients. The genotype data would then be correlated with several measures of hypertrophy.

These modifiers may help researchers better understand the molecular mechanisms involved in the development of LVH. They will likely allow for the improved understanding of HCM patho-aetiology and may improve risk profiling. Furthermore, as genetic modifiers appear sufficient to completely prevent disease expression in some HCM carriers, they may point to new targets for intervention, for example metabolic modulation. Such understanding may eventually lead to strategies aimed at preventing the development of pathological cardiac hypertrophy both in HCM and possibly other hypertrophic disorders including hypertension and diabetes.

4.10 CONCLUSION

Mutations in the *TTN* gene have been found to play a role in the development of HCM. The aim of this study was thus to identify novel interactors of the 11-domain super-repeat region of titin as candidate modifiers (or possible disease causing mutations) of hypertrophy in HCM in order to better understand the mechanisms leading to hypertrophy. Interactions between the 11-domain super-repeat region of titin and FLNC, PEBP4, H-FABP3, MYOM2 and MYOM1 were identified using yeast two-hybrid analysis and verified by means of colocalisation. Once interactors

were identified, it was possible to subsequently hypothesize on the functional role that the interactions with titin may play in the development of HCM.

Filamin C, PEBP4, H-FABP3, MYOM2 and MYOM1 have multiple complex functions, some of which have been found to be important in muscle development and are able to be linked to HCM via their interactions with titin. In this study the speculations are that it is possible that the *FLNC* gene could be a candidate for cardiac diseases, especially cardiomyopathies that are associated with hypertrophy or developmental defects (Van der Ven *et al.*, 2006). As titin is known to play a functional role in muscle assembly as well as passive resting tension (Maruyama, 1997), the putative interaction of titin and PEBP4 is speculated to be indicative of the formation of the interstitial fibrosis and myocyte disarray seen in HCM. Heart-type fatty acid-binding protein 3 has a number of clinical applications including prognostic value to predict recurrent cardiac events and is used as an early marker for acute myocardial infarction; to differentiate between cardiac and skeletal muscle injuries; the estimation of myocardial infarct size; the clinical assessment of congestive heart failure and as a potential biomarker of cardiac ischemia (Azzazy *et al.*, 2006) and its suggested interaction with titin is speculated to play a role in inhibiting its functional abilities, thus leading to the possible worsening of disease. Myomesin 2 is jointly responsible with MYOM1 for the formation of a head structure on one end of the titin string that connects the Z and M bands of the sarcomere (Fürst *et al.*, 1999) and this is speculated to be linked to a developmental error with the result being a defect in sarcomeric structure formation, which could result in pathologies such as HCM. Thus, the interactors could play a functional role in the manner in which titin is

involved in HCM. The biological significance of the interactions still need to be determined categorically and remain a priority for future studies in this field.

APPENDIX I**REAGENTS, BUFFERS, SOLUTIONS AND MEDIA****1. Electrophoresis stock solutions****10% Ammonium Persulfate**

Ammonium Persulfate	10g
Sterile water	10mL

Mix well and store at 4°C

20X SB Stock Solution

di-Sodium tetraborate decahydrate	38.14g
Sterile water to a final volume of one litre	

1X SB Solution

20X SB Stock Solution	50mL
Sterile water to a final volume of one litre	

2. Gels**2% Agarose gel**

Agarose	2g
SB Buffer (1X)	100mL

Microwave for 1 min on maximum power and add 5µL ethidium bromide (10mg/mL) when the temperature reaches ±55°C

3. Loading dyes

Ethidium Bromide Stock (10mg/mL)

Ethidium bromide 500mg

Sterile water 50mL

Stir well on magnetic stirrer for four hours and store in a dark container at 4°C

Bromophenol Blue loading dye

Bromophenol blue 0.1% (w/v)

Sterile water to a final volume of 100mL and store at 4°C

4. Yeast media

YPDA media

Difco peptone 10g

Yeast extract 10g

Glucose 10g

L-adenine hemisulphate (0.2% stock solution) 7.5mL

Add sterile water to a final volume of 500mL and autoclave at 121°C for 15 min

YPDA agar plates

Difco peptone 10g

Yeast extract 10g

Glucose 10g

L-adenine hemisulphate (0.2% stock solution) 7.5mL

Bacto agar 10g

Add sterile water to a final volume of 500mL and autoclave at 121°C for 15 min.

Allow to cool to a temperature of $\pm 55^{\circ}\text{C}$ before pouring the plates. Allow plates to set for 2-5 hours and store at room temperature for up to three weeks.

SD Media

Glucose	12g
Yeast nitrogen base without amino acids	4g
SD amino acid supplement	0.4g
Sterile water to a final volume of 600mL	

SD agar plates

Glucose	12g
Yeast nitrogen base without amino acids	4g
SD amino acid supplement	0.4g
Bacto agar	12g

Add sterile water to a final volume of 600mL and autoclave at 121°C for 15 min.

Allow to cool to $\pm 55^{\circ}\text{C}$ before pouring the plates. Allow plates to set for 2-5 hours and store at room temperature for up to three weeks.

TDO media

Glucose	12g
Yeast nitrogen base without amino acids	4g
SD ^{-L-W-H} amino acid supplement	0.4g

Add sterile water to a final volume of 600mL and autoclave at 121°C for 15 min.

TDO agar plates

Glucose	12g
Yeast nitrogen base without amino acids	4g
SD ^{-L-W-H} amino acid supplement	0.4g
Bacto agar	12g

Add sterile water to a final volume of 600mL and autoclave at 121°C for 15 min.

Allow to cool to $\pm 55^{\circ}\text{C}$ before pouring the plates. Allow plates to set for 2-5 hours and store at room temperature for up to three weeks.

QDO media

Glucose	12g
Yeast nitrogen base without amino acids	4g
SD ^{-L-W-H-Ade} amino acid supplement	0.4g

Add sterile water to a final volume of 600mL and autoclave at 121°C for 15 min.

QDO agar plates

Glucose	12g
Yeast nitrogen base without amino acids	4g
SD ^{-Leu-Trp-His-Ade} amino acid supplement	0.4g
Bacto agar	12g

Add sterile water to a final volume of 600mL and autoclave at 121°C for 15 min.

Allow to cool to $\pm 55^{\circ}\text{C}$ before pouring the plates. Allow plates to set for 2-5 hours and store at room temperature for up to three weeks.

X- α -Galactosidase Solution (5mg/mL)

X- α -Galactosidase	25mg
----------------------------	------

Dimethylformamide	1mL
-------------------	-----

Make a 25mg/mL stock solution. Dilute with Dimethylformamide to a 5mg/mL working solution.

5. Yeast transformation reagents

1M LiAc

LiAc	5.1g
------	------

Make up to 50mL with sterile water

100Mm LiAc

1M LiAc	5mL
---------	-----

Make up to 50mL with sterile water

50% Polyethylene glycol (PEG)

PEG 4000	25g
----------	-----

Make up to 50mL with sterile water

6. Eukaryotic cell culture media

Complete growth media

DMEM (4.5g/L glucose, with L-glutamine)	178mL
Foetal calf serum	20mL
Penicillin/streptomycin	2mL

Pre-warmed to 37°C before use

Serum-free media

DMEM (4.5g/L glucose, with L-glutamine)	100mL
---	-------

Pre-warmed to 37°C before use

Differentiating growth media

DMEM (4.5g/L glucose, with L-glutamine)	196mL
Horse serum	2mL
Penicillin/streptomycin	2mL

Pre-warmed to 37°C before use

Phosphate Buffered Saline (PBS)

PBS tablet (Sigma)	one tablet
ddH ₂ O	200mL

Dissolve tablet in ddH₂O and store solution at 0-5°C

7. Solutions used for the establishment of bacterial competent cells

CAP-Buffer

CaCl ₂	2.21g
Glycerol	37.5mL
Piperazine-N,N'-bis(2-ethanesulfonic acid) (PIPES)	0.76g

Sterile water to a final volume of 250mL, adjust pH to 7.0 and store at 4°C

8. Bacterial media

LB media

Bacto tryptone	5g
Yeast extract	2.5g
NaCl	5g

Sterile water to a final volume of 500mL, autoclave and add appropriate antibiotic (Ampicillin 20mg/L, Kanamycin 5mg/L) to the media when the temperature reaches $\pm 55^{\circ}\text{C}$.

LB agar plates

Bacto tryptone	5g
Yeast extract	2.5g
NaCl	5g
Bacto agar	8g

Sterile water to a final volume of 500mL, autoclave and add appropriate antibiotic (Ampicillin 20mg/L, Kanamycin 5mg/L) to the media when the temperature reaches $\pm 55^{\circ}\text{C}$ prior to pouring. Allow plates to set for 2-5 hours and store at room temperature for up to three weeks.

9. Yeast plasmid purification solutions

Yeast Lysis Buffer

SDS	1%
Triton X-100	2%
NaCl	100mM
Tris, pH 8	100mM
EDTA, pH 8	1mM

10. Colocalisation

Mowiol

- 30.0g glycerol (analytical grade)
- 12.0g Mowiol 4-88 (e.g. Calbiochem #475904)
- 30.0mL ddH₂O
- Add 60.0mL 0.2 M Tris buffer pH 8.5 and stir overnight at room temperature
- Heat to 50°C and stir for another hour, to dissolve the remaining Mowiol
- Centrifuge mixture at 5000g for 15 min to remove any undissolved particles
- Aliquot supernatant at 5mL and store at -20°C until use
- Prior to use, add some (tip of a small spatula) anti-fading agent (n-propylgallate, Sigma) to 5mL of Mowiol. Warm to 50°C for one hour and

invert tube frequently to dissolve anti-fading agent. Centrifuge to sediment any remaining particles and to remove air bubbles.

- The final mixture is stable for several weeks at 4°C in the dark

NB: Do not use once Mowiol has turned a yellowish colour.

APPENDIX II**CALCULATING YEAST MATING EFFICIENCIES****Calculating yeast mating efficiencies (Calculations based on Clontech Manual)**

Count number of colonies on all plates with 30-300 colonies after 4 days

$$\text{\#colony forming units (cfu)/mL} = \frac{\text{cfu} \times 1000 \mu\text{L/mL}}{\text{Volume plated } (\mu\text{L}) \times \text{dilution factor}}$$

1. Number of cfu/mL on SD^{-Leu} plates = viability of prey partner
2. Number of cfu/mL on SD^{-Trp} plates = viability of bait partner
3. Number of cfu/mL on SD^{-Leu-Trp} plates = viability of diploids
4. Lowest number of cfu/mL of SD^{-Leu} or SD^{-Trp} plates indicates limiting partner

$$5. \text{ Mating efficiency} = \frac{\text{\#cfu/mL of diploid} \times 100}{\text{\#cfu/mL of limiting partner}}$$

Library titre

Count number of colonies on all plates with 30-300 colonies after 4 days

$$\text{cfu/mL} = \frac{\text{\#colonies}}{\text{Plating volume (mL)} \times \text{dilution factor}}$$

Number of colonies screened

\#clones screened = \#cfu/mL of diploids x final resuspension volume

Haemocytometric cell count

A Neubauer haemocytometer (Superior, Berlin, Germany) was used to perform haemocytometric cell counts to determine the titre of the bait culture used in the library mating experiment. A glass coverslip was placed over the counting surface before aliquoting the sample onto the haemocytometer. About 50 μ L of a 1 in 10 dilution of bait culture was then pipetted into one of the haemocytometer's V-shaped wells. This allowed for the area under the coverslip to fill up with the sample by means of capillary action. The counting chamber was then placed under a microscope (Nikon TMS, Nikon Instruments, New York, USA) and the counting area was brought into focus under low magnification. The number of cells in the large central quadrant of the haemocytometer were counted and this value was used to calculate the number of cells per millilitre using the following formula:

Number of cells/mL = number of cells x dilution factor x 10^4 (a constant used due to the depth of the haemocytometer being 0.1mm)

APPENDIX III

STRAIN PHENOTYPES

BACTERIAL STRAIN PHENOTYPE

E.coli strain DH5 α

Φ 80d lacZ Δ M15 recA1, endA1, Gry A96 thi-1, hsdR17 supE44, relA1, deoR
 Δ (lacZYA argF)u169

YEAST STRAIN PHENOTYPES

S.cerevisiae strain AH109

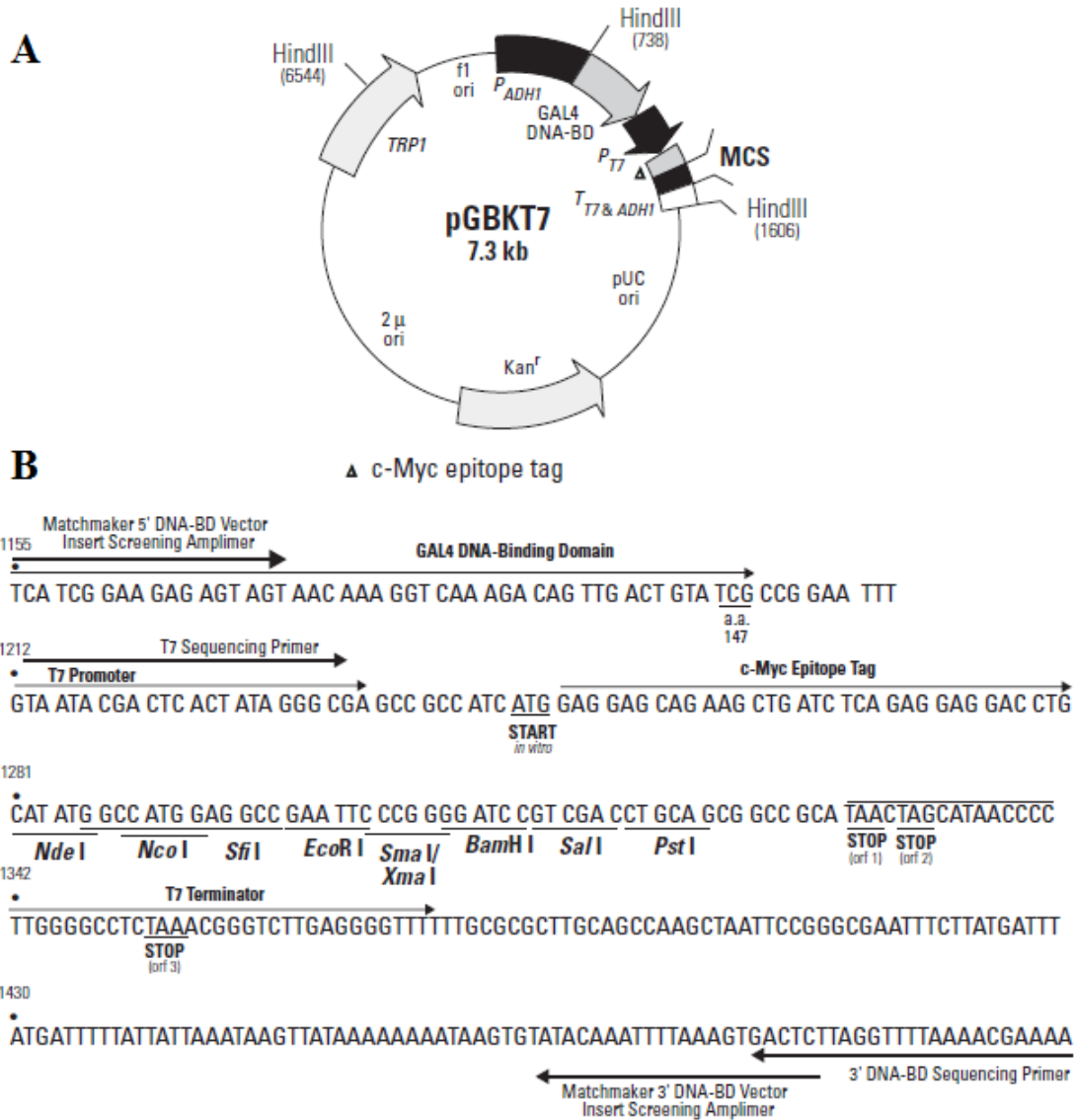
MAT α , trp1-901, leu2-3, ura3-5, his3-200, gal4 Δ , gal80 Δ , LYS2::GAL1uas-
GAL1TATA-HIS3, GAL2UAS-GAL2TATA-ADE2, URA3::MEL1UAS-
MEL1TATA-lacZ
(James *et al.*, 1996)

S.cerevisiae strain Y187

MAT α , ura3-52, his3-200, ade2-101, trp1-901, leu2-3, 112, gal4 Δ , met-, gal80 Δ ,
URA3::GAL1UAS-GAL1TATA-lacZ
(Harper *et al.*, 1993)

APPENDIX IV

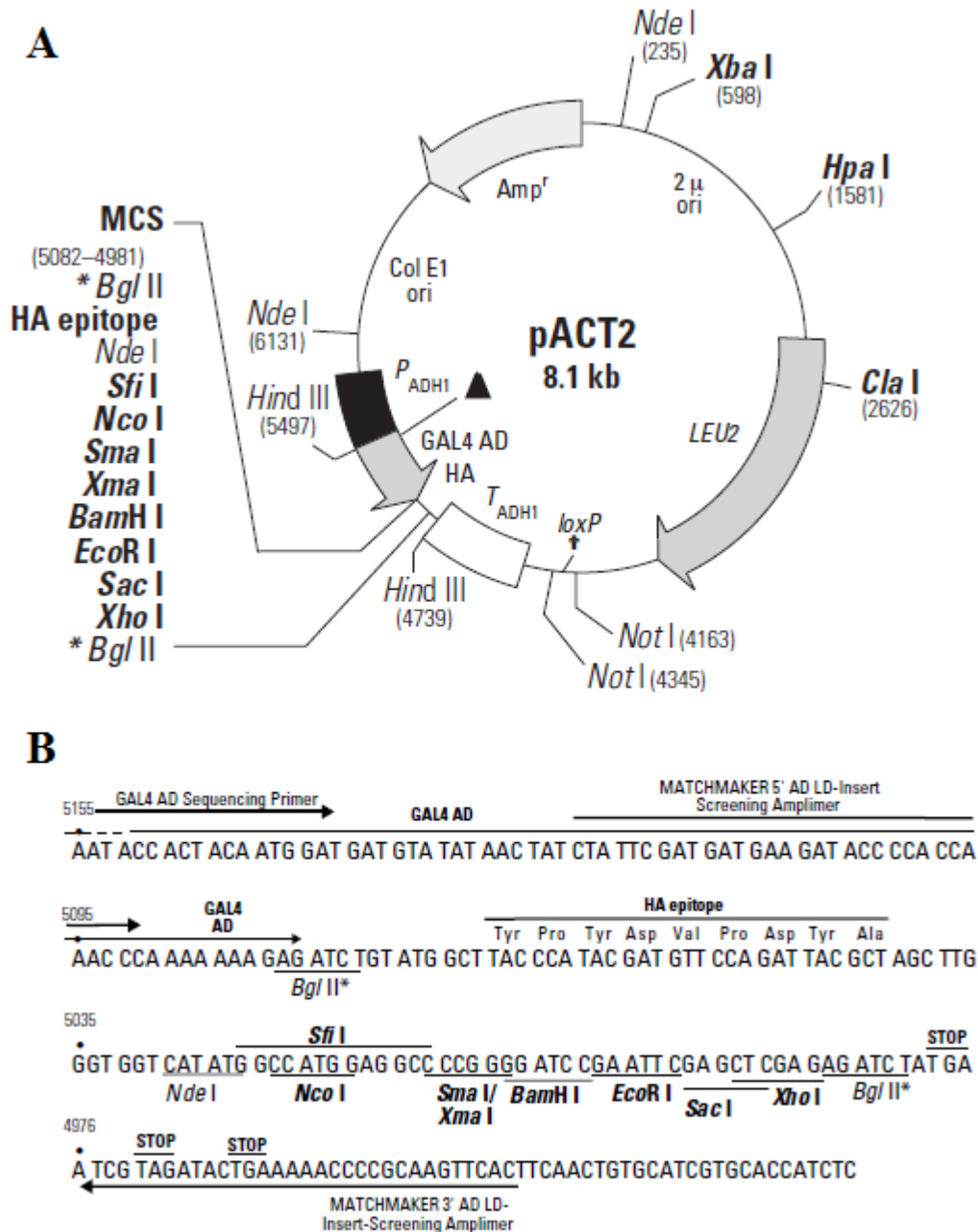
VECTORS



Restriction map and multiple cloning site (MCS) of the Y2H bait vector- pGBKT7.

A) The vector layout, the position of the kanamycin resistance gene (*Kan^r*), *TRP1* and GAL4-BD coding sequences, the f1 bacteriophage, yeast 2 μ and pUC plasmid origins of replication, the T7 RNA polymerase promoter sequence, the HA epitope, the truncated *S.cerevisiae* ADH1 promoter sequence and the c-Myc epitope tag (Δ).

B) The nucleotide sequence of the pGBKT7 MCS. All the restriction enzyme sites are indicated, the GAL4-BD coding sequence, the T7 promoter sequence, the c-Myc epitope tag and the vector specific primers are indicated on the sequence (Taken from the vector information sheet, PT3248-5, CAT# 630489 & 630443).



Restriction map and multiple cloning site (MCS) of the Y2H prey vector- pACT2.

A) The vector layout, the position of the ampicillin resistance gene (*Amp^r*), *LEU2* and GAL4-AD coding sequences, the yeast 2 μ and pBR plasmid origins of replication, the T7 RNA polymerase promoter sequence, the HA epitope and the truncated *S.cerevisiae* ADH1 promoter sequence.

B) The nucleotide sequence of the pACT2 MCS. All the restriction enzyme sites are indicated, the GAL4-AD coding sequence, the T7 promoter sequence, the HA epitope tag and the vector specific primers are indicated on the sequence (Taken from the vector information sheet, PT3022-5, CAT# 638822).

REFERENCES

1. **Agarkova I, Auerbach D, Ehler E and Perriard J.** A Novel Marker for Vertebrate Embryonic Heart, the EH-myomesin Isoform. *J Biol Chem.* 2000; **275**: 10256–10264.
2. **Agarkova I and Perriard J.** The M-band: an elastic web that crosslinks thick filaments in the center of the sarcomere. *Trends in Cell Biology* 2005; **15**: 477-485.
3. **Andersen JL, Peter Schjerling P and Saltin B.** The cellular biology of muscle helps to explain why a particular athlete wins and suggests what future athletes might do to better their odds. *Scientific American* 2000; September: 48-55.
4. **Andersen PS, Havndrup O, Hougs L, Sørensen KM, Jensen M, Larsen LA, Hedley P, Thomsen ARB, Moolman-Smook J, Christiansen M, and Bundgaard H.** Diagnostic Yield, Interpretation, and Clinical Utility of Mutation Screening of Sarcomere Encoding Genes in Danish Hypertrophic Cardiomyopathy Patients and Relatives. *Human Mutation* 2008; **30**: 363–370.
5. **Anderson BR and Granzier HL.** Titin-based tension in the cardiac sarcomere: Molecular origin and physiological adaptations. *Progress in Biophysics and Molecular Biology* 2012; **110**: 204-217.

6. **Arad M, Seidman JG and Seidman CE.** Phenotypic diversity in hypertrophic cardiomyopathy. *Human Molecular Genetics* 2002; **11**: 2499–2506.
7. **Arber S, Hunter JJ, Ross J, Hongo M, Sansig G, Borg J, Perriard J, Chien KR and Caroni P.** MLP-Deficient Mice Exhibit a Disruption of Cardiac Cytoarchitectural Organization, Dilated Cardiomyopathy, and Heart Failure. *Cell* 1997; **88**: 393–403.
8. **Ashbaugh CD, Warren HB, Carey VJ and Wessels MR.** Molecular analysis of the role of the group A streptococcal cysteine protease, hyaluronic acid capsule, and M protein in a murine model of human invasive soft-tissue infection. *J Clin Invest.* 1998; **102**: 550-560.
9. **Auerbach D, Bantle S, Keller S, Hinderling V, Leu M, Ehler E, and Perriard J.** Different Domains of the M-Band Protein Myomesin Are Involved in Myosin Binding and M-Band Targeting. *Molecular Biology of the Cell* 1999; **10**: 1297–1308.
10. **Azzazy HME, Pelsers MMAL and Christenson RH.** Unbound Free Fatty Acids and Heart-Type Fatty Acid–Binding Protein: Diagnostic Assays and Clinical Applications. *Clinical Chemistry* 2006; **52**: 19–29.
11. **Banfield MJ, Barker JJ, Perry ACF and Brady RL.** Function from structure? The crystal structure of human phosphatidylethanolamine-binding

- protein suggests a role in membrane signal transduction. *Structure* 1998; **6**: 1245–1254.
12. **Bang M, Mudry RE, McElhinny AS, Trombitás K, Geach AJ, Yamasaki R, Sorimachi H, Granzier H, Gregorio CC and Labeit S.** Myopalladin, a Novel 145-Kilodalton Sarcomeric Protein with Multiple Roles in Z-Disc and I-Band Protein Assemblies. *The Journal of Cell Biology* 2001a; **153**: 413–427.
 13. **Bang M, Centner T, Fornoff F, Geach AJ, Gotthardt M, McNabb M, Witt CC, Labeit D, Gregorio CC, Granzier H, Labeit S.** The Complete Gene Sequence of Titin, Expression of an Unusual \approx 700-kDa Titin Isoform, and Its Interaction With Obscurin Identify a Novel Z-Line to I-Band Linking System. *Circulation Research* 2001b; **89**: 1065-1072.
 14. **Bantle S, Keller S, Haussmann I, Auerbach D, Perriard E, Mühlebach S, and Perriard J.** Tissue-specific Isoforms of Chicken Myomesin Are Generated by Alternative Splicing. *J Biol Chem.* 1996; **271**: 19042–19052.
 15. **Bähler M, Eppenberger HM and Wallimann T.** Novel Thick Filament Protein of Chicken Pectoralis Muscle: the 86 kd Protein. *J Mol Biol.* 1985; **186**: 393-401.
 16. **Bellin RM, Huiatt TW, Critchley DR and Robson RM.** Synemin may function to directly link muscle cell intermediate filaments to both myofibrillar Z-lines and costameres. *J Biol Chem.* 2001; **276**: 32330–32337.

17. **Bennett PM, Fürst DO and Gautel M.** The C-protein (myosin binding protein C) family: Regulators of contraction and sarcomere formation? *Rev Physiol Biochem Pharmacol.* 1999; **138**: 203-234.
18. **Bertoncini P, Schoenauer R, Agarkova I, Hegner M, Perriard J and Güntherodt H.** Study of the Mechanical Properties of Myomesin Proteins Using Dynamic Force Spectroscopy. *J Mol Biol.* 2005; **348**: 1127–1137.
19. **Blair E, Redwood C, De Jesus Oliveira M, Moolman-Smook JC, Brink PA, Corfield VA, Östman-Smith I, Watkins H.** Mutations of the Light Meromyosin Domain of the β -Myosin Heavy Chain Rod in Hypertrophic Cardiomyopathy. *Circulation Research* 2002; **90**: 263-269.
20. **Carlsson L and Thornell LE.** Desmin-related myopathies in mice and man. *Acta Physiol Scand.* 2001; **171**: 341-348.
21. **Causier B and Davies B.** Analysing protein-protein interactions with the yeast two-hybrid system. *Plant Molecular Biology* 2002; **50**: 855–870.
22. **Cazorla O, Freiburg A, Helmes M, Centner T, McNabb M, Wu Y, Trombitás K, Labeit S and Granzier H.** Differential Expression of Cardiac Titin Isoforms and Modulation of Cellular Stiffness. *Circulation Research* 2000; **86**: 59-67.

23. **Chung M, Tsoutsman T and Semsarian C.** Hypertrophic cardiomyopathy: from gene defect to clinical disease. *Cell Research* 2003; **13**: 9-20.
24. **Chung CS and Granzier HL.** Contribution of titin and extracellular matrix to passive pressure and measurement of sarcomere length in the mouse left ventricle. *Journal of Molecular and Cellular Cardiology* 2011; **50**: 731–739.
25. **Colan SD, Sanders SP, MacPherson D and Borow KM.** Left ventricular diastolic function in elite athletes with physiologic cardiac hypertrophy. *J Am Coll Cardiol.* 1985; **6**: 545-549.
26. **Craig RW and Padrón R.** Molecular Structure of the Sarcomere. Myology, 3rd Edition, *The McGraw-Hill Companies, Inc.* 2004.
27. **Czajlik A, Thompson GS, Khan GN, Kalverda AP, Homans SW, Trinick J.** ¹H, ¹⁵N and ¹³C backbone chemical shift assignment of the titin A67-A68 domain tandem. *Biomol NMR Assign.* 2012; **6**: 39-41.
28. **De Lange WJ.** An Investigation of Myosin Binding Protein C Mutations in South Africa and a Search for Ligands Binding to Myosin Binding Protein C. PhD thesis. University of Stellenbosch, Department of Biomedical Sciences; 2004.
29. **Devereux RB, Wachtell K, Gerds E, Boman K, Nieminen MS, Papademetriou V, Rokkedal J, Harris K, Aurup P and Dahlöf B.**

- Prognostic Significance of Left Ventricular Mass Change During Treatment of Hypertension. *The Journal of the American Medical Association* 2004; **292**: 2350-2356.
30. **Devereux RB and Roman MJ.** Inter-relationships between hypertension, left ventricular hypertrophy and coronary heart disease. *J Hypertens.* 1993; **11**: 3-9.
31. **Dorland's Illustrated Medical Dictionary** 31st Edition, Saunders, an imprint of *Elsevier Inc.* 2007.
32. **Ehler E, Rothen BM, Hämmerle SP, Komiyama M and Perriard J.** Myofibrillogenesis in the developing chicken heart: assembly of Z-disk, M-line and the thick filaments. *Journal of Cell Science* 1999; **112**: 1529-1539.
33. **Einheber, S. and Fischman, D.** Isolation and characterization of a cDNA clone encoding avian skeletal muscle C-protein : an intracellular member of the immunoglobulin superfamily. *Proc Natl Acad Sci. USA* 1990; **87**: 2157-2161.
34. **Elliott GF, Lowy J and Worthington CR.** An X-ray and light-diffraction study of the filament lattice of striated muscle in the living state and in rigor. *J Mol Biol.* 1963; **6**: 295-305.
35. **Eppenberger HM, Perriard JC, Rosenberg UB and Strehler EE.** The Mr 165,000 M-protein myomesin: A specific protein of cross-striated muscle cells. *J Cell Biol.* 1981; **89**: 185-193.

36. *ExPASy Proteomics Server* Swiss Institute of Bioinformatics, 2011.
37. **Freiburg A, Trombitas K, Hell W, Cazorla O, Fougerousse F, Centner T, Kolmerer B, Witt C, Beckmann JS, Gregorio CC, Granzier H and Labeit S.** Series of Exon-Skipping Events in the Elastic Spring Region of Titin as the Structural Basis for Myofibrillar Elastic Diversity. *Circulation Research* 2000; **86**: 1114-1121.
38. **Frey N, Luedde M and Katus HA.** Mechanisms of disease: hypertrophic cardiomyopathy. *Nature* 2012; **9**: 91-100.
39. **Frey N and Olson EN.** Cardiac hypertrophy: the good, the bad, and the ugly. *Annu Rev Physiol.* 2003; **65**: 45-79.
40. **Fujita M, Mitsuhashi H, Isogai S, Nakata T, Kawakami A, Nonaka I, Noguchi S, Hayashi YK, Nishino I, Kudo A.** Filamin C plays an essential role in the maintenance of the structural integrity of cardiac and skeletal muscles, revealed by the medaka mutant *zacro*. *Developmental Biology* 2012; **361**: 79-89.
41. **Fürst DO, Osborn M, Nave R and Weber K.** The Organization of Titin Filaments in the Half-Sarcomere Revealed by Monoclonal Antibodies in Immunoelectron Microscopy: A Map of Ten Nonrepetitive Epitopes Starting at

- the Z Line Extends Close to the M Line. *The Journal of Cell Biology* 1988; **106**: 1563-1572.
42. **Fürst DO, Nave R, Osborn M and Weber K.** Repetitive titin epitopes with a 42 nm spacing coincide in relative position with known A band striations also identified by major myosin-associated proteins. An immunoelectron-microscopical study on myofibrils. *Journal of Cell Science* 1989; **94**: 119-125.
43. **Fürst DO, Obermann WM and van der Ven PF.** Structure and assembly of the sarcomeric M band. *Rev Physiol Biochem Pharmacol.* 1999; **138**: 163-202.
44. **Fürst DO and Gautel M.** The Anatomy of a Molecular Giant: How the Sarcomere Cytoskeleton is Assembled from Immunoglobulin Superfamily Molecules. *J Mol Cell Cardiol.* 1995; **27**: 951-959.
45. **Gambert S, Vergely C, Filomenko R, Moreau D, Bettaieb A, Opie LH and Rochette L.** Adverse effects of free fatty acid associated with increased oxidative stress in postischemic isolated rat hearts. *Molecular and Cellular Biochemistry* 2006; **283**: 147–152.
46. **Garcia R, Grindlay J, Rath O, Fee F and Kolch W.** Regulation of human myoblast differentiation by PEBP4. *EMBO reports* 2009; **10**: 278-284.
47. **García-Castro M, Reguero JR, Batalla A, Díaz-Molina B, González P, Alvarez V, Cortina A, Cubero GI and Coto E.** Hypertrophic

- Cardiomyopathy: Low Frequency of Mutations in the β -Myosin Heavy Chain (*MYH7*) and Cardiac Troponin T (*TNNT2*) Genes among Spanish Patients. *Clinical Chemistry* 2003; **49**: 1279-1285.
48. **Gaussin V.** Offbeat mice. *Anat Rec A Discov Mol Cell Evol Biol.* 2004; **280**: 1022-1026.
49. **Gautel M.** Cytoskeletal protein kinases: titin and its relations in mechanosensing. *Pflugers Arch - Eur J Physiol.* 2011; **462**: 119–134.
50. **Gautel M, Goulding D, Bullard B, Weber K and Fürst DO.** The central Z-disk region of titin is assembled from a novel repeat in variable copy numbers. *Journal of Cell Science* 1996; **109**: 2747-2754.
51. **Gautel M, Mues A, Young P.** Control of sarcomeric assembly: The flow of information on titin. *Rev Physiol Biochem Pharmacol.* 1999; **138**: 97-137.
52. **Gautel M and Goulding D.** A molecular map of titin/connectin elasticity reveals two different mechanisms acting in series. *FEBS Lett.* 1996; **385**: 11-14.
53. **Glatz JFC and Storch J.** Unravelling the significance of cellular fatty acid-binding proteins. *Curr Opin Lipidol.* 2001; **12**: 267-274.

54. **Glatz JFC and Van der Vusse GJ.** Cellular Fatty Acid-Binding Proteins: Their Function and Physiological Significance. *Prog Lipid Res.* 1996; **35**: 243-282.
55. **Gordon AM, Homsher E, Regnier M.** Regulation and contraction in striated muscle. *Physiol Rev.* 2000; **80**: 853-924.
56. **Gotthardt M, Hammer RE, Hübner N, Monti J, Witt CC, McNabb M, Richardson JA, Granzier H, Labeit S and Herz J.** Conditional expression of mutant M-line titins results in cardiomyopathy with altered sarcomere structure. *J Biol Chem.* 2003; **278**: 6059–6065.
57. **Granzier H and Labeit S.** Cardiac titin: an adjustable multi-functional spring. *Journal of Physiology* 2002; **541**: 335–342.
58. **Granzier H and Labeit S.** The Giant Protein Titin : A Major Player in Myocardial Mechanics, Signaling, and Disease. *Circulation Research* 2004; **94**: 284-295.
59. **Granzier H and Labeit S.** Structure-Function Relations of the Giant Protein Titin in Striated and Smooth Muscle Cells. *Muscle Nerve* 2007; **36**: 740–755.
60. **Gregorio CC, Trombitás K, Centner T, Kolmerer B, Stier G, Kunke K, Suzuki K, Obermayr F, Herrmann B, Granzier H, Sorimachi H and Labeit S.** The NH2 terminus of titin spans the Z-disc: its interaction with a

- novel 19 kD ligand (T-cap) is required for sarcomeric integrity. *J Cell Biol.* 1998; **143**: 1013-1027.
61. **Gregorio CC, Granzier H, Sorimachi H and Labeit S.** Muscle assembly: a titanic achievement? *Curr Opin Cell Biol.* 1999; **11**: 18-25.
62. **Grove BK, Kurer V, Lehner C, Doetschman TC, Perriard J and Eppenberger HM.** A new 185,000 dalton skeletal muscle protein detected by antibodies. *J Cell Biol.* 1984; **98**: 518-524.
63. **Grove BK, Cerny L, Perriard J and Eppenberger HM.** Myomesin and M-Protein: Expression of Two M-Band Proteins in Pectoral Muscle and Heart during Development. *The Journal of Cell Biology* 1985; **101**: 1413-1421.
64. **Grove BK, Cerny L, Perriard J, Eppenberger HM and Thornell LE.** Fiber type-specific distribution of M-band proteins in chicken muscle. *J Histochem Cytochem.* 1989; **37**: 447-454.
65. **Haider AW, Larson MG, Benjamin EJ and Levy D.** Increased left ventricular mass and hypertrophy are associated with increased risk for sudden death. *J Am Coll Cardiol.* 1998; **32**: 1454-1459.
66. **Hanson J, Huxley HE.** Structural basis of the cross-striations in muscle. *Nature* 1953; **172**: 530-532.

67. **Hanson J, Huxley HE.** Quantitative studies on the structure of cross-striated myofibrils: II. Investigations by biochemical techniques. *Biochim Biophys Acta* 1957; **23**: 250-260.
68. **Hart G.** Exercise-induced cardiac hypertrophy: a substrate for sudden death in athletes? *Experimental Physiology* 2003; **88**: 639-644.
69. **Hengst U, Albrecht H, Hess D and Monard D.** The Phosphatidylethanolamine-binding Protein Is the Prototype of a Novel Family of Serine Protease Inhibitors. *J Biol Chem.* 2001; **276**: 535–540.
70. **Herman DS, Lam L, Taylor MRG, Wang L, Teekakirikul P, Christodoulou D, Conner L, DePalma SR, McDonough B, Sparks E, Teodorescu DL, Cirino AL, Banner NR, Pennell DJ, Graw S, Merlo M, Di Lenarda A, Sinagra G, Bos JM, Ackerman MJ, Mitchell RN, Murry CE, Lakdawala NK, Ho CY, Barton PJ, Cook SA, Mestroni L, Seidman JG and Seidman CE.** Truncations of titin causing dilated cardiomyopathy. *N Engl J Med* 2012; **366**: 619-628.
71. **Herrmann H and Aebi U.** Intermediate filaments and their associates: Multi-talented structural elements specifying cytoarchitecture and cytodynamics. *Curr Opin Cell Biol.* 2000; **12**: 79-90.
72. **Herwald H, Cramer H, Mörgelin M, Russell W, Sollenberg U, Norrby-Teglund A, Flodgaard H, Lindbom L and Björck L.** M protein, a classical

bacterial virulence determinant, forms complexes with fibrinogen that induce vascular leakage. *Cell* 2004; **116**: 367-379.

73. **Hornemann T, Kempa S, Himmel M, Hayess K, Fürst DO and Wallimann T.** Muscle-type creatine kinase interacts with central domains of the M-band proteins myomesin and M-protein. *J Mol Biol.* 2003; **332**: 877–887.
74. **Horowitz R.** The physiological role of titin in striated muscle. *Rev Physiol Biochem Pharmacol* 1999; **138**: 57-96.
75. **Horowitz R, Kempner ES, Bisher ME and Podolsky RJ.** A physiological role for titin and nebulin in skeletal muscle. *Nature* 1986; **323**: 160-164.
76. **Horowitz R, Luo G, Zhang JQ and Herrera AH.** Nebulin and nebulin-related proteins in striated muscle. *Adv Biophys* 1996; **33**: 143-150.
77. **Hudson B, Hidalgo C, Saripalli C and Granzier H.** Hyperphosphorylation of Mouse Cardiac Titin Contributes to Transverse Aortic Constriction-Induced Diastolic Dysfunction. *Circulation Research* 2011; **109**: 858-866.
78. **Huxley HE.** Electron microscope studies of the organization of the filaments in striated muscle. *Biochim Biophys Acta* 1953a; **12**: 387-394.

79. **Huxley HE.** X-ray analysis and the problem of muscle. *Proc R Soc Lond Biol.* 1953b; **141**: 59-62.
80. **Huxley HE.** The double array of filaments in cross-striated muscle. *J Biophys Biochem Cytol.* 1957; **3**: 631-648.
81. **Huxley HE.** Electron microscope studies on the structure of natural and synthetic protein filaments from striated muscle. *J Mol Biol.* 1963; **7**: 281-308.
82. **Huxley HE and Hanson J.** Changes in the cross-striations of muscle during contraction and stretch and their structural interpretation. *Nature* 1954; **173**: 973-976.
83. **Huxley HE and Hanson J.** Quantitative studies on the structure of cross-striated myofibrils. I. Investigations by interference microscopy. *Biochim Biophys Acta* 1957; **23**: 229-249.
84. **Huxley AF and Niedegerke R.** Structural changes in muscle during contraction. Interference microscopy of living muscle fibres. *Nature* 1954; **173**: 971-973.
85. **Irving T, Wu Y, Bekyarova T, Farman GP, Fukuda N and Granzier H.** Thick-Filament Strain and Interfilament Spacing in Passive Muscle: Effect of Titin-Based Passive Tension. *Biophysical Journal* 2001; **100**: 1499–1508.

86. **James P, Halladay J and Craig EA.** Genomic Libraries and a Host Strain Designed for Highly Efficient Two-Hybrid Selection in Yeast. *Genetics* 1996; **144**: 1425-1436.

87. **Kaiser CM, Bujalowski PJ, Ma L, Anderson J, Epstein HF and Oberhauser AF.** Tracking UNC-45 Chaperone-Myosin Interaction with a Titin Mechanical Reporter. *Biophysical Journal* 2012; **102**: 2212–2219.

88. **Kaufman BD, Auerbach S, Reddy S, Manliot C, Deng L, Prakash A, Printz BF, Gruber D, Papavassiliou DP, Hsu DT, Sehnert AJ, Chung WK and Mital S.** RAAS gene polymorphisms influence progression of pediatric hypertrophic cardiomyopathy. *Hum Genet* 2007; **122**: 515–523.

89. **Keren A, Syrris P and McKenna WJ.** Hypertrophic cardiomyopathy: the genetic determinants of clinical disease expression. *Nature* 2008; **5**: 158-168.

90. **Kim H and Storch J.** Mechanism of Free Fatty Acid Transfer from Rat Heart Fatty Acid-binding Protein to Phospholipid Membranes. *J Biol Chem.* 1992; **267**: 20051-20056.

91. **King NMP, Methawasin M, Nedrud J, Harrell N, Chung CS, Helmes M and Granzier H.** Mouse intact cardiac myocyte mechanics: cross-bridge and titin-based stress in unactivated cells. *J. Gen. Physiol.* 2010; **137**: 81-91.

92. **Kley RA, Hellenbroich Y, Van der Ven PFM, Fürst DO, Huebner A, Bruchertseifer V, Peters SA, Heyer CM, Kirschner J, Schröder R, Fischer D, Müller K, Tolksdorf K, Eger K, Germing A, Brodherr T, Reum C, Walter MC, Lochmüller H, Ketelsen U and Vorgerd M.** Clinical and morphological phenotype of the filamin myopathy: a study of 31 German patients. *Brain* 2007; **130**: 3250-3264.
93. **Knöll R, Hoshijima M and Chien KR.** Z-line proteins: implications for additional functions. *European Heart Journal Supplements* 2002; **4**: 113-117.
94. **Kolmerer B, Witt CC, Freiburg A, Millevoi S, Stier G, Sorimachi H, Pelin K, Carrier L, Schwartz K, Labeit D, Gregorio CC, Linke WA and Labeit S.** The titin cDNA sequence and partial genomic sequences: Insights into the molecular genetics, cell biology and physiology of the titin filament system. *Rev Physiol Biochem* 1999; **138**: 19-55.
95. **Komuro I and Yazaki Y.** Control of Cardiac Gene Expression by Mechanical Stress. *Annual Review of Physiology* 1993; **55**: 55-75.
96. **Kontogianni-Konstantopoulos A, Catino DH, Strong JC, Randall WR, Bloch RJ.** Obscurin regulates the organization of myosin into A bands. *American Journal of Physiology-Cell Physiology* 2004; **287**: 209-217.

97. **Koren MJ, Devereux RB, Casale PN, Savage DD and Laragh JH.** Relation of left ventricular mass and geometry to morbidity and mortality in uncomplicated essential hypertension. *Ann Int Med.* 1991; **114**: 345-352.
98. **Krans JL.** The Sliding Filament Theory of Muscle Contraction. *Nature Education* 2010; **3**: 66.
99. **Krüger M and Linke WA.** The Giant Protein Titin: A Regulatory Node That Integrates Myocyte Signaling Pathways. *J Biol Chem.* 2011; **286**: 9905–9912.
100. **Kushmerick MJ.** Energy balance in muscle activity: Simulations of ATPase coupled to oxidative phosphorylation and to creatine kinase. *Comp Biochem Physiol B Biochem Mol Biol.* 1998; **120**: 109-123.
101. **Labeit S, Gautel M, Lakey A, and Trinick J.** Towards a molecular understanding of titin. *EMBO J.* 1992; **11**: 1711–1716.
102. **Labeit S, Kolmerer B and Linke WA.** The giant protein titin. Emerging roles in physiology and pathophysiology. *Circulation Research* 1997; **80**: 290-294.
103. **Labeit S and Kolmerer B.** Titins: giant proteins in charge of muscle ultrastructure and elasticity. *Science* 1995; **270**: 293-296.
104. **Lange S, Xiang F, Yakovenko A, Vihola A, Hackman P, Rostkova E, Kristensen J, Brandmeier B, Franzen G, Hedberg B, Gunnarsson LG,**

- Hughes SM, Marchand S, Sejersen T, Richard I, Edström L, Ehler E, Udd B, Gautel M.** The Kinase Domain of Titin Controls Muscle Gene Expression and Protein Turnover. *Science* 2005; **308**: 1599-1603.
105. **Lange S, Ehler E and Gautel M.** From A to Z and back? Multicompartment proteins in the sarcomere. *Trends in Cell Biology* 2006; **16**: 11–18.
106. **Lehman W, Galińska-Rakoczy A, Hatch V, Tobacman LS and Craig R.** Structural Basis for the Activation of Muscle Contraction by Troponin and Tropomyosin. *J Mol Biol.* 2009; **388**: 673–681.
107. **Leinwand LA, Tardiff JC and Gregorio CC.** Mutations in the Sensitive Giant Titin Result in a Broken Heart. *Circulation Research* 2012; **111**: 158-161.
108. **Levy D, Labib SB, Anderson KM, Christiansen JC, Kannel WB and Castelli WP.** Determinants of sensitivity and specificity of electrocardiographic criteria for left ventricular hypertrophy. *Circulation* 1990; **81**: 815-820.
109. **LeWinter MM, Wu Y, Labeit S and Granzier H.** Cardiac titin: structure, functions and role in disease. *Clin Chim Acta* 2007; **375**: 1-9.
110. **Lieber RL and Bodine-Fowler SC.** Skeletal muscle mechanics: implications for rehabilitation. *Phys Ther.* 1993; **73**: 844-856.

111. **Lijnen P and Petrov V.** Renin-Angiotensin System, Hypertrophy and Gene Expression in Cardiac Myocytes. *Journal of Molecular and Cellular Cardiology* 1999; **31**: 949–970.
112. **Lim D, Lutucuta S, Bachireddy P, Youker K, Evans A, Entman M, Roberts R and Marian AJ.** Angiotensin II Blockade Reverses Myocardial Fibrosis in a Transgenic Mouse Model of Human Hypertrophic Cardiomyopathy. *Circulation* 2001; **103**: 789-791.
113. **Linke WA.** Stretching molecular springs: elasticity of titin filaments in vertebrate striated muscle. *Histology and Histopathology* 2000; **15**: 799-811.
114. **Linke WA.** Sense and stretchability: The role of titin and titin-associated proteins in myocardial stress-sensing and mechanical dysfunction. *Cardiovascular Research* 2008; **77**: 637–648.
115. **Linke WA, Rudy DE, Centner T, Gautel M, Witt C, Labeit S and Gregorio CC.** I-Band Titin in Cardiac Muscle Is a Three-Element Molecular Spring and Is Critical for Maintaining Thin Filament Structure. *Journal of Cell Biology* 1999; **146**: 631-644.
116. **Linke WA, Kulke M, Li H, Fujita-Becker S, Neagoe C, Manstein DM, Gautel M and Julio M. Fernandez JM.** PEVK Domain of Titin: An Entropic

- Spring with Actin-Binding Properties. *Journal of Structural Biology* 2002; **137**: 194–205.
117. **Lopaschuk GD**. Targets for modulation of fatty acid oxidation in the heart. *Curr Opin Investig Drugs*. 2004; **5**: 290-294.
118. **Lopaschuk GD, Ussher JR, Folmes CDL, Jaswal JS and Stanley WC**. Myocardial Fatty Acid Metabolism in Health and Disease. *Physiol Rev* 2010; **90**: 207–258.
119. **Loell BH and Carabello BA**. Left Ventricular Hypertrophy : Pathogenesis, Detection, and Prognosis. *Circulation* 2000; **102**: 470-479.
120. **Luther PK**. Three-dimensional structure of a vertebrate muscle Z-band: Implications for titin and α -actinin binding. *J Struct Biol*. 2000; **129**: 1-16.
121. **Luther PK and Squire JM**. Three-dimensional structure of the vertebrate muscle M-region. *J Mol Biol*. 1978; **125**: 313-324.
122. **Luther PK and Squire JM**. Muscle Z-band ultrastructure: Titin Z-repeats and Z-band periodicities do not match. *J Mol Biol*. 2002; **319**: 1157-1164.
123. **Lypowy J, Ieng-Yi Chen I and Abdellatif M**. An Alliance between Ras GTPase-activating Protein, Filamin C, and Ras GTPase-activating Protein SH3

- Domain-binding Protein Regulates Myocyte Growth. *J Biol Chem.* 2005; **280**: 25717–25728.
124. **Mani RS and Kay CM.** Interaction studies of the 165 000 dalton protein component of the M-line with the S2 subfragment of myosin. *Biochim Biophys Acta.* 1978; **536**: 134-141.
125. **Marian AJ.** Pathogenesis of diverse clinical and pathological phenotypes in hypertrophic cardiomyopathy. *Lancet* 2000; **355**: 58–60.
126. **Marian AJ.** Modifier genes for hypertrophic cardiomyopathy. *Curr Opin Cardiol.* 2002; **17**: 242–252.
127. **Maron BJ.** Hypertrophic Cardiomyopathy. A Systematic Review. *JAMA* 2002; **287**: 1308-1320.
128. **Maron BJ, Bonow RO, Cannon RO, Leon MB and Epstein SE.** Hypertrophic Cardiomyopathy. *N Engl J Med* 1987; **316**: 780-789.
129. **Maron BJ, Gardin JM, Flack JM, Gidding SS, Kurosaki TT, Bild DE.** Prevalence of Hypertrophic Cardiomyopathy in a General Population of Young Adults. *Circulation* 1995; **92**: 785-789.
130. **Maron BJ, Olivotto I, Spirito P, Casey SA, Bellone P, Gohman TE, Graham KJ, Burton DA and Cecchi F.** Epidemiology of Hypertrophic

- Cardiomyopathy-Related Death: Revisited in a Large Non-Referral-Based Patient Population. *Circulation* 2000; **102**: 858-864.
131. **Maron BJ, McKenna WJ, Danielson GK, Kappenberger LJ, Kuhn HJ, Seidman CE, Shah PM, Spencer WH, Spirito P, Ten Cate FJ and Wigle ED.** American College of Cardiology/European Society of Cardiology Clinical Expert Consensus Document on Hypertrophic Cardiomyopathy. *Journal of the American College of Cardiology* 2003; **42**: 1687–1713.
132. **Maruyama K.** Connectin/titin, giant elastic protein of muscle. *The FASEB Journal* 1997; **11**: 341-345.
133. **Maruyama K.** Comparative aspects of muscle elastic proteins. *Rev Physiol Biochem Pharmacol.* 1999; **138**: 1-18.
134. **Masaki T and Takaiti O.** M-protein. *J Biochem* 1974; **75**: 367-380.
135. **Mateja RD, Greaser ML and De Tombe PP.** Impact of titin isoform on length dependent activation and cross-bridge cycling kinetics in rat skeletal muscle. *Biochimica et Biophysica Acta* 2012 [in press].
136. **Mayans O, Van der Ven PFM, Wilm M, Mues A, Young P, Fürst DO, Wilmanns M and Mathias Gautel M.** Structural basis for activation of the titin kinase domain during myofibrillogenesis. *Nature* 1998; **395**, 863-869.

137. **McClellan G, Kulikovskaya I and Winegrad S.** Changes in Cardiac Contractility Related to Calcium-Mediated Changes in Phosphorylation of Myosin-Binding Protein C. *Biophysical Journal* 2001; **81**: 1083–1092.
138. **McElhinny AS, Kakinuma K, Sorimachi H, Labeit S and Gregorio CC.** Muscle-specific RING finger-1 interacts with titin to regulate sarcomeric M-line and thick filament structure and may have nuclear functions via its interaction with glucocorticoid modulatory element binding protein-1. *The Journal of Cell Biology* 2005; **157**: 125–136.
139. **McLeod CJ, Bos JM, Theis JL, Edwards WD, Gersh BJ, Ommen SR and Ackerman MJ.** Histologic characterization of hypertrophic cardiomyopathy with and without myofilament mutations. *American Heart Journal* 2009; **158**: 799-805.
140. **Means AR.** The clash in titin. *Nature* 1998; **395**: 846-847.
141. **Millevoi S, Trombitas K, Kolmerer B, Kostin S, Schaper J, Pelin K, Granzier H and Labeit S.** Characterization of nebulin and nebulin and emerging concepts of their roles for vertebrate Z-discs. *J Mol Biol.* 1998; **282**: 111-123.
142. **Moolman-Smook JC, De Lange W, Corfield VA and Brink PA.** Expression of HCM causing mutations: lessons learnt from genotype-phenotype studies of

- the South African founder *MYH7* A797T mutation. *Journal of Medical Genetics* 2000; **37**: 951-956.
143. **Moreira ES, Wiltshire TJ, Faulkner G, Nilforoushan A, Vainzof M, Suzuki OT, Valle G, Reeves R, Zatz M, Passos-Bueno MR and Jenne DE.** Limb-girdle muscular dystrophy type 2G is caused by mutations in the gene encoding the sarcomeric protein telethonin. *Nat Genet* 2000; **24**: 163-166.
144. **Morioka N, Shigematsu Y, Hamada M and Higaki J.** Circulating Levels of Heart-Type Fatty Acid-Binding Protein and Its Relation to Thallium-201 Perfusion Defects in Patients With Hypertrophic Cardiomyopathy. *The American Journal of Cardiology* 2005; **95**: 1334-1337.
145. **Murray JT, Campbell DG, Pegg M, Mora A and Cohen P.** Identification of filamin C as a new physiological substrate of PKB α using KESTREL. *Biochem. J.* 2004; **384**: 489-494.
146. **Musa H, Meek S, Gautel M, Peddie D, Smith AJH and Peckham M.** Targeted homozygous deletion of M-band titin in cardiomyocytes prevents sarcomere formation. *Journal of Cell Science* 2006; **119**: 4322-4331.
147. **Nair SSD, Leitch JW, Falconer J and Garg ML.** Prevention of Cardiac Arrhythmia by Dietary (n-3) Polyunsaturated Fatty Acids and Their Mechanism of Action. *The Journal of Nutrition* 1997; **127**: 383.

148. **Nave R, Fürst DO and Weber K.** Visualization of the Polarity of Isolated Titin Molecules: A Single Globular Head on a Long Thin Rod As the M Band Anchoring Domain? *The Journal of Cell Biology* 1989; **109**: 2177-2187.

149. **Nedrud J, Labeit S, Gotthardt M and Granzier H.** Mechanics on Myocardium Deficient in the N2B Region of Titin: The Cardiac-Unique Spring Element Improves Efficiency of the Cardiac Cycle. *Biophysical Journal* 2011; **101**: 1385–1392.

150. **Niimura H, Patton KK, McKenna WJ, Soultis J, Maron BJ, Seidman JG and Seidman CE.** Sarcomere Protein Gene Mutations in Hypertrophic Cardiomyopathy of the Elderly. *Circulation* 2002; **105**: 446-451.

151. **Noguchi J, Yanagisawa M, Imamura N, Kasuya Y, Sakurai T, Tanakaj T and Masaki T.** Complete Primary Structure and Tissue Expression of Chicken Pectoralis M-protein. *J Biol Chem.* 1992; **267**: 20302-20310.

152. **Nowak KJ.** Trusting new age weapons to tackle titin. *Brain* 2012; **135**: 1663–1667.

153. **Nunzi MG and Franzini-Armstrong C.** The structure of smooth and striated portions of the adductor muscle of the valves in a scallop. *Journal of Ultrastructure Research* 1981; **76**: 134-148.

154. **Obermann WMJ, Gautel M, Steiner F, Van der Ven PFM, Weber K and Fürst DO.** The structure of the sarcomeric M band: Localization of defined domains of myomesin, M-protein, and the 250-kD carboxy-terminal region of titin by immunoelectron microscopy. *J Cell Biol.* 1996; **134**: 1441-1453.
155. **Obermann WMJ, Gautel M, Weber K and Fürst DO.** Molecular structure of the sarcomeric M band: mapping of titin and myosin binding domains in myomesin and the identification of a potential regulatory phosphorylation site in myomesin. *The EMBO Journal* 1997; **16**: 211-220.
156. **Offer G.** The molecular basis of muscular contraction. 1974: 623-671.
157. **Offer G, Moos C and Starr R.** A New Protein of the Thick Filaments of Vertebrate Skeletal Myofibrils. *J Mol Biol.* 1973; **74**: 653-676.
158. **Olson AK, Ledee D, Iwamoto K, Kajimoto M, O'Kelly Priddy C, Isern N and Portman MA.** C-Myc induced compensated cardiac hypertrophy increases free fatty acid utilization for the citric acid cycle. *J Mol Cell Cardiol.* 2012, doi:10.1016/j.yjmcc.2012.07.005 [in press].
159. **Parry DA and Steinert PM.** Intermediate filaments: molecular architecture, assembly, dynamics and polymorphism. *Q Rev Biophys.* 1999; **32**: 99-187.

160. **Pask HT, Jones KL and Luther PK.** M-band structure, M-bridge interactions and contraction speed in vertebrate cardiac muscles. *J Muscle Res Cell Motil.* 1994; **15**: 633-645.
161. **Patel R, Nagueh SF, Tsybouleva N, Abdellatif M, Lutucuta S, Kopelen HA, Quinones MA, Zoghbi WA, Entman M, Roberts R and Marian AJ.** Simvastatin Induces Regression of Cardiac Hypertrophy and Fibrosis and Improves Cardiac Function in a Transgenic Rabbit Model of Human Hypertrophic Cardiomyopathy. *Circulation* 2001; **104**: 317-324.
162. **Pilz S, Scharnag H, Tiran B, Wellnitz B, Seelhorst U, Boehm BO and März W.** Elevated plasma free fatty acids predict sudden cardiac death: a 6.85-year follow-up of 3315 patients after coronary angiography. *European Heart Journal* 2007; **28**: 2763–2769.
163. **Pollard TD.** Actin. *Curr Opin Cell Biol.* 1990; **2**: 33-40.
164. **Poon E, Howman EV, Newey SE and Davies KE.** Association of syncoilin and desmin: Linking intermediate filament proteins to the dystrophin-associated protein complex. *J Biol Chem.* 2002; **277**: 3433-3439.
165. **Porter JD, Merriam AP, Gong B, Kasturi S, Zhou X, Hauser KF, Andrade FH and Cheng G.** Postnatal suppression of myomesin, muscle creatine kinase and the M-line in rat extraocular muscle. *The Journal of Experimental Biology* 2003; **206**: 3101-3112.

166. **Price MG and Gomer RH.** Skelemin, a cytoskeletal M-disc periphery protein, contains motifs of adhesion/recognition and intermediate filament proteins. *J Biol Chem.* 1993; **268**: 21800-21810.
167. **Rawlins J, Bhan A and Sharma S.** Left ventricular hypertrophy in athletes. *European Journal of Echocardiography* 2009; **10**: 350–356.
168. **Reddy KB, Gascard P, Price MG, Negrescu EV and Fox JEB.** Identification of an interaction between the M-band protein skelemin and b-integrin subunits. *J Biol Chem.* 1998; **273**: 35039-35047.
169. **Revera M, Van der Merwe L, Heradien M, Goosen A, Corfield VA, Brink PA, Moolman-Smook JC.** Long-term follow-up of R403W_{MYH7} and R92W_{TNNT2} HCM families: mutations determine left ventricular dimensions but not wall thickness during disease progression. *Cardiovascular Journal of Africa* 2007; **18**: 146-153.
170. **Revera M, Van der Merwe L, Heradien M, Goosen A, Corfield VA, Brink PA and Moolman-Smook JC.** Troponin T and β -myosin mutations have distinct cardiac functional effects in hypertrophic cardiomyopathy patients without hypertrophy. *Cardiovascular Research* 2008; **77**: 687-694.
171. **Roberts R and Marian AJ.** Can an Energy-Deficient Heart Grow Bigger and Stronger? *Journal of the American College of Cardiology* 2003; **41**: 1783-1785.

172. **Satoh M, Takahashi M, Sakamoto T, Hiroe M, Marumo F and Kimura A.** Structural Analysis of the Titin Gene in Hypertrophic Cardiomyopathy: Identification of a Novel Disease Gene. *Biochemical and Biophysical Research Communications* 1999; **262**: 411-417.
173. **Schoenauer R, Bertoncini P, Machaidze G, Aebi U, Perriard J, Hegner M and Agarkova I.** Myomesin is a Molecular Spring with Adaptable Elasticity. *J Mol Biol.* 2005; **349**: 367–379.
174. **Schoenauer R, Emmert MY, Felley A, Ehler E, Brokopp C, Weber B, Nemir M, Faggian GG, Pedrazzini T, Falk V, Hoerstrup SP and Agarkova I.** EH-myomesin splice isoform is a novel marker for dilated cardiomyopathy. *Basic Research in Cardiology* 2011; **106**: 233-247.
175. **Schreiber A, Specht B, Pelsers MMAL, Glatz JFC, Borchers T and Spener F.** Recombinant Human Heart-Type Fatty Acid-Binding Protein as Standard in Immunochemical Assays. *Clin Chem Lab Med* 1998; **36**: 283–288.
176. **Schunkert H, Bröckel U, Hengstenberg C, Luchner A, Muscholl MW, Kurzidim K, Kuch B, Döring A, Riegger GAJ and Hense H.** Familial Predisposition of Left Ventricular Hypertrophy. *Journal of the American College of Cardiology* 1999; **33**: 1685-1691.

177. **Seidman JG and Seidman C.** The genetic basis for cardiomyopathy: from mutation identification to mechanistic paradigms. *Cell* 2001; **104**: 557-567.
178. **Severs NJ.** The cardiac muscle cell. *BioEssays* 2000; **22**: 188–199.
179. **Sharp A and Mayet J.** Regression of left ventricular hypertrophy: hoping for a longer life. *Journal of Renin-Angiotensin-Aldosterone System* 2002; **3**: 141-144.
180. **Short B.** Titin isn't a sleeping giant. *The Journal of Cell Biology* 2011: 597.
181. **Silverthorn DU.** Human Physiology An Integrated Approach, 4th Edition. *Pearson Education Inc.* 2007: 403-404.
182. **Sjöström M and Squire JM.** Fine structure of the A-band in cryo-sections. The structure of the A-band of human skeletal muscle fibres from ultra-thin cryo-sections negatively stained. *J Mol Biol.* 1977 **109**: 49-68.
183. **Sobhanifar S.** Yeast Two Hybrid Assay: A Fishing Tale. *BioTeach Journal* 2003; **1**: 81-88.
184. **Solaro RJ and Rarick HM.** Troponin and tropomyosin. Proteins that switch on and tune in the activity of cardiac myofilaments. *Circulation Research* 1998; **83**: 471-480.

185. **Soteriou A, Gamage M and Trinick J.** A survey of interactions made by the giant protein titin. *Journal of Cell Science* 1993; **104**: 119-123.

186. **Spirito P, Seidman CE, McKenna WJ and Maron BJ.** The Management of Hypertrophic Cardiomyopathy. *N Engl J Med* 1997; **336**: 775-785.

187. **Spirito P and Maron BJ.** Relation Between Extent of Left Ventricular Hypertrophy and Age in Hypertrophic Cardiomyopathy. *JACC* 1989; **13**: 820-823.

188. **Stahl SW, Puchner EM, Alexandrovich A, Gautel M and Gaub HE.** A Conditional Gating Mechanism Assures the Integrity of the Molecular Force-Sensor Titin Kinase. *Biophysical Journal* 2011; **101**: 1978–1986.

189. **Steiner F, Weber K and Fürst DO.** M band proteins myomesin and skelemin are encoded by the same gene: Analysis of its organization and expression. *Genomics* 1999; **56**: 78-89.

190. **Stöllberger C, Slany J, Brainin M and Finsterer J.** Angiotensin-Converting Enzyme Inhibitors and Stroke Prevention: What About the Influence of Atrial Fibrillation and Antithrombotic Therapy? *Stroke* 2003; **34**: 208.

191. **Stromer MH.** Intermediate (10 nm) filaments in muscle, in Goldman RD and Steinert PM (eds): *Cellular and Molecular Biology of Intermediate Filaments*. New York: Plenum Press, 1990: 19.

192. **Stromer MH.** Immunocytochemistry of the muscle cell cytoskeleton. *Microsc Res Tech* 1995; **31**: 95-105.
193. **Sussman MA, Lim HW, Gude N, Taigen T, Olson EN, Robbins J, Colbert MC, Gualberto A, Wieczorek DF and Molkentin JD.** Prevention of Cardiac Hypertrophy in Mice by Calcineurin Inhibition. *Science* 1998; **281**: 1690-1693.
194. **Takezawa Y, Kim D, Ogino M, Sugimoto Y, Kobayashi T, Arata T and Wakabayashi K.** Backward Movements of Cross-Bridges by Application of Stretch and by Binding of MgADP to Skeletal Muscle Fibers in the Rigor State as Studied by X-Ray Diffraction. *Biophysical Journal* 1998; **76**: 1770–1783.
195. **Taylor M, Graw S, Sinagra G, Barnes C, Slavov D, Brun F, Pinamonti B, Salcedo EE, Sauer W, Pyxaras S, Anderson B, Simon B, Bogomolovas J, Labeit S, Granzier H and Mestroni L.** Genetic Variation in Titin in Arrhythmogenic Right Ventricular Cardiomyopathy - Overlap Syndromes. *Circulation*. 2011; **124**: 876-885.
196. **Trinick J.** Elastic filaments and giant proteins in muscle. *Current opinion in cell biology* 1991; **3**: 112-119.
197. **Trinick J.** Titin and nebulin: protein rulers in muscle? *Trends in Biomedical Sciences* 1994; **19**: 405-409.

198. **Trinick J.** Titin as a scaffold and spring. *Current Biology* 1996; **6**: 258-260.
199. **Trinick J and Lowey S.** M-protein from chicken pectoralis muscle: Isolation and characterization. *J Mol Biol.* 1977; **113**: 343-
200. **Trinick J and Tskhovrebova L.** Titin: a molecular control freak. *Trends in Cell Biol.* 1999; **9**: 377-380.
201. **Tskhovrebova L and Trinick J.** Titin: Properties Family Relationships. *Nature Reviews* 2003; **4**: 679-689.
202. **Tskhovrebova L and Trinick J.** Roles of Titin in the Structure and Elasticity of the Sarcomere. *Journal of Biomedicine and Biotechnology* 2010: 1-7.
203. **Tskhovrebova L and Trinick J.** Making Muscle Elastic: The Structural Basis of Myomesin Stretching. *PLoS Biology* 2012; **10**: 1-3.
204. **Tsoutsman T, Lam L and Semsarian C.** Genes, Calcium and Modifying Factors in Hypertrophic Cardiomyopathy. *Clinical and Experimental Pharmacology and Physiology* 2006; **33**: 139-145.
205. **Turnacioglu KK, Mittal B, Dabiri GA, Sanger JM and Sanger JW.** Zeugmatin is part of the Z-band targeting region of titin. *Cell Structure and Function* 1997; **22**: 73-82.

206. **Van Criekinge W and Beyaert R.** Yeast Two-Hybrid: State of the Art. *Biological Procedures Online* 1999; **2**: 1-38.
207. **Van der Merwe L, Cloete R, Revera M, Heradien M, Goosen A, Corfield VA, Brink PA, Moolman-Smook JC.** Genetic variation in angiotensin-converting enzyme 2 gene is associated with left ventricular hypertrophy in hypertrophic cardiomyopathy. *Human Genetics* 2008; **124**: 57-61.
208. **Van der Ven PFM, Ehler E, Vakeel P, Eulitz S, Schenk JA, Milting H, Micheel B and Fürst DO.** Unusual splicing events result in distinct Xin isoforms that associate differentially with filamin c and Mena/VASP. *Experimental Cell Research* 2006; **312**: 2154-2167.
209. **Van der Ven PF and Fürst DO.** Assembly of titin, myomesin and M-protein into the sarcomeric M band in differentiating human skeletal muscle cells in vitro. *Cell Structure and Function* 1997; **22**: 163-171.
210. **Van Nieuwenhoven FA, Kleine AH, Wodzig KWH, Hermens WT, Kragten HA, Maessen JG, Punt CD, Van Dieijen MP, Van der Vusse GJ and Glatz JFC.** Discrimination Between Myocardial and Skeletal Muscle Injury by Assessment of the Plasma Ratio of Myoglobin Over Fatty Acid-Binding Protein. *Circulation* 1995; **92**: 28-2854.

211. **Verdecchia P, Schillaci G, Borgioni C, Ciucci A, Gattobigio R, Zampi I, Reboldi G and Porcellati C.** Prognostic Significance of Serial Changes in Left Ventricular Mass in Essential Hypertension. *Circulation* 1998; **97**: 48-54.
212. **Verdecchia P, Schillaci G, Reboldi G, Franklin SS and Porcellati C.** Different Prognostic Impact of 24-Hour Mean Blood Pressure and Pulse Pressure on Stroke and Coronary Artery Disease in Essential Hypertension. *Circulation* 2001; **103**: 2579-2584.
213. **Vigoreaux JO.** The muscle Z band: lessons in stress management. *Journal of Muscle Research and Cell Motility* 1994; **15**: 237-255.
214. **Vinkemeier U, Obermann W, Weber K and Fürst DO.** The globular head domain of titin extends into the center of the sarcomeric M band. *Journal of Cell Science* 1993; **106**: 319-330.
215. **Voelkel T and Linke WA.** Conformation-regulated mechanosensory control via titin domains in cardiac muscle. *Pflugers Arch - Eur J Physiol* 2011; **462**: 143–154.
216. **Wang S, Lo M, Shang C, Kao S and Tseng Y.** Role of M-Line Proteins in Sarcomeric Titin Assembly During Cardiac Myofibrillogenesis. *Journal of Cellular Biochemistry* 1998; **71**: 82–95.

217. **Wang X, Li N, Liu B, Sun H, Chen T, Li H, Qiu J, Zhang L, Wan T and Cao X.** A Novel Human Phosphatidylethanolamine-binding Protein Resists Tumor Necrosis Factor α -induced Apoptosis by Inhibiting Mitogen-activated Protein Kinase Pathway Activation and Phosphatidylethanolamine Externalization. *J Biol Chem.* 2004; **279**: 45855–45864.
218. **Wang X, Li N and Li H.** Silencing of Human Phosphatidylethanolamine-Binding Protein 4 Sensitizes Breast Cancer Cells to Tumor Necrosis Factor- α -Induced Apoptosis and Cell Growth Arrest. *Clin Cancer Res.* 2005; **11**: 7545-7553.
219. **Wang K and Ramirez-Mitchell R.** A network of transverse and longitudinal intermediate filaments is associated with sarcomeres of adult vertebrate skeletal muscle. *J Cell Biol.* 1983; **96**: 562-570.
220. **Wang K and Wright J.** Architecture of the sarcomere matrix of skeletal muscle. Immunoelectron microscopic evidence that suggests a set of parallel inextensible nebulin filaments anchored at the Z line. *J Cell Biol.* 1988; **107**: 2199-2212.
221. **Watkins H, Seidman JG and Seidman CE.** Familial hypertrophic cardiomyopathy: A genetic model of cardiac hypertrophy. *Hum Mol Genet.* 1995; **4**: 1721-1727.

222. **Wigle ED, Rakowski H, Kimball BP and Williams WG.** Hypertrophic Cardiomyopathy Clinical Spectrum and Treatment. *Circulation* 1995; **92**: 1680-1692.
223. **Witt CC, Burkart C, Labeit D, McNabb M, Wu Y, Granzier H and Labeit S.** Nebulin regulates thin filament length, contractility, and Z-disk structure in vivo. *The EMBO Journal* 2006; **25**: 3843–3855.
224. **Wolfrum C, Borrmann CM, Torsten Borchers T and Spener F.** Fatty acids and hypolipidemic drugs regulate peroxisome proliferator-activated receptors α - and γ -mediated gene expression via liver fatty acid binding protein: A signaling path to the nucleus. *PNAS* 2001; **98**: 2323–2328.
225. **Woodcock EA and Matkovich SJ.** Cardiomyocytes structure, function and associated pathologies. *The International Journal of Biochemistry & Cell Biology* 2005; **37**: 1746–1751.
226. **Xu C, Craig R and Tobacman L.** Tropomyosin positions in regulated thin filaments revealed by cryoelectron microscopy. *Biophys J* 1999; **77**: 985.
227. **Young P, Ferguson C, Bañuelos S and Gautel M.** Molecular structure of the sarcomeric Z-disk: two types of titin interactions lead to an asymmetrical sorting of α -actinin. *The EMBO Journal* 1998; **17**: 1614–1624.

228. **Young P, Ehler E and Gautel M.** Obscurin, a giant sarcomeric Rho guanine nucleotide exchange factor protein involved in sarcomere assembly. *J Cell Biol.* 2001; **154**: 123-136.
229. **Zot AS and Potter JD.** Structural aspects of troponin-tropomyosin regulation of skeletal muscle contraction. *Annu Rev Biophys Biophys Chem* 1987; **16**: 535-559.

Webpages:

<http://eu.idtdna.com/Scitools/Scitools.aspx>

<http://www.acris-antibodies.com/target/myomesin-2-antibody.htm>

<http://www.clontech.com/>

<http://www.ncbi.nlm.nih.gov/Entrez>

<http://www.pharmacology2000.com/>